(NASA-CR-144811) MULTISPECTRAL COLOR PHOTOGRAPHY FOR MINERAL EXPLORATION BY THE REMOTE SENSING OF BIOGEOCHEMICAL ANOMALIES (Long Island Univ.) 147 p HC A07/MF A01 CSCL 14E G3/43

N77-10806

Unclas
07139

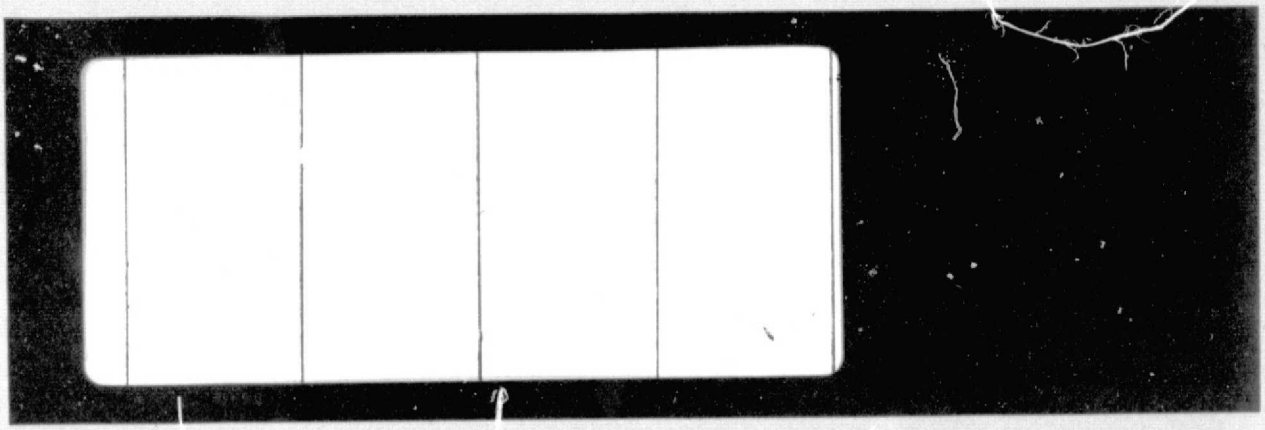

SCIENCE ENGINEERING RESEARCH GROUP

C. W. POST CENTER
LONG ISLAND UNIVERSITY

Science Engineering Research Group
Long Island University
C.W. Post Center
Greenvale, New York 11548

Multispectral Color Photography for Mineral Exploration by the Remote Sensing of Biogeochemical Anomalies

by

Edward Yost

August 1975

Prepared for:

NASA Goddard Space Flight Center
Greenbelt, Maryland 20771

Under Contract #NGR-33-151-007

Abstract

A two-phase experiment was conducted to evaluate selected band multispectral photography as a mineral exploration tool by detecting stress on trees caused by underground mineralization.

Ground truth consisted of two test sites in the Prescott National Forest within which the mineralization had been established by a drilling program. Species of trees were categorized as background, intermediate, and anomalous based upon where they grew with respect to this underlying mineralization. Analysis of soil geochemistry and the metal content of ashed samples of the trees in relation to the inferred locus of subsurface mineralization showed that: (1) Copper content in soil one foot below the surface was not related to copper content of any of the tree species, (2) copper content of the trees was related to distance from a drill hole in the core zone of mineralization, (3) the trace metal content of Ponderosa Pine trees growing over the subsurface copper anomaly was five times greater than Ponderosa Pine growing 560 feet away.

Computer analysis of the reflectance spectra of mineralized trees measured during the first phase of the experiment confirmed that the relative percent reflectance differences of Ponderosa Pine, Alligator Bark Juniper, and Emory Oak growing in anomalous areas was less than that of the same tree species growing in background areas. Subsequent analysis of the reflectance spectra obtained during the experiment's second phase showed that the differences in reflectance between Pinion Pine trees exceeded that which could be attributed to subsurface mineralization.

Visual examination of comparative image densities on multispectral negatives obtained with six different filter sets indicated that "anomalous" Ponderosa Pine could be best differentiated from "background" Ponderosa Pine using spectral bands: 406-480 nm, 505-558 nm, 585-680 nm, and 810-855 nm. Qualitative photo interpretation of multispectral images obtained in these spectral bands using an additive color viewer showed that the color saturation of "anomalous" Ponderosa Pine was too subtle to be detected by a human observer.

Quantitative measurements of image densities showed that spectral bands 406-480 nm, 505-558 nm, and 585-680 nm form a three-dimensional vector space within which "anomalous" Ponderosa Pine tended to be separate from "background" Ponderosa Pine. A linear decision rule was developed from these measurements which resulted in correctly classifying all background Ponderosa Pine and also correctly classifying anomalous Ponderosa Pine five out of six times.

Acknowledgements

The experiments reported herein were the joint efforts of Columbia University's Geology Department and Long Island University's Science Engineering Research Group.

Selection of the test site, design of the ground truth, and strategy for soil geochemistry, as well as vegetation biogeochemistry was performed by Professor Peter Ypma. The tactics of the sampling program, construction of tree location maps, and making of sample analyses were done by Dr. William Drake. Spectral reflectance measurements were collected by Messrs. Karl Grodewald, Richard Rehrig, and John Trevor. Mr. Robert Anderson was aerial photographer, photo scientist, and photo interpreter. What deficiencies may exist are the responsibility of the author.

Edward Yost
Long Island University
August 1975

Table of Contents

Section I

Introduction

Described herein is the second part of an experiment in the application of biogeochemical remote sensing for mineral exploration using selected narrow band multispectral photography.

The location of the two test sites used in these experiments (one adjacent to the other) in the Prescott National Forest is shown in Figure I below.

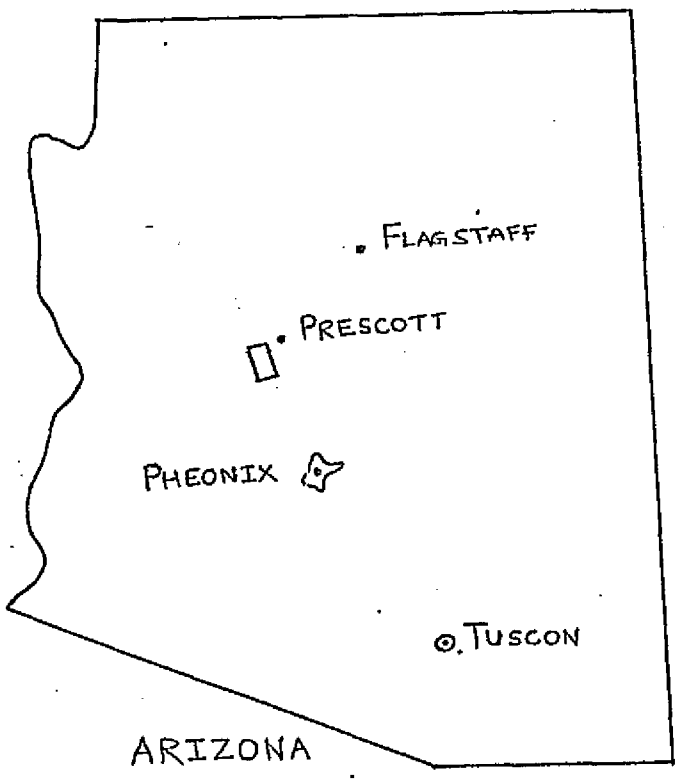

Figure I. The location of the Copper Creek and Copper Basin test sites near Prescott, Arizona.

The detailed situation of the two test sites in the Iron Springs, Arizona and Kirkland, Arizona 15 minute quadrangle topographic maps is shown in Figure 2. The Copper Basin site is four miles west of 34°30'N, 112°30' west and the Copper Creek site is four miles southwest of these coordinates.

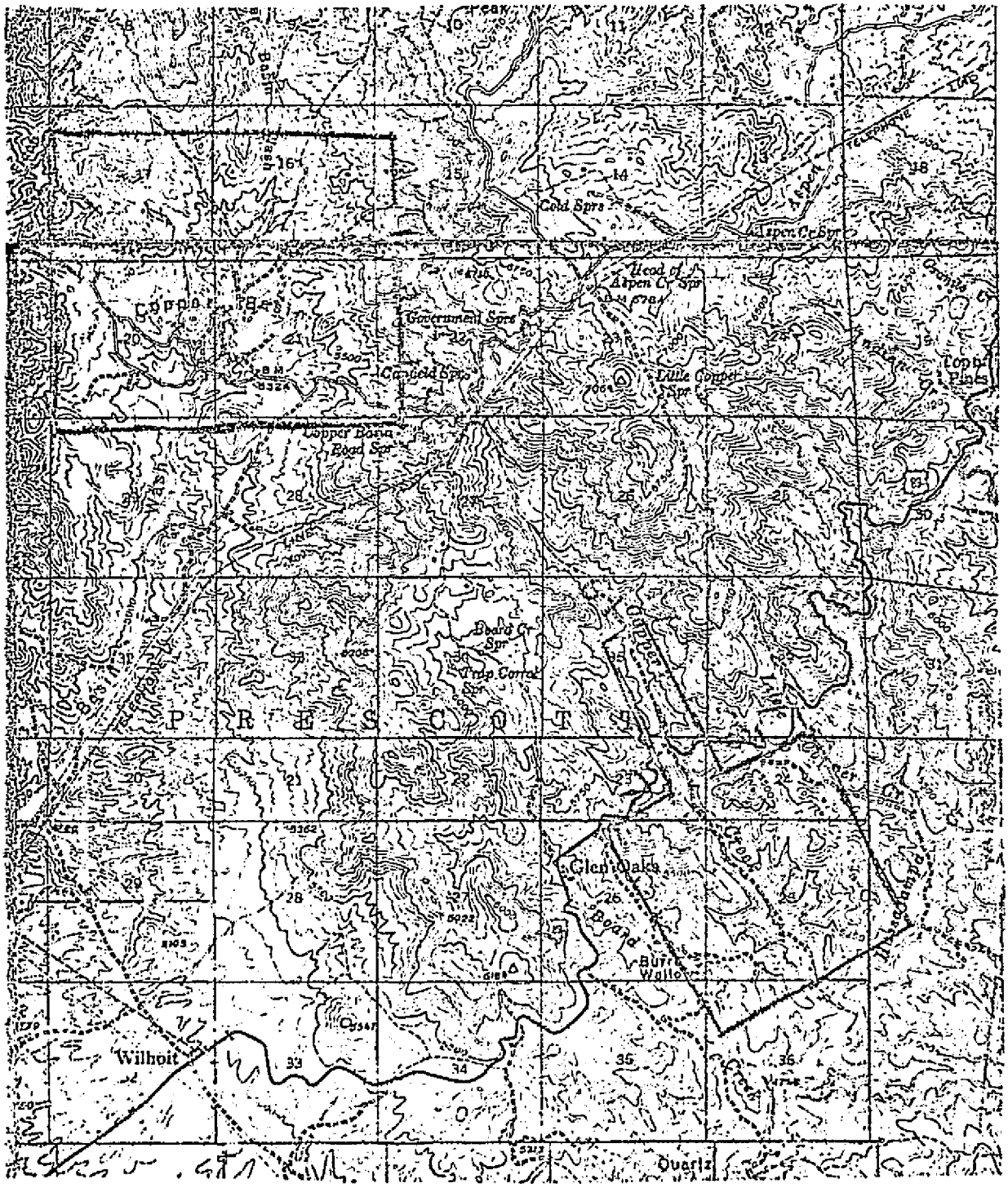

Figure 2. Location of the Copper Basin and Copper Creek test sites on the Iron Springs, Arizona and Kirkland, Arizona 15 minute topographic maps.

The first part of the experiment was conducted in the fall of 1971 at which time the copper content of three species of trees growing in Copper Creek was measured, along with associated soil samples. The areas were categorized as background, intermediate, and anomalous (core zone) based on the proximity to a sub-surface copper anomaly, the location of which had been established by drilling by others prior to our commencing this experiment. At the same time as the trace metal content of the trees was measured, a truck-mounted telespectroradiometer was used to obtain the reflectance spectra of selected anomalous, intermediate, and background trees. As described in Section 2, all three tree species growing in the anomalous core zone exhibited a reduced spectral reflectance compared to those trees growing in the background areas. Appendix A contains detailed maps of the tree and soil sample locations,as well as the copper content of soil samples and trace copper content of the trees in the Copper Basin test site.

The second part of the experiment conducted in the fall of 1972 was designed to obtain narrow band multispectral photography of the Copper Creek test site and of a second test site at Copper Basin. Selected sets of four narrow band filters were established from the reflectance spectra obtained in the fall of 1971. These filter sets were used on a four-lens multispectral camera to obtain 1:8,000 scale multispectral photography of both test sites. Simultaneously, the reflectance spectra of tree species at Copper Basin were obtained along with soil geochemistry and the trace metal content of the dominant tree species growing there. Again, the areas were divided into background, intermediate, and anomalous. Appendix B contains detailed maps of the locations at which tree and soil samples were obtained in Copper Basin. Appendix C tabularizes the copper and molybdenum trace metal content of ashed samples of tree needles, as well as the soil

sample copper and molybdenum content.

The objective of the second part of the experiment was to see if: (1) trees growing in anomalous "core zone" of both test sites could be detected in the multispectral photographic imagery, and (2) if a chain of causality could be established between the soil geochemistry, the trace metal content of the trees, the reflectance spectra of the trees, and the images of the trees on multispectral photography.

Section 2

Background

Remote sensing techniques in the visible and infrared spectral regions, as applied to mineral exploration, can be categorized as follows:

1. Differences in vegetation due to geochemical anomalies (Yost, 1971).
2. Structural discontinuities such as lineaments, faults, fault pattern, doming, fold, and deformation style as related to mineral deposits.
3. Alteration of host rock due to mineralization related processes.
4. Rock type and texture as a general geologic mapping tool and guide to mineral deposits.

In most studies that have been made on the subject of remote sensing applied to mineral exploration, scanning of surface phenomena such as rock and soil characteristics and structural features as related to mineral deposits have been most emphasized. Pilot studies of this sort were carried out in desert areas. The results were interesting because of the surprisingly high resolution that still can be achieved from high flying aircraft (with 90% of the total atmosphere between them and their target). Large parts of the earth are soil and vegetation covered. Very little is known about these areas. Large scale exploration for mineral deposits under such conditions is carried out mainly by a ground survey for rock outcrops, their structure, a geochemical soil or stream-sediment analysis or geobotanical sampling.

The recent establishment of a correlation between the reflectance spectra of the foliage of plants or trees with heavy metal content of the soil has been a major step toward the application of remote sensing for mineral potential of the large vegetation covered parts of the world. In studies performed by Canney (1970) and Yost (1971) it was shown that at the 95% confidence level significant differences are found in the chlorophyll reflection band at 550 nanometers and in the mesophyll reflection band in the 700-900 nm range between balsam fir and red spruce growing on normal and geochemically anomalous soils.

A study of the vegetation in the Copper Creek region of Arizona was undertaken to amplify these earlier findings of correlation between reflectance spectra characteristics of vegetation and geochemical anomalies due to heavy metal accumulations in the soil upon which the vegetation is growing.

Preliminary Results of Spectral Measurements from Copper Creek, Arizona

The in situ spectral reflectance of three types of trees growing along Copper Creek was measured. The tree groups included Alligator Bark Juniper, Ponderosa Pine, and Emory Oak. The stands are not particularly isolated, but rather grow indispersed. A total of 142 trees were measured and were classified according to the geology of the terrain rather than the top soil mineralization. This classification method was selected primarily because there exists areas along the creek on which a large amount of transported soil has been deposited. The deep root system of the trees permits uptake of minerals into the leaves from depths below that of the top soil. A set of 44 trees were measured in a region classified as "background" and the copper mineralization was about 100 ppm. The trees growing

over a copper anomaly had about 500 ppm on the average and a total of 31 trees in this group were measured. An "intermediate" set of 42 trees, having an average copper content of 200 ppm, were also measured. In addition, two other areas containing transported soil on the surface of the terrain were measured and the tree copper mineralization ranged between 0 ppm to about 250 ppm. These groups, however, were growing in an intermediate area and were classified as such regardless of their copper content.

A series of four spectral reflectance scans was made on each tree. Each scan consists of three sets of measurements at each wavelength ranging from 400 nanometers to 1100 nanometers. This quantity of data (which is automatically punched in ASCII code onto paper tape) is necessary in order to assure that statistically accurate measurements will result. For each species of vegetation a subset of individual trees was selected from the anomalous, intermediate, and background groups. The spectra of these trees were averaged for each group and plotted as shown in Figures 3, 4, and 5.

It should be noted that from 400 nm to 675 nm, the percent directional reflectance scale goes from 0 to 10% along the y axis. From 700 nm to 1050 nm, the reflectance scale along the y axis ranges from 0 to 100%. This scale expansion was included to show the subtle spectral changes which take place in the visible spectrum. Referring to the spectra of Alligator Bark Juniper of Figure 3, the trees growing over the copper anomaly exhibit a lower percent directional reflectance than either the intermediate or background groups. This is true in both the visible and the near-infrared wavelength regions.

The intermediate group appears to reflect slightly more radiation than the background group in the blue spectral band from 400 to 500 nm.

Notice that in addition to the obvious change in amplitude between the anomalous and background groups in the visible region that there are two wavelength intervals in which the distribution itself has been altered. The first interval exists between 400 nm and 525 nm and the second ranges from 580 nm to about 675 nm. The background and intermediate groups exhibit shallow gradients in these regions which are characteristically different from the anomalous trees. Also, a slight increase in reflectance is seen at 650 nm for the background and intermediate groups. In the infrared spectrum the background trees reflect everywhere higher than the anomalous and the reflectance of the intermediate set is where one might reasonably expect it to be, between the former two.

Figure 4 shows the reflectance spectra of the three sub-groups of Ponderosa Pine. The anomalous set exhibits lower reflectance than either the background or the intermediate trees in the same way that the Juniper trees did. However, the intermediate group does not overlap the background set at any wavelength. The relative reflectance in the blue spectral region from 400 to 500 nm is flat in the same way as Juniper. This effect, which was also seen between 580 and 675 nm in Juniper, is not nearly as apparent in the Pine, although the increase in reflectance at 650 nm is considerably more pronounced. Both the visible and near-infrared spectra of Juniper and Pine possess one more characteristic. The background and intermediate groups have approximately the same reflectance distribution and amplitude. That is, their color is quite similar. The anomalous trees display a distinct decrease in both their blue and yellow-orange reflectance which would make their foliage appear greener (less blue) than the other two groups.

Figure 5 shows the reflectance spectra for the three classes of Emory Oak. At first glance there might appear to be no difference between these

Figure 3.
Alligator Bark Juniper

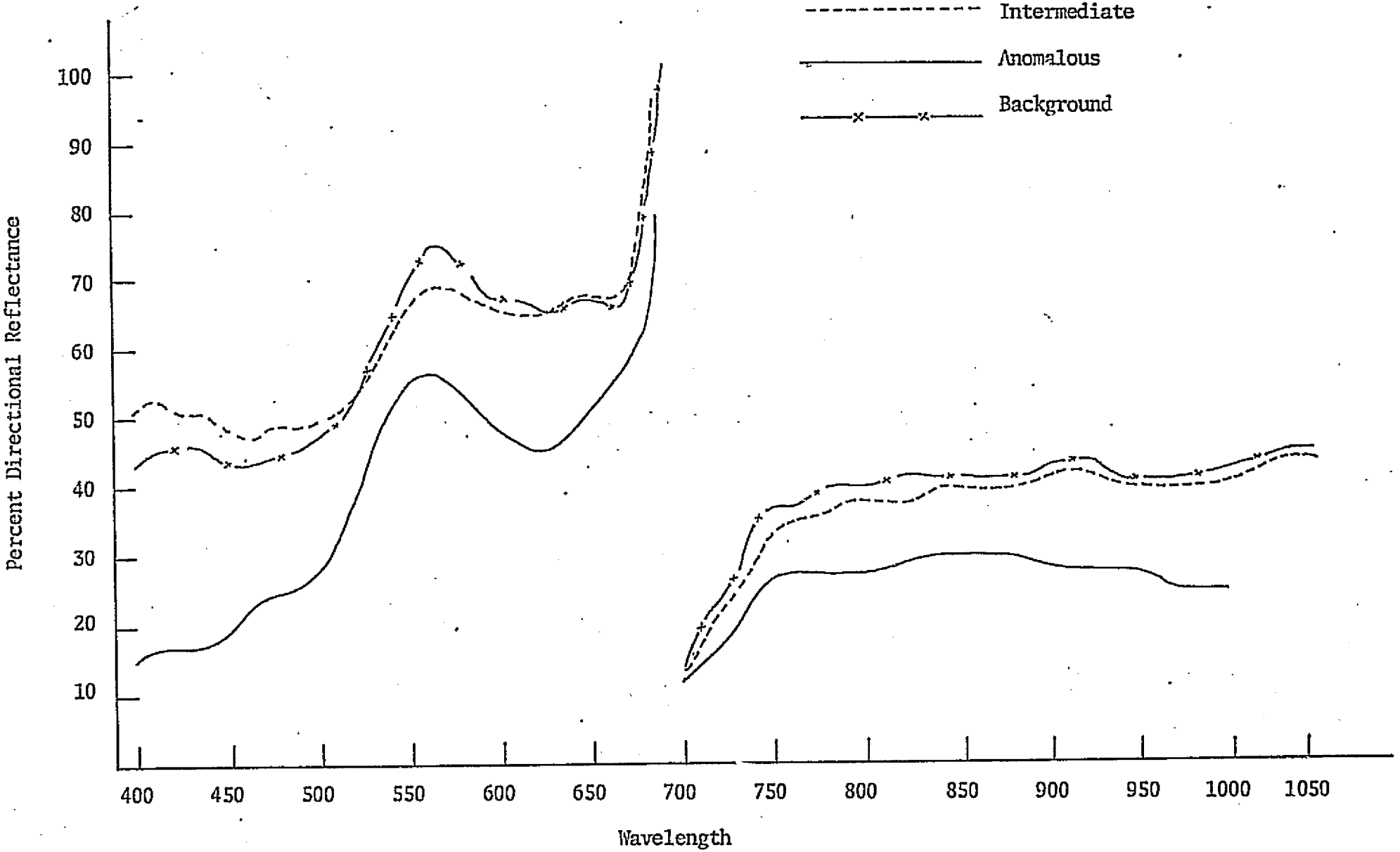

Figure 4.

Ponderosa Pine

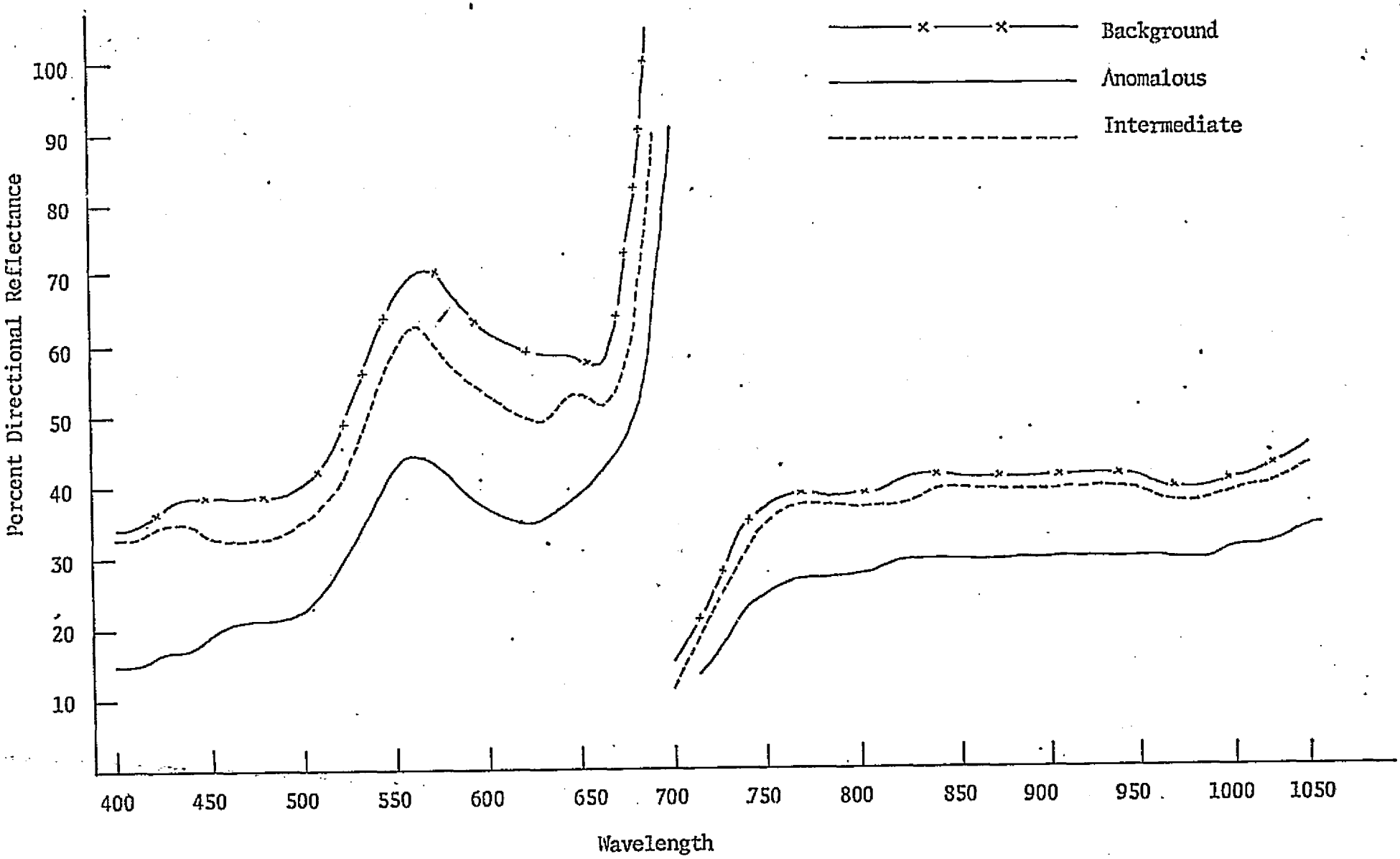

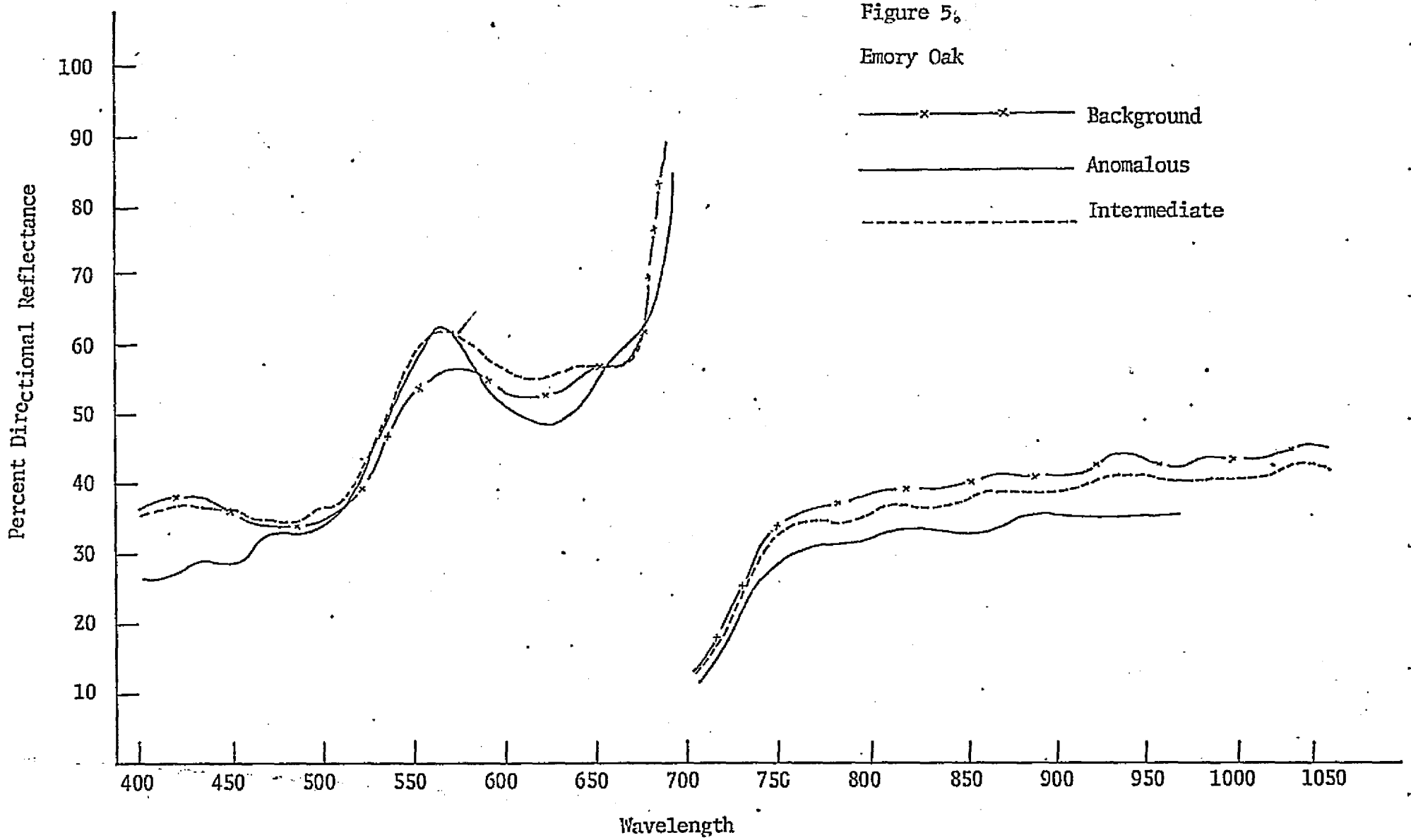
Figure 5.
Emory Oak
Background
Anomalous
Intermediate
Percent Directional Reflectance
100
90
80
70
60
50
40
30
20
10
400
450
500
550
600
650
700
750
800
850
900
950
1000
1050
Wavelength

spectra in the visible wavelength region. Notice, however, that the reflectance of the background and intermediate groups in the 400-500 nm band is considerably higher than that of the anomalous trees; a similar situation exists from 580 to 650 nm. This is exactly the same change om spectral distribution which was seen in the case of the Juniper and Pine groups. This fact is significant in that multispectral techniques are based upon differences in spectral distribution, rather than amplitude differences. Once again, the infrared interval for Emory Oak follows the pattern set by the Juniper and Ponderosa Pine.

It is apparent from these preliminary results that the spectra of each species measured is definitely related to the soil in which the vegetation is growing. The results are consistent both within and between the groups. Two spectral regions (from 400 to 500 nm and from 580 to 650 nm) can be used to filter a multispectral camera to obtain excellent imagery which will exhibit copper anomalies in additive color. Any portion of the near-infrared from 700 nm to 1100 nm could also be used as a filter.

Multispectral Color Photography

The initial results of the in situ spectra clearly indicated that the percent directional reflectance of vegetation is related to the subsurface soil mineralization. Multispectral sensors (which are correctly filtered to exclude unwanted radiation from being imaged on the film) have been successfully employed to detect subtle geophysical phenomena from aircraft altitudes ranging between 3,000 and 30,000 feet. Based upon the above findings- two distinct tasks were performed:

-- After selection of the optimal camera filtration, multispectral color and color infrared imagery was obtained of the Copper Creek, Arizona, area. Ground truth was also taken for verification purposes.

-- The final results of the multispectral photo interpretation were compared with geologic ground truth to determine the degree of accuracy with which soils anomalous in copper can be detected using this multispectral remote sensor.

The advantage of this approach is that it permits a logical association to be made between geologic ground truth, vegetation spectra, known anomalies and unknown anomalies at a variety of altitudes.

The ability of multispectral color photography to differentiate a multiplicity of subtle spectral differences in vegetation has been conducted since 1964 (cf. Yost & Wenderoth, 1967). The capability of multispectral photography for detecting and displaying environmental phenomenon for the first time has been documented (Yost & Wenderoth, 1968). A variety of multispectral photographic procedures for speciating trees and crops by analytical measurement of the chromaticity of multispectral images have been developed (Wenderoth & Yost, 1968; Yost & Wenderoth, 1969). In addition, entirely new techniques have been brought into practice which permit detection of very subtle spectral differences which are often masked by large brightness differences existing in natural vegetation.

The multispectral color photographic system combines abridged spectral photographic data collection in four spectral bands in the .36 to .9 micron region of the spectrum with colorimetric data reduction using additive color techniques.

This remote sensing technique allows the scientist to select any spectral band in the near-ultraviolet, visible, or near-infrared region of the spectrum in which to collect spectral photography and provides him with a device to combine the photos into a single color picture. The viewer also provides the scientist with the capability of altering the color of the presentation in order to enhance the particular relationships he may

detect throughout the entire spectral region (360-900 nm). Four spatially identical photos are produced and all images appear in identical coordinate positions as measured from the principal point of each photograph.

Section 3

Spectral Reflectance Measurements

In situ spectral reflectance measurements and multispectral photography were obtained at the Copper Basin and Copper Creek south of Prescott, Arizona. The equipment and techniques used are described herein. Reflectance measurements were analyzed to select filters for multispectral photography.

Spectral Reflectance Measurements

The quantitative spectral analysis of soils, vegetation, and rocks requires that simultaneous and accurate measurements of incident and reflected radiation be made. Since the spectral energy reflected by an object varies with that which is incident upon it, these spectroradiometric measurements must be made at the same instant of time.

Whereas a radiometer measures in units of energy rate intensity such as microwatts per centimeter square, a spectroradiometer measures in units of energy rate intensity per bandwidth, such as microwatts per centimeter square per nanometer. This latter system of units is most meaningful for measurements of radiation since a graph of the spectral distribution of radiant intensity versus wavelength can be obtained. The area under such a curve can be made numerically and dimensionally equal to energy available in the spectral bands of the multispectral camera.

A computerized telespectroradiometer was utilized to collect the in situ reflectance spectra. This truck-mounted instrument is positioned

adjacent to the target to be measured, the detector head extended in the air to obtain the similar downward perspective as the multispectral camera. The instrument measures and stores in the computer memory the reflectance of a standard white plate which is placed in the field of view of the spectroradiometer. The reference plate is then removed and the spectra of the target is obtained. The computer enters all the necessary instrument corrections, divides the standard white plate reference readings into the target readings at each discrete wavelength measured and prints out the result on a teletypewriter. Figure 6 shows this truck-mounted instrument in operation at the test site.

The detector head mounted atop the extended ladder is comprised of an imaging optical system, a circular interference filter monochromator, visible and infrared photomultiplier detectors, and an electronic amplifier. The circular filter is indexed into position in the optical system in front of the detector which selects the particular wavelwngth to be measured. Usually 80 discrete wavelengths are measured between 400 nm and 1100 nm.

The ratio of target reflectivity to standard reflectance reference is automatically calculated by the instrument and displayed under computer control. The computer is programmed with a list of spectral ranges (visible and infrared), data points (discrete wavelengths of interest), and the number of scans per data point. The computer incorporated in the spectroradiometer is a 16-bit word length general purpose computer having a 4096 work (8K byte) memory. Four hardware accumulators are used in addition to a PC register. The basic control program resides in 3000 core locations and includes a floating point interpretive package. The 1000 remaining locations are used for temporary data storage during target data acquisition. The basic control program takes radiometric

Figure 6. Truck-mounted telespectroradiometer.

measurements at pre-determined wavelengths, stored in a look-up table. For reflectance measurements a white standard reflector is compared to the target and the relative reflectance of the target is computed as a ratio of the target to the standard. The computer then uses this responsivity data to calculate the radiance of a target.

The telespectroradiometer used to collect the data contains two spectral channels - one covering from 400 to 700 nm (visible), the other from 675 to 1350 nm (infrared). The system is comprised of an optical head which contains the telescope optics, a sensing head containing the photomultiplier detectors, and input-output control console which contains the computer, motor drives, analog-to-digital converter, and teletypewriter.

The system is designed to have flexibility in the spectral region of operation and in its mode of operation. The primary filter assembly of the system utilizes a circular variable interference filter which allows continuous variance of the spectral region transmitted to the detector as a function of the angular position of the filter. The spectral response typically covers a two-octave range of wavelengths with an average spectral resolution of 2 1/2%. The system operates in an incrementally stepped mode which provides the ability to take precise measurements at each wavelength. Time is allowed for gain ranging, amplifier settling, and multiple readings for computer averaging.

The automatic telespectroradiometer used to collect the data consists of four basic units: The optical head, the sensing head, the control cabinet, and the output unit.

The telespectroradiometer contains a 300 mm focal length refractive optical system with a 50 mm diameter entrance aperture. The mechanical configuration of the optical head of the system is shown in Figure 7. The incoming radiation is focused by the objective lens on an intermediate focal plane where an adjustable field stop is located to define the system's field of view.

The radiation passing through the field stop is refocused by the transfer optics onto the front surface of the circular variable filter. The radiation traversing the filter is refocused by a relay lens onto the detector.

The circular variable filter is motor-driven under computer control. The direct coupled angular encoder provides a feedback signal to the computer of the instantaneous position of the circular variable filter. The computer program specifies the angular position at which measurements will be made and monitors the optical encoder output until the correct

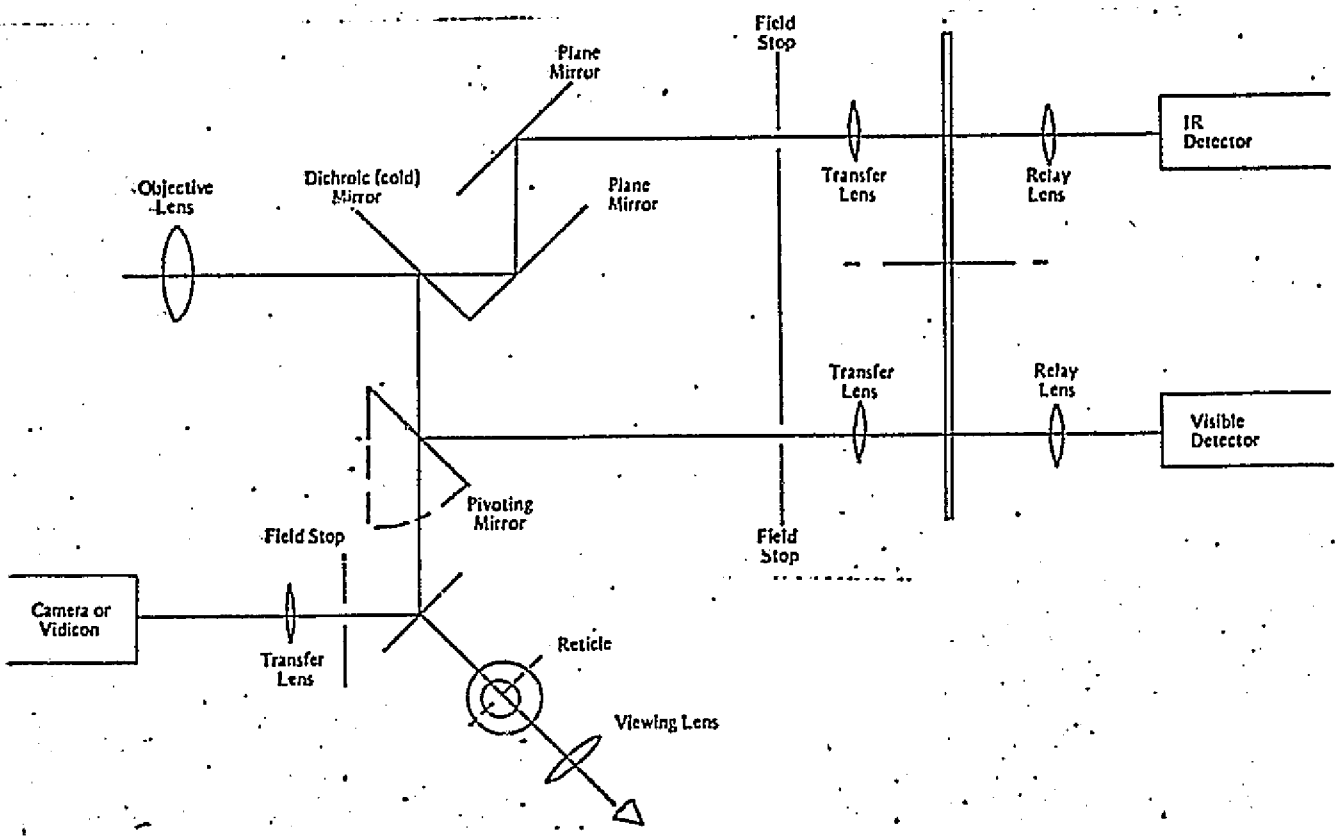

Figure 7. Telespectroradiometer optical schematic.

angular orientation is achieved.

The electrical signals generated by the detector(s) are amplified by a picoammeter amplifier with remote gain-ranging controlled by the computer program. The high-level, low-impedance analog output of the amplifier may be transmitted up to a distance of 250 feet to the computer, allowing completely remote operation. Also located in the optics package are the shutter and viewing mirror solenoids, optical encoder buffer amplifiers, and line drivers.

The picoammeter is a two-stage, solid-state amplifier using compact metal-film feedback resistors and solid-state switching for range selection. The program-controlled or manually-controlled shutter allows dark current measurement and corrections to be made under program control

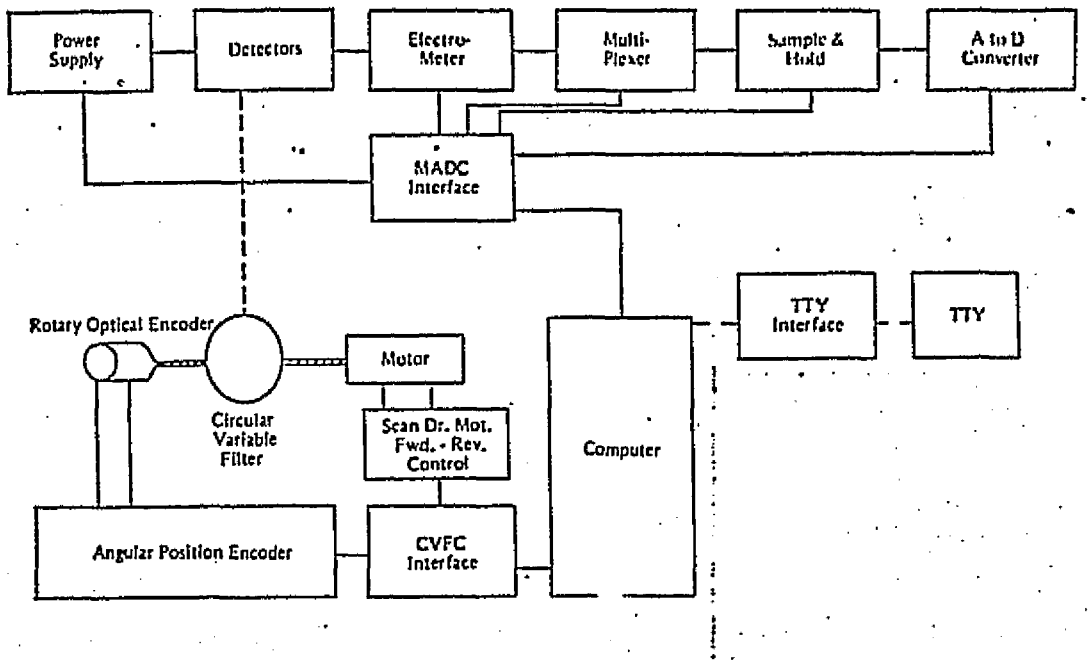

Figure 8. Telespectroradiometer electronics block diagram.

without operator intervention. A block diagram of the electronic circuitry is given in Figure 8.

The analog signal from the optical detector is fed to the analog multiplexer of the analog-to-digital input channel. The multiplexer selects the picoammeter output for conversion or other accessory functions, such as internal self-check functions. The multiplexer output drives the sample-and-hold and the eleven-bit analog-to-digital converter. The multiplexer, sample-and-hold and analog-to-digital converter are controlled by the MADC interface which also contains the picoammeter gain control registers, shutter and viewing mirror solenoid buffer registers.

The encoder outputs drive the decoder nodule which, in turn, drives the present position register in the CVFC interface. The present position register supplies the computer program with the current angular rotational position of the circular interference filter. The CVFC interface contains

auxiliary buffer registers for operating the motor drives and synchronization control modules.

Copper Creek Reflectance Measurements

The spectral reflectance measurements obtained at the Copper Creek test site during 1971 were reanalyzed using newly developed computer programs for computing relative percent reflectance differences. The reflectance spectra of trees growing in the "core zone" of copper mineralization were compared to trees growing in "background" areas having normal soil mineralization.

The average of spectral reflectance measurements of eight Ponderosa Pine are shown in Figure 9a. These trees grow in soil having an average mineralization of 76 ppm. The eight trees sampled had a copper content of 145 ppm in the dry ashed sample.. The reflectance spectra of areas of intermediate mineralization and the core zone are also shown in Figure 9. The average surface soil copper content in the core zone was 456 ppm, while ashed samples of Ponderosa Pine contained an average of 569 ppm copper.

The average reflectance spectra of these trees have been compiled in Appendix . These reflectance spectra were used to compute the relative percent reflectance of Ponderosa Pine growing in the intermediate and anomalous areas of soil mineralization as follows:

$$R_r = \frac{R_a - R_b}{R_a} \times 100$$

where R_r = relative reflectance ratio (percent)

R_b = the percent directional spectral reflectance of "background" group of trees

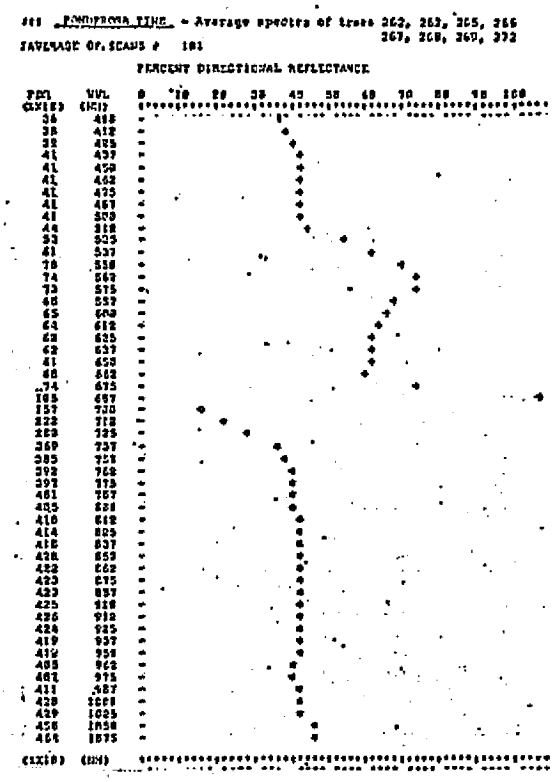

9a. Background Mineralization
Soil: 76 ppm cu

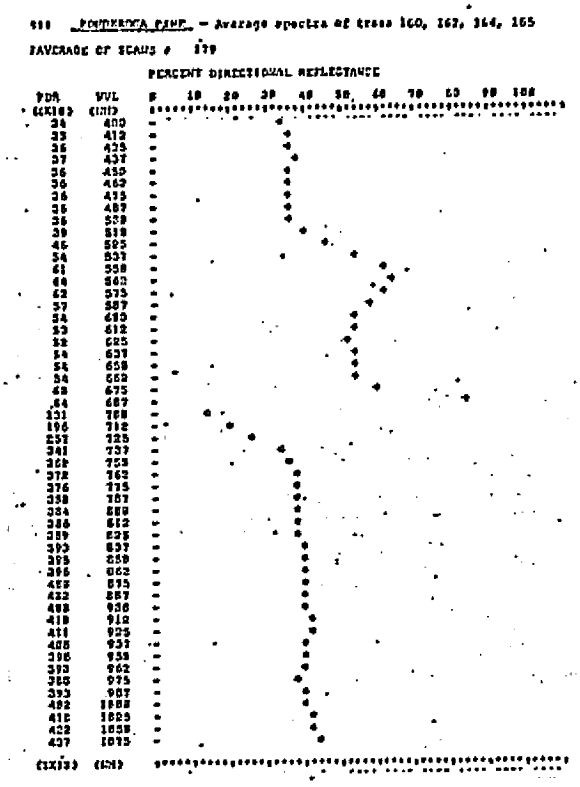

9b. Intermediate Mineralization
Soil: 376 ppm cu

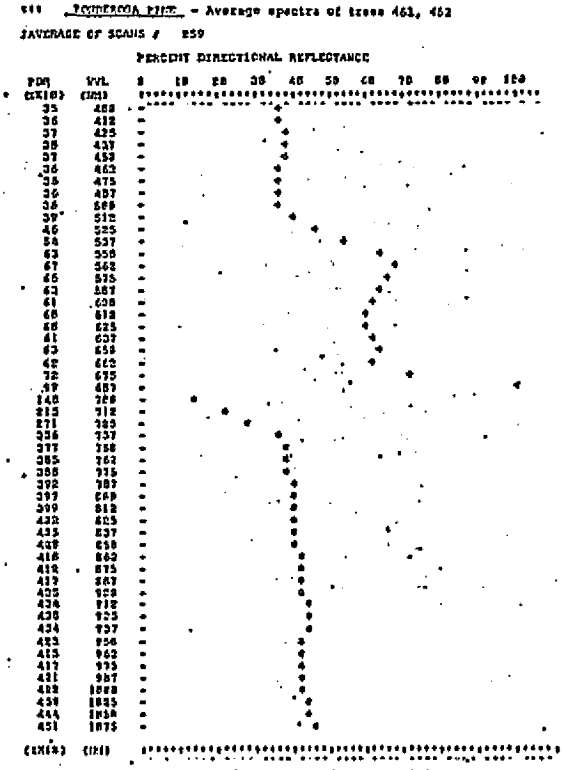

9c. Intermediate Mineralization
Soil: 407 ppm cu

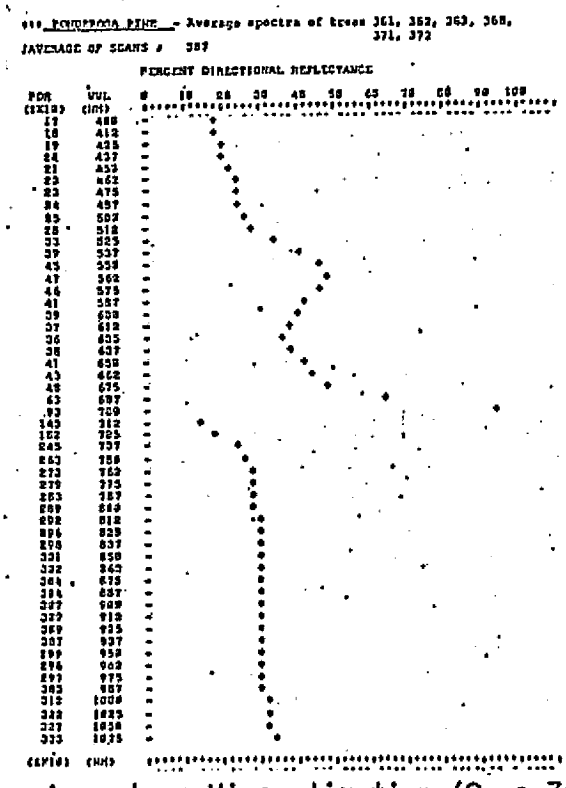

9d. Anoamlous Mineralization (Core Zone)
Soil: 456 ppm cu

Figure 9. Reflectance spectra of Ponderosa Pine at the Copper Creek test site. Pines growing in soil with copper concentration have reduced reflectance.

S101 RELATIVE REFLECTANCE RATIOS (PERCENT)

BASE SCAN NUMBER IS: 101 Background

SCAN #>	179	259	387
WVL	Inter-mediate	Inter-mediate	Anomalous Core Zone
400	-5.42	-4.00	-54.85
412	-7.04	-5.96	-55.01
425	-7.85	-6.02	-54.18
437	-10.35	-7.07	-52.77
450	-12.56	-9.04	-50.00
462	-12.40	-11.39	-44.30
475	-12.78	-11.52	-43.85
487	-13.39	-12.15	-43.17
500	-12.93	-12.18	-40.04
512	-13.13	-12.21	-38.47
525	-13.17	-12.79	-38.75
537	-12.29	-12.12	-36.87
550	-12.39	-10.20	-36.29
562	-13.04	-9.61	-36.26
575	-14.82	-9.23	-37.76
587	-15.99	-7.47	-39.91
600	-16.58	-5.63	-41.15
612	-17.22	-5.26	-42.10
625	-16.36	-2.64	-42.14
637	-13.22	-.16	-38.67
650	-11.48	+2.32	-33.77
662	-10.86	+3.56	-29.03
675	-19.61	-3.81	-35.42
687	-20.40	-5.38	-40.23
700	-16.65	-5.20	-40.57
712	-11.73	-3.21	-37.24
725	-8.24	-3.08	-34.98
737	-7.45	-3.34	-33.62
750	-5.83	-2.03	-31.80
762	-5.26	-1.89	-30.50
775	-5.30	-2.04	-29.78
787	-5.32	-2.17	-29.40
800	-5.29	-2.10	-28.76
812	-5.84	-2.71	-28.80
825	-6.07	-2.90	-28.62
837	-5.99	-3.06	-28.69
850	-5.84	-2.81	-28.35
862	-6.22	-2.89	-28.53
875	-5.26	-2.51	-28.15
887	-5.04	-1.51	-28.32
900	-3.94	+.16	-27.80
912	-3.64	+2.00	-27.54
925	-3.00	+3.24	-27.24
937	-2.77	+3.58	-26.94
950	-3.38	+2.80	-27.52
962	-3.86	+2.47	-26.97
975	-4.65	+2.43	-27.04
987	-4.34	+2.49	-26.31
1000	-4.32	+.50	-25.74
1025	-4.43	+.02	-25.11
1050	-6.10	-1.13	-27.33
1075	-5.95	-2.95	-28.36

Table 1. The ratio of percent reflectance of Ponderosa Pine growing in soil of normal background mineralization compared to pinos growing in soils of intermediate and anomalous mineralization.

R_a = the percent directional reflectance of the anomalous (or intermediate) group of trees.

The data was computed for each wavelength and is tabulated in Table I. As can be seen, the relative differences in percent reflectance is less for the intermediate areas and least for the anomalous core zones.

Figure 10 below shows the average relfectance spectra of Emory Oak growing in the Copper Creek core zone compared to the background area. The oaks growing in the core zone have less reflectance throughout the spectrum than do background oaks, except in the 512-575 nm spectral band. Oaks growing in the core zone were found to contain an average of 222 ppm copper in the ashed samples, while in the background they contained, on the average, 36 ppm copper in ashed samples.

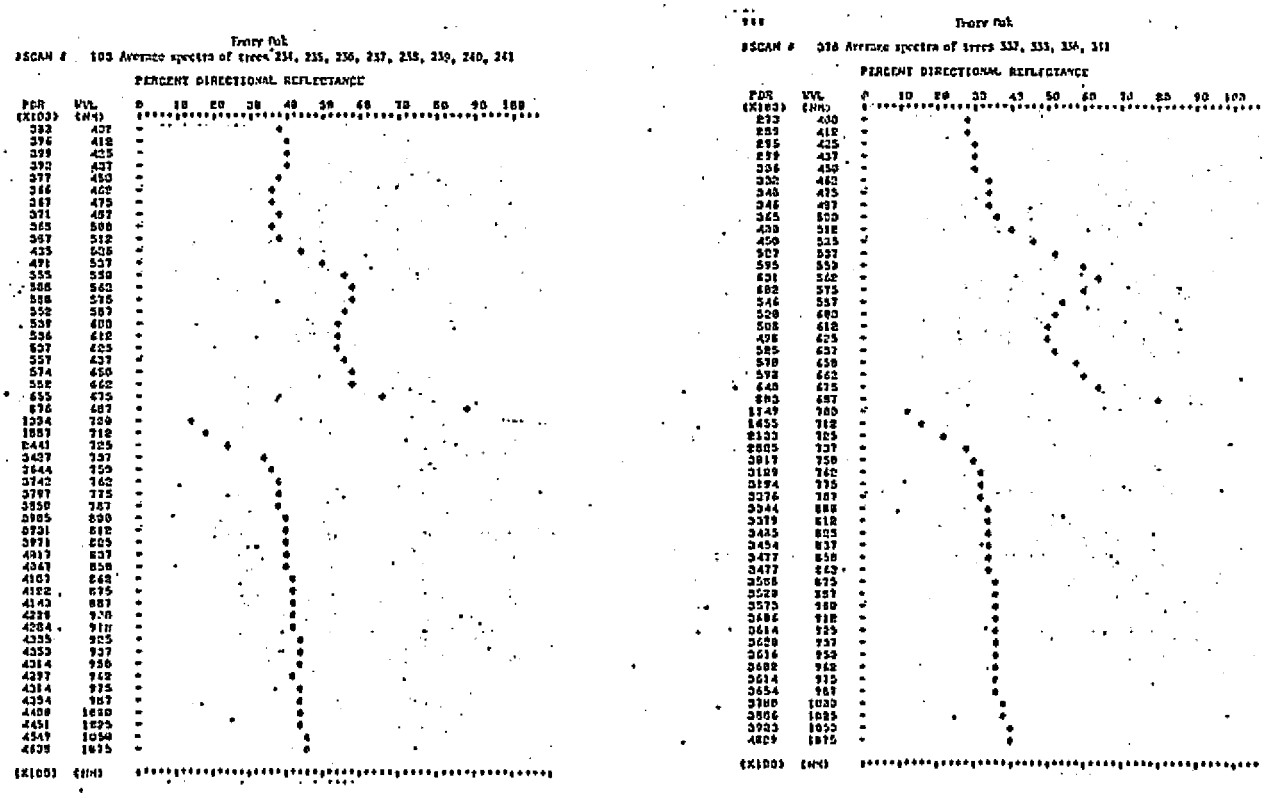

10a. Background

10b. Anomalous

Figure 10. Emory Oak reflectance spectra at the Copper Creek test site. Oaks growing in high copper concentrate soil have reduced spectral reflectance.

The average reflectance spectra of Alligator Bark Juniper growing in background and anomalous core zone areas of Copper Creek are shown in Figure 11 below. Juniper, like pine and oak, have reduced reflectance throughout the spectrum when growing in soil with anomalous copper content.

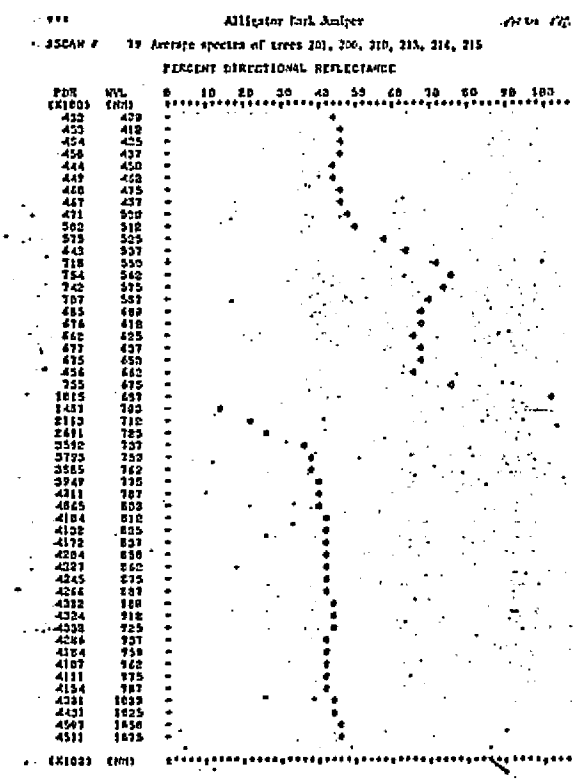

Background (11a)

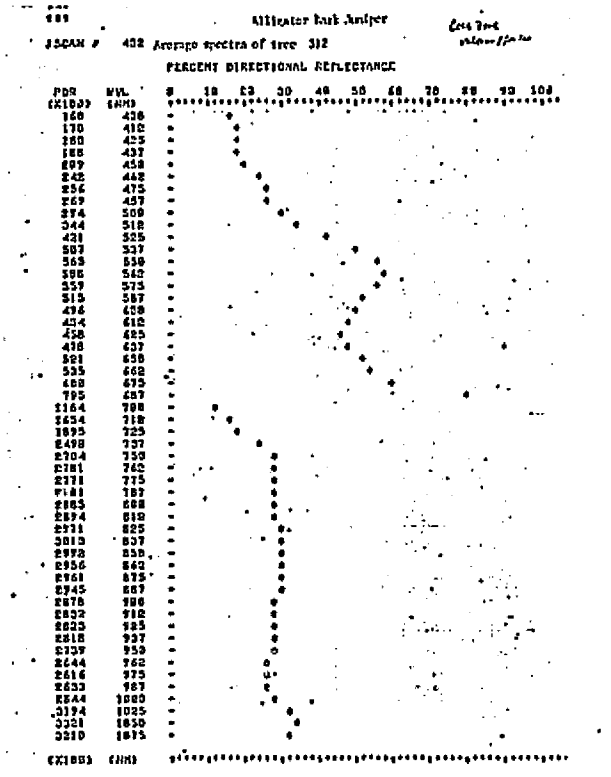

Anomalous (11b)

Figure 11. Alligator Bark Juniper reflectance spectra at the Copper Creek test site. Junipers growing in soils with high copper content have reduced spectral reflectance.

The relationship between the average copper content of soil samples and the average copper content of ashed samples of Ponderosa Pine, Emory Oak,

Alligator Bark Juniper in the background, intermediate, and core zone are shown in the graph below.

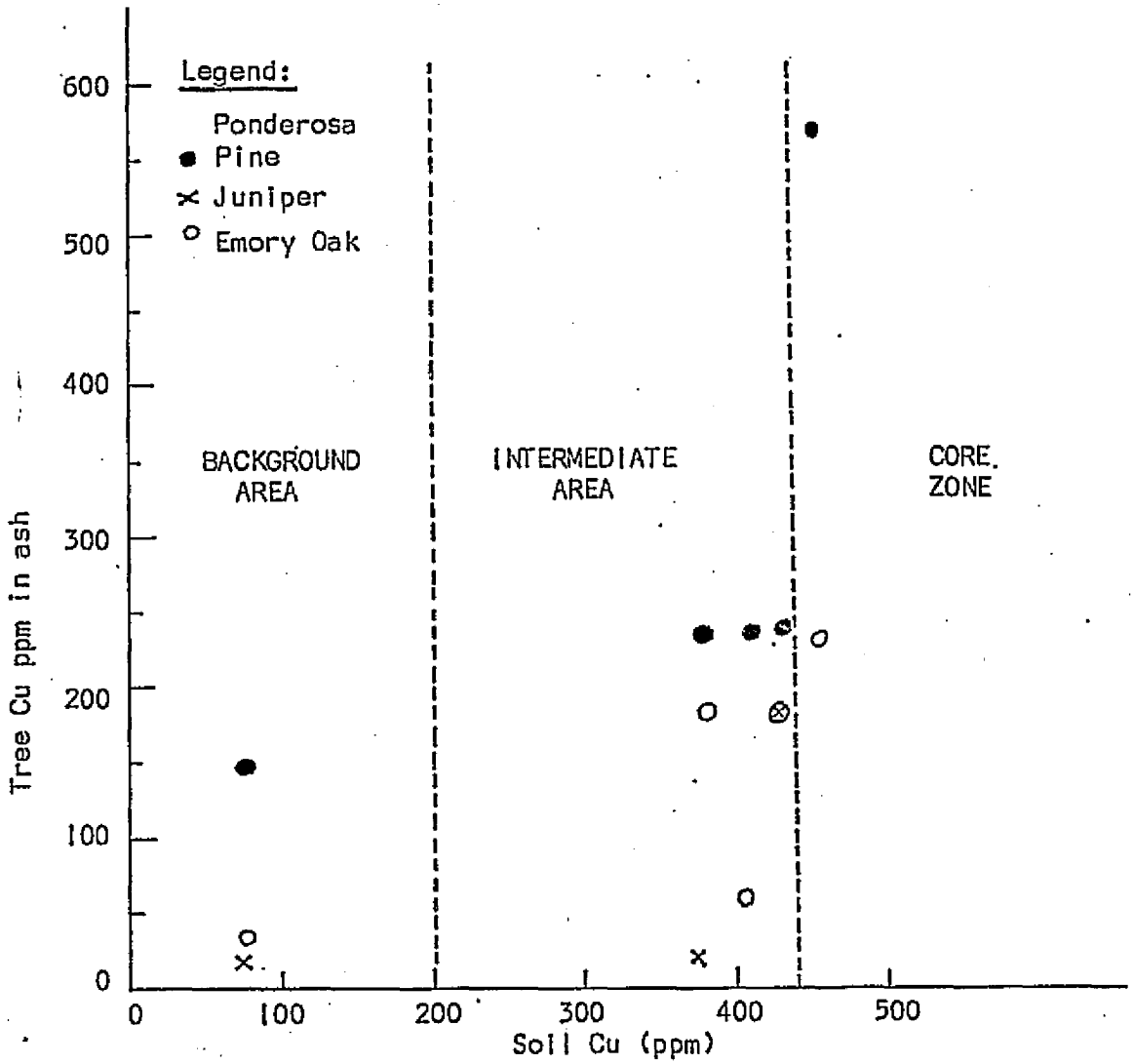

Figure 12. Average copper content of ashed samples of three trees compared to the average copper content of soil in which they grow; Copper Creek, Prescott National Forest, Arizona.

Spectral reflectance measurements of Manzanita growing in Copper Basin were made in background and anomalous areas of the basin. Manzanita growing in the background area contained an average of 100 ppm copper and 4 ppm molybdenum in the ashed samples, whereas Manzanita growing in the area of anomalous soil mineralization contained an average of 2520 ppm copper and 106 ppm molybdenum in the ashed samples. These reflectance spectra are shown in Figure 13 below. The percent relative directional reflectance was computed and is shown in Table 2 from which it can be seen that Manzanita with background copper content exhibits reduced spectral reflectance compared to that containing anomalous amounts of copper and molybdenum. It should be noted that these data are measured from two samples of Manzanita growing in each area.

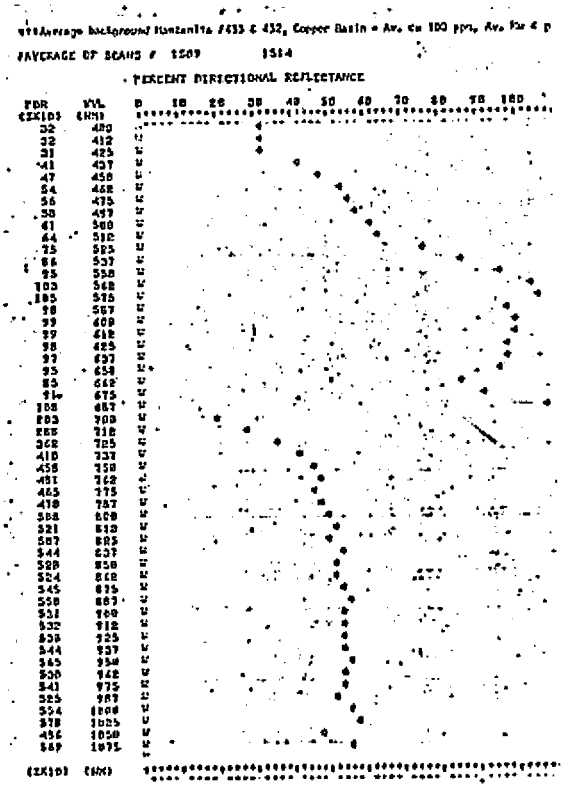

13a. Background

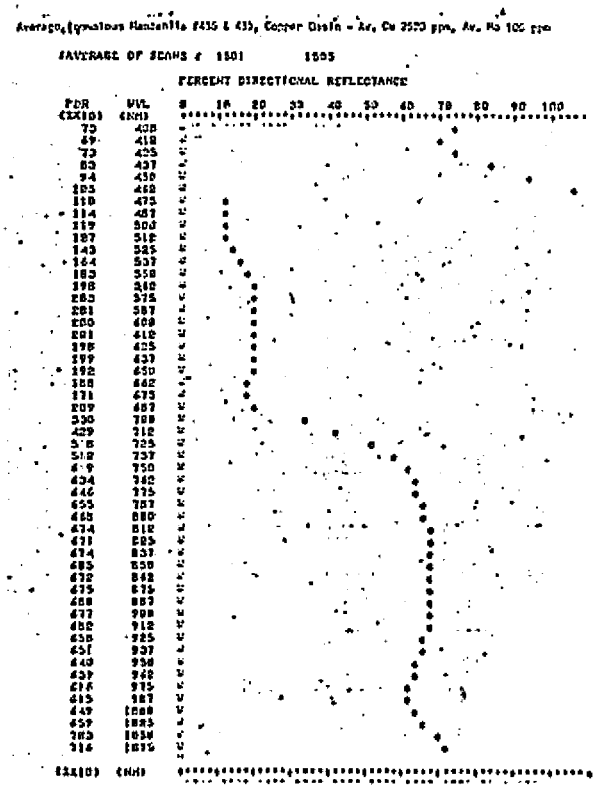

13b. Anomalous

Figure 13. Reflectance spectra of Manzanita growing in background and anomalous areas of Copper Basin, Arizona.

S1501 RELATIVE REFLECTANCE RATIOS (PERCENT)

BASE SCAN NUMBER IS: 1501 Anomalous Manzanita, Copper Basin

SCAN #> 1509 Background Manzanita, Copper Basin

WVL	
400	-56.16
412	-53.62
425	-57.53
437	-50.60
450	-50.00
462	-48.57
475	-49.09
487	-49.12
500	-48.73
512	-49.60
525	-47.55
537	-47.56
550	-48.08
562	-47.97
575	-48.27
587	-51.24
600	-50.50
612	-50.74
625	-50.50
637	-51.25
650	-50.52
662	-54.78
675	-46.78
687	-48.32
700	-38.48
712	-32.86
725	-30.11
737	-29.55
750	-26.00
762	-24.13
775	-28.01
787	-28.24
800	-25.14
812	-22.70
825	-24.44
837	-19.28
850	-24.08
862	-22.02
875	-19.25
887	-19.11
900	-21.56
912	-21.99
925	-18.46
937	-16.43
950	-11.71
962	-17.05
975	-12.17
987	-14.63
1000	-14.63
1025	-12.29
1050	-30.86
1075	-20.53

Table 2. The ratio of relative percent reflectance of background Manzanita compared to Manzanita containing anomalous amounts of copper. Background Manzanita exhibits reduced spectral reflectance.

The reflectance spectra of fifteen Pinion Pine growing in areas of background and anomalous soil mineralization were measured and are shown in Appendix H. The reflectance spectra of an average of four background Pinion Pine and one anomalous Pine is shown in Figure 14. The ratio of relative percent directional reflectance of the average background reflectance spectra of these four trees compared to four Pinion Pine growing in anomalous soil was computed and is shown in Table 3. The infrared reflectance of anomalous Pinion Pine is greater in all anomalous Pinion Pine measured than in background, while the visible reflectance exhibits no clear pattern of reflectance.

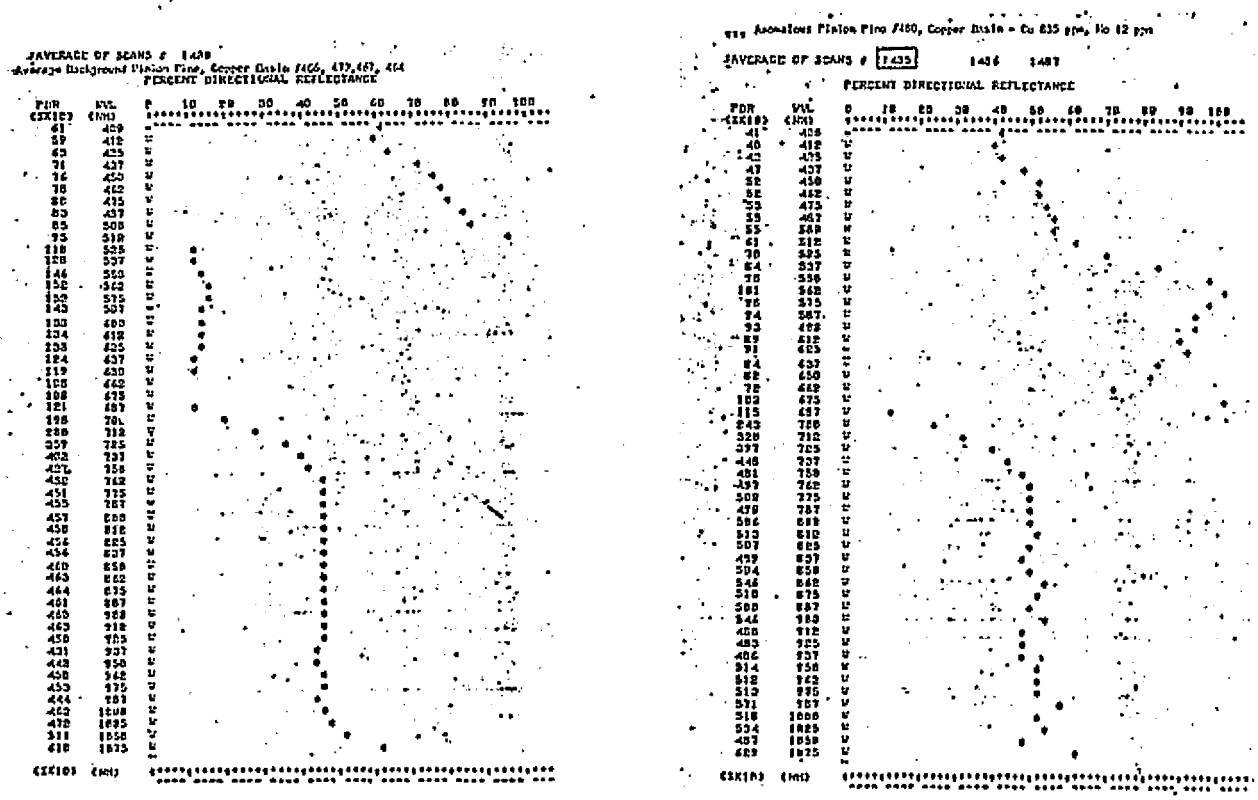

14a. Background

Anomalous 14b.

Figure 14. Percent directional reflectance of Pinion Pine growing in areas of Copper Basin, Arizona containing background and anomalous soil mineralization.

S1400 RELATIVE REFLECTANCE RATIOS (PERCENT)

BASE SCAN NUMBER IS: 1400 Average Background Pinion Pine

SCAN #>	1473	1485	1489	1493
WVL	Anomalous Pine-485	Anomalous Pine-480	Anomalous Pine-482	Anomalous Pine-487
400	+13.33	-31.66	+38.33	-51.66
412	+10.34	-31.03	+34.48	-46.55
425	+11.29	-32.25	+33.87	-46.77
437	+17.14	-32.85	+38.57	-44.28
450	+20.00	-30.66	+38.66	-42.66
462	+20.77	-32.46	+41.55	-40.25
475	+22.78	-32.91	+43.03	-39.24
487	+20.73	-32.92	+39.02	-39.02
500	+23.80	-34.52	+44.04	-38.09
512	+20.21	-35.10	+40.42	-39.36
525	+20.18	-35.77	+40.36	-37.61
537	+25.19	-33.85	+36.22	-37.79
550	+22.06	-32.41	+33.79	-39.31
562	+23.84	-33.11	+31.78	-38.41
575	+23.17	-35.09	+32.45	-39.07
587	+23.94	-33.80	+35.21	-36.61
600	+20.43	-32.11	+33.57	-37.22
612	+20.30	-33.08	+34.58	-36.09
625	+19.37	-29.45	+33.33	-34.88
637	+17.88	-31.70	+28.45	-34.95
650	+18.64	-30.50	+32.20	-33.89
662	+17.75	-32.71	+30.84	-31.77
675	+45.79	-4.67	+32.71	-7.47
687	+40.83	-4.16	+29.16	+1.66
700	+50.76	+23.35	+34.01	+36.54
712	+39.78	+14.69	+32.25	+40.86
725	+34.35	+10.89	+31.00	+41.06
737	+30.92	+11.72	+28.42	+45.63
750	+28.87	+12.91	+27.93	+45.30
762	+30.37	+10.19	+27.49	+45.67
775	+32.88	+11.55	+23.77	+50.88
787	+34.80	+7.92	+28.63	+47.35
800	+31.57	+10.96	+26.31	+45.61
812	+34.13	+12.25	+28.88	+47.26
825	+38.90	+11.42	+29.23	+49.45
837	+35.16	+7.47	+31.42	+48.35
850	+37.90	+9.80	+28.75	+47.71
862	+35.93	+18.18	+27.92	+50.64
875	+31.10	+10.15	+26.56	+50.32
887	+32.17	+8.69	+32.17	+51.30
900	+33.11	+18.95	+26.36	+45.96
912	+31.16	+5.62	+29.22	+46.96
925	+35.85	+7.57	+26.50	+45.21
937	+30.23	+13.02	+21.86	+44.18
950	+29.93	+16.55	+21.76	+48.07
962	+33.91	+12.03	+28.88	+39.60
975	+32.07	+13.49	+15.92	+39.60
987	+35.66	+28.89	+16.70	+40.18
1000	+32.32	+12.36	+25.16	+36.22
1025	+33.12	+13.37	+40.76	+35.88
1050	+32.74	-4.50	+40.78	+29.01
1075	+1.31	+3.28	+13.30	+28.73

Table 3. The ratio of percent reflectance of four Pinion Pine with anomalous copper and molybdenum content compared to Pinion Pine containing background amounts of these metals.

The homogeniety of the reflectance measurements of individual trees was examined by computing the ratios of relative percent directional reflectance for four anomalous and four background Pinion Pine trees. These ratios are shown in Figure 15. Should the trees in each group have a homogeneous spectral reflectance, the data shown in Figure 15 should be zero. The magnitude of these ratios shows the vast lack of homogeniety in the reflectance of Pinion Pine, independent of mineralization.

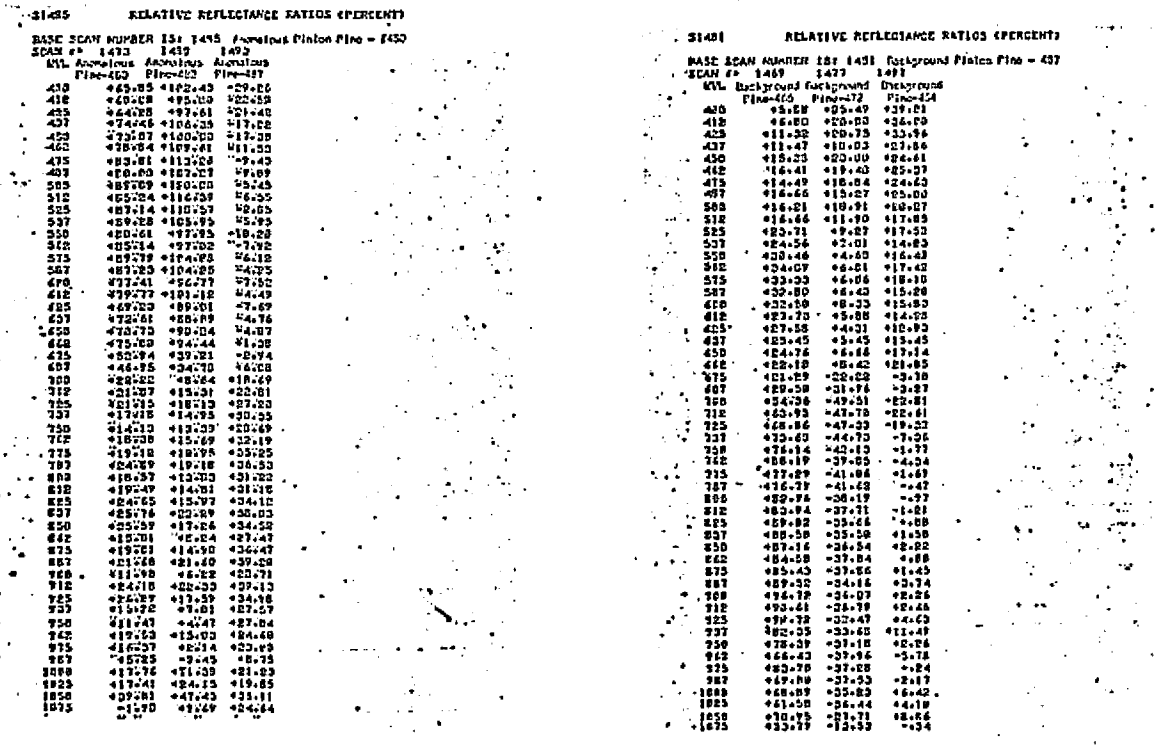

15a. Anomalous

Background 15b.

Figure 15. The ratios of percent reflectance of individual Pinion Pine trees growing in the anomalous and background areas of Copper Basin, Arizona.

Section 4

MUSTISPECTRAL PHOTOGRAPHY

Three multispectral photographic flights were made over the Copper Creek and Copper Basin test areas. These flights were performed on 30 and 31 October 1972 and on 1 November 1972. The weather varied from scattered clouds to clear.

Multispectral Photographic Equipment

The Spectral Data Model 10 multispectral camera system shown in Figure 16was used to obtain the imagery. The camera body contains a four slit focal plane shutter assembly with a spectral filter in front

Figure 16. Spectral Data Model 10 multispectral camera system.

of each lens. Each lens can be focused for the wavelength transmitted by the particular filter used in order to achieve maximum image resolution. The camera also incorporates image motion compensation and data annotation feature.

Based upon an analysis of the reflectance spectra taken in 1971, six (6) sets of four multispectral filters were flown on the first flight. The purpose of this test was to empirically determine the four filters which produced the best image contrast between ammalous and background trees. These six filter sets had been selected using the relative log reflectance difference spectra discussed in the preceeding chapter.

The optical characteristics of these filter sets is tabularized below:

Table 4. Test multispectral filter sets.

Test Filter Set Number	Peak Transmission (nm)	Half Peak Bandpass (nm)
T1	440	406-480
	520	505-558
	620	585-680
	848	810-855
T2	440	406-480
	625	600-650
	675	650-700
	848	810-855
T3	440	406-480
	625	600-650
	675	650-700
	525	495-555
T4	445	425-465
	725	700-750
	683	647-699
	525	495-555
T5	450	400-500
	515	495-535
	625	600-650
	825	800-850
T6	440	406-480
	683	685-710
	625	600-700
	723	712-745

Based on a visual analysis of the resultant multispectral imagery, two prime sets were chosen for use as follows:

Prime Filter Set Number	Peak Transmission (nm)	Half Peak Bandpass (nm)
P1	445	425-465
	625	600-650
	675	650-700
	825	800-850
P2	440	406-480
	520	505-558
	620	585-680
	848	810-855

Table 5. Prime sets of multispectral filters.

Standard Kodak 2424 black-and-white film was used in the camera. The multispectral photography was processed in a Kodak Versamat II-C continuous film processor using Hunt's (Type A) chemistry. Control was maintained by use of an EG&G Mark IV sensitometer in order to obtain the desired processing characteristics. The characteristic curves (density vs. exposure for white light) for these flights are shown in Figure 17.

Positive transparencies with balanced exposure in all four spectral bands were made on EK2424 duplicating film using a Spectral Data Model 41 optical projection printer. This printer contains four lamps, the intensity of which can be controlled independently, thereby allowing a considerable amount of compensation for residual exposure errors which may exist between the four multispectral negative images acquired by the airborne camera. Such differential exposure errors can result from changes in the distribution of the solar illuminant, atmospheric haze, and changes in the reflectance of vegetation, soil and rocks between the condition which existed when the aperatures of the camera lenses (with filters attached)

were calibrated and the conditions which existed when the airborne multispectral photography was obtained. Figure 18 shows the optical projection printer.

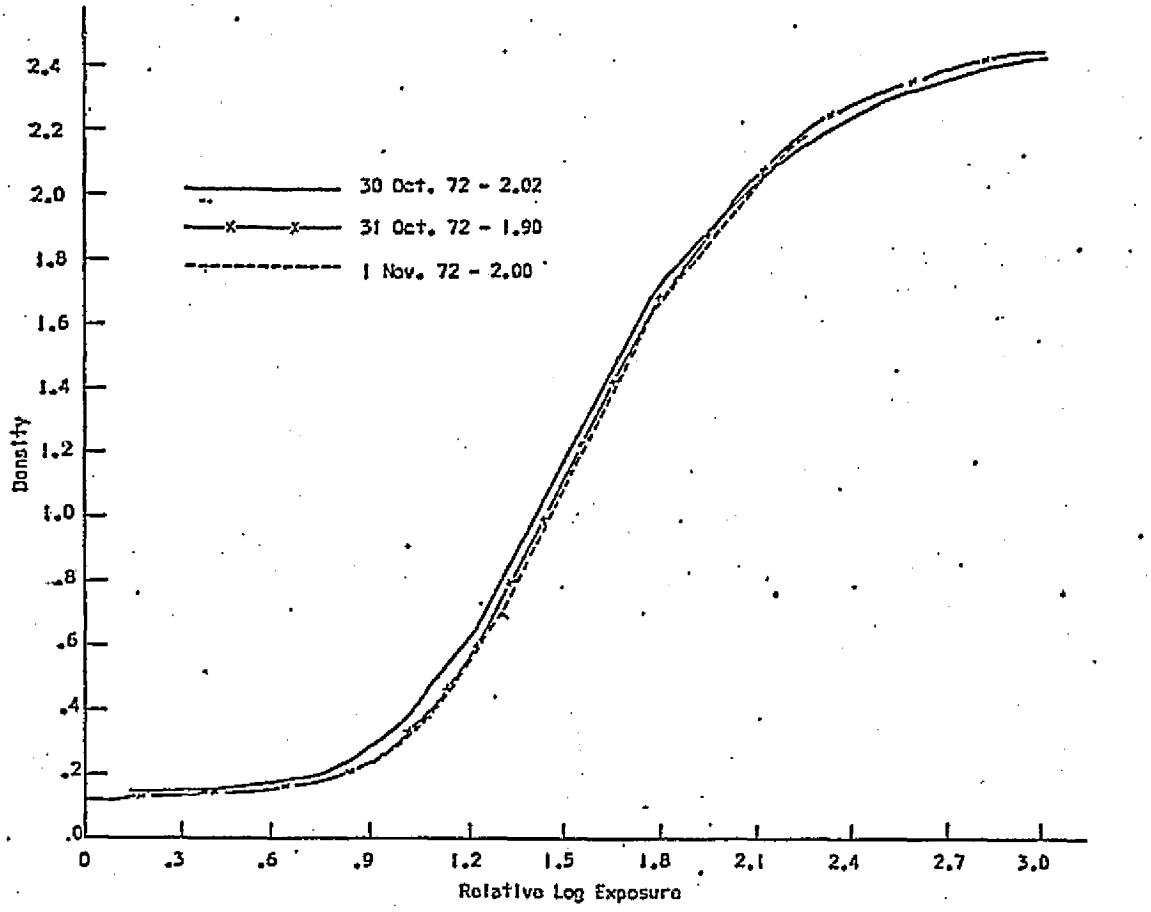

Figure 17. Processing characteristic curves for the multispectral camera black-and-white negatives.

The multispectral viewer shown in Figure 19 was used to recombine the black-and-white multispectral images in additive color. This viewer contains four seperate optical projection systems, one for each of the four black-and-white multispectral images. These projection optics each contain a long focal length scale correction lens in addition to the primary projection lens. The four illumination systems (one for each projection lens) contain sets of blue, green and red filters. The imagery can also be viewed in black-and-white without filters. The resolution

Figure 18. Spectral Data Model 41 Optical Projection Printer.

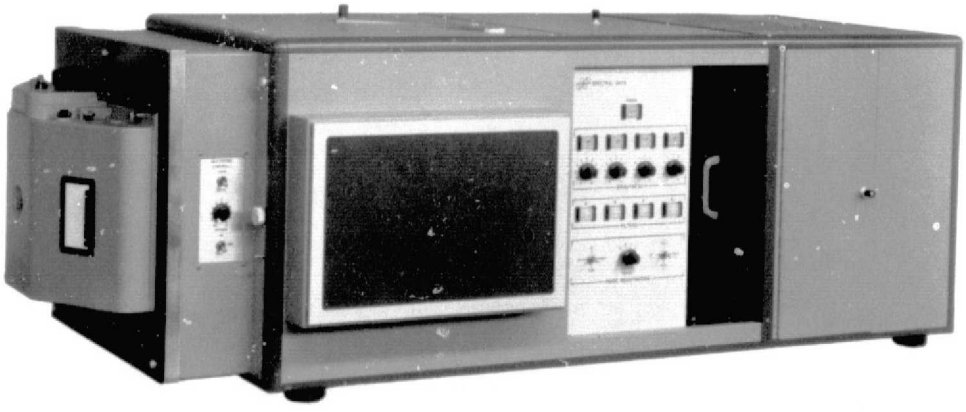

Figure 19. Spectral Data Model 76 Additive Color Viewer.

accuracy on the screen is such that a composite resolution of twenty-five lines per multimeter at four times enlargement of the photo scale is produced. The additive color photographs shown in the subsequent sections of this report were produced by photographing the multispectral viewer screen using Ektacolor film.

Mission logs for all flights are shown in Appendix J. The average flight altitude was between 3500 feet and 4000 feet above terrain. Representative samples of the imagery acquired are shown in Figures 20 and 21. Figure 20 shows four black-and-white multispectral images of the core zone acquired using filter set P2 (see Table 5). Figure 21 shows images of the intermediate areas. Both images were taken within ten seconds of each other on 1 November 1972 at 1330 PST.

406-480 nm Band

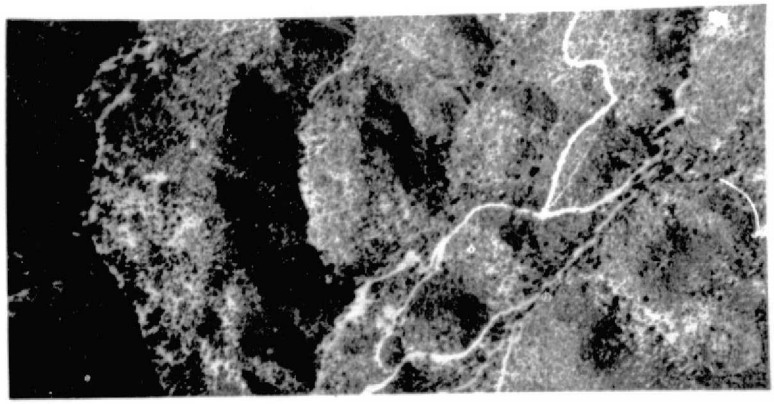

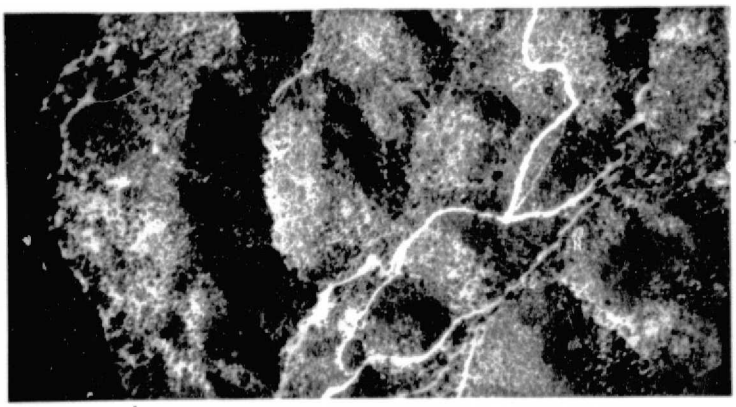

505-558 nm Band

585-680 nm Band

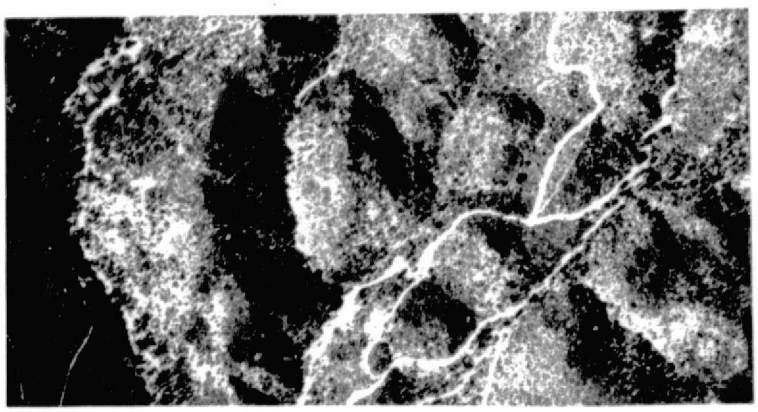

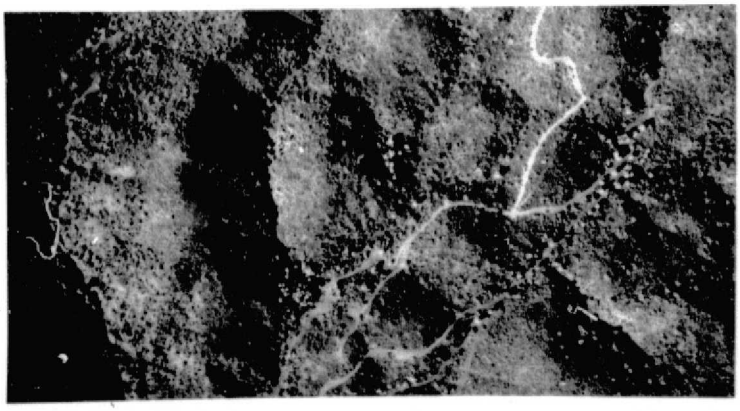

810-855 nm Band

Figure 20. Multispectral photographs of the Copper Creek core zone of anomalous mineralization taken 1 November 1972 at 1330 4,000 feet AGL (9,000 feet ASL).

406-480 nm Band

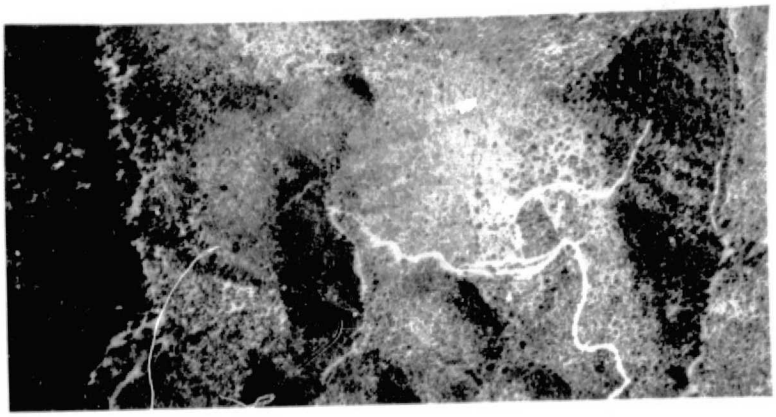

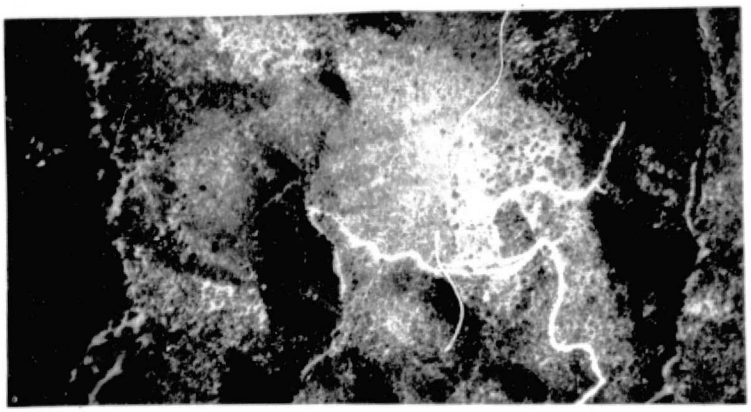

505-558 nm Band

585-680 nm Band

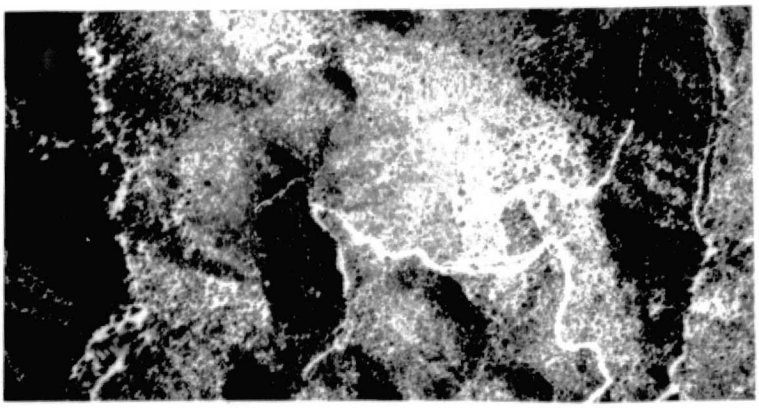

810-855 nm Band

Figure 21. Multispectral photographs of the Copper Creek area of intermediate mineralization taken 1 November 1972 at 1330 4,000 feet AGL (9,000 feet ASL).

Section 5

Analysis of Multispectral Photographic Imagery

In order to locate each tree sampled in the background, intermediate, and anomalous (core zone) areas of both Copper Creek and Copper Basin, uncontrolled mosaics were made of both areas. Figure 23 on the following page is a reproduction of the mosaic of the Copper Creek site. The mosaic of Copper Basin constituted a single flight strip across the basin coinciding with the soil geochemical and geobotanical traverse.

Twenty-six black-and-white 4X enlargements were made of a single band of multispectral photography. These 8 x 16 inch prints covered all the trees sampled in both areas.

Figure 22. Using annotated enlargements.

Figure 23. Uncontrolled mosaic of the Copper Creek site.

Upon these black-and-white prints were annotated every tree, the trace metal content of which had been measured. The accuracy of these annotations was verified by extensive field checking.

The Copper Creek area was selected for detailed image analysis because the terrain was relatively undisturbed by drilling and mining operations.

Biogeochemistry by Species in the Core Zone

In order to determine the tree images that would be best to quantitatively measure, an analysis of both the tree and soil copper content in the core zone was made. Soil copper content was compared with ashed samples of tree copper content growing in close proximity thereto (within 30 feet or less of the point where the soil sample was made). These results, shown in Figure 24, were unspectacular.

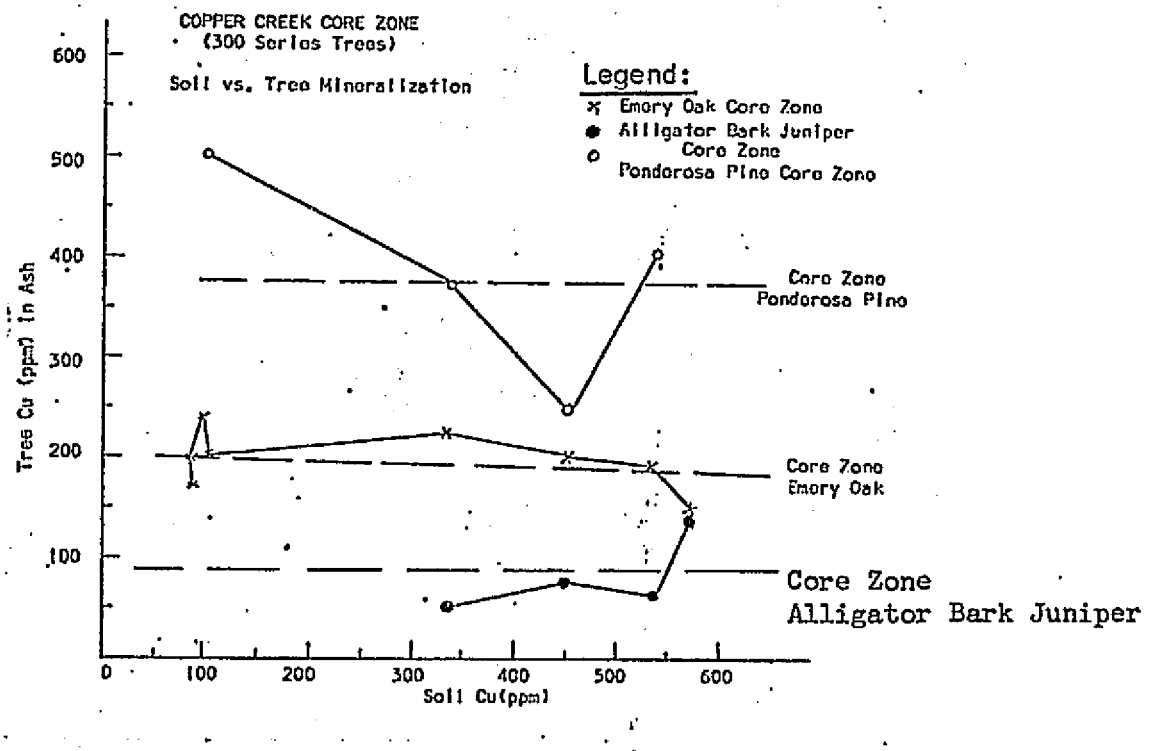

Figure 24. Soil vs. tree mineralization in the anomalous core zone of Copper Creek.

As can be seen from the preceding graph, there appears to be little relationship between copper content of the soil measured about one foot beneath the surface and the copper content of the ashed samples of the trees. It should be noted that the average copper content of Juniper is one quarter that of Ponderosa Pine and Oak one half of Ponderosa Pine.

An analysis was then done of the metal content of the three tree species as a function of the distance from a drill hole in the core zone. The assupption was that the drill hole approximated the sub-surface center of mineralization. As can be seen from Figure 25 below, the results were encouraging.

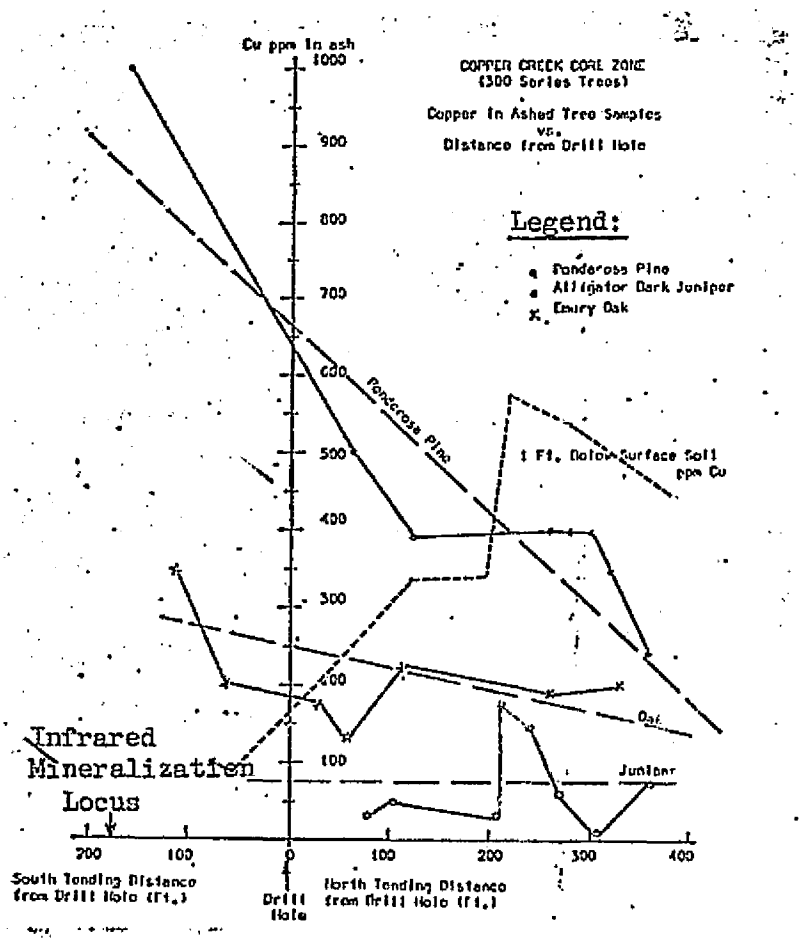

Figure 25. Tree copper content in relation to distance from the core zone drill hole.

Both Ponderosa Pine and Emory Oak showed a definite relationship between the distance from the drill hole and the copper content of their ash. Ponderosa Pine was, by far, the better "indicator" specie, having five times the metal content over the inferred sub-surface mineralization locus as existed 560 feet away from the locus.

Additive Color Multispectral Photography

An extensive analysis was performed of the multispectral imagery using additive color viewing techniques described in Section 4. Figures 26 and 27 show the Copper Creek anomalous core zone. The general location of the trees sampled is shown in the top black-and-white photo. The bottom photo is a color reproduction of the additive color viewer screen in which the 406 to 480 band is imaged as green, the 805 to 855 nm band is imaged as red.

An area of intermediate mineralization in Copper Creek is shown in Figure 28 . Here the general location of the species of the tree samples have been annotated. Figure 29 shows the corresponding additive color viewer image.

Although there appeared to be a slight color difference in the Ponderosa Pine trees in the core zone compared to both the intermediate and background areas of mineralization, the difference was so subtle that it was not noticeable in going from one frame of multispectral imagery to the next.

Quantitative Image Measurement

Density measurements were made of the multispectral images of Ponderosa Pines growing in the anomalous core zone and in the background area of Copper Creek. Seven large well-defined tree crowns were selected in each area. The multispectral imagery was registered on the additive color viewer screen, the specific tree crown identified, and a brightness measurement made of

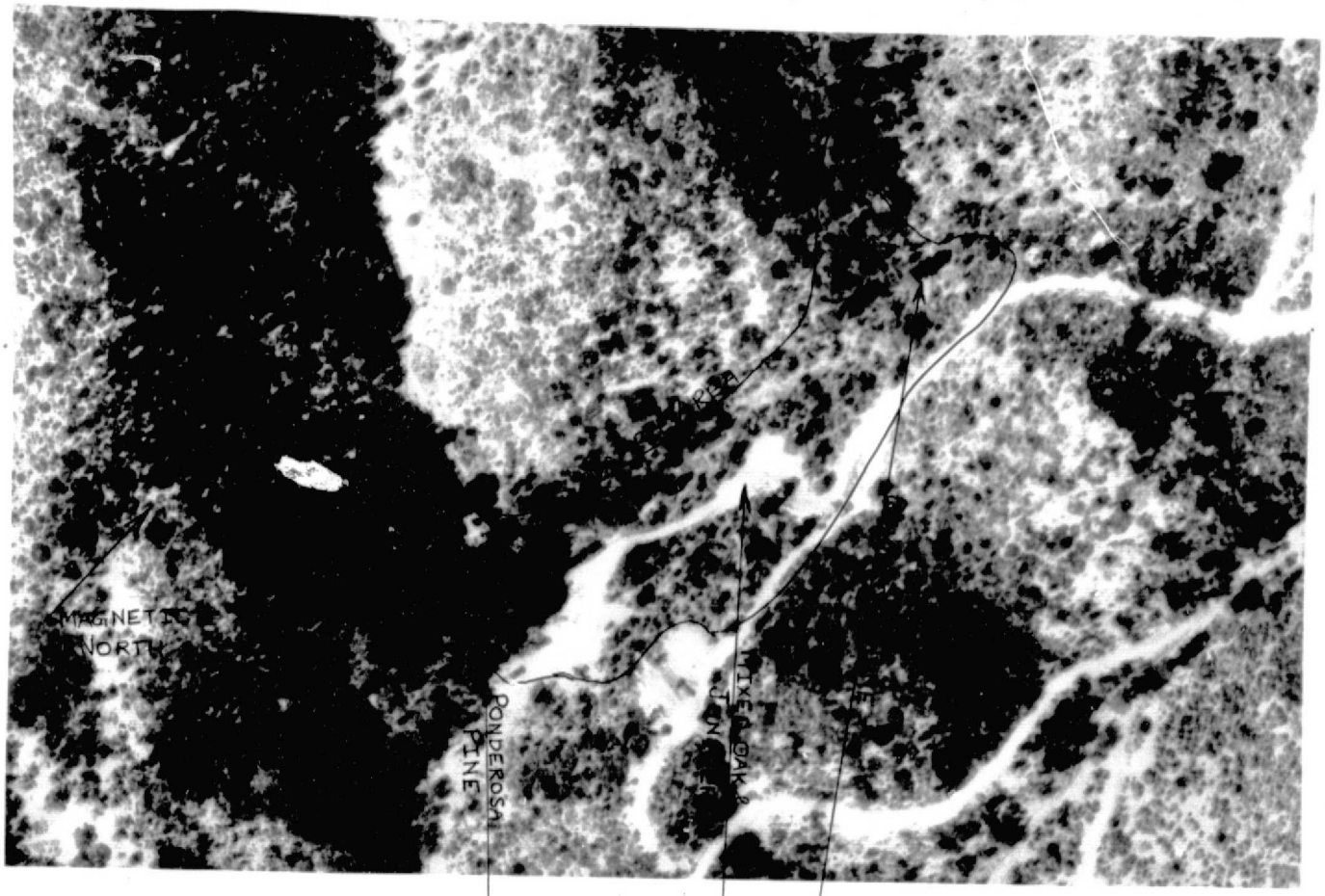

Figure 26. Copper Creek core zone.

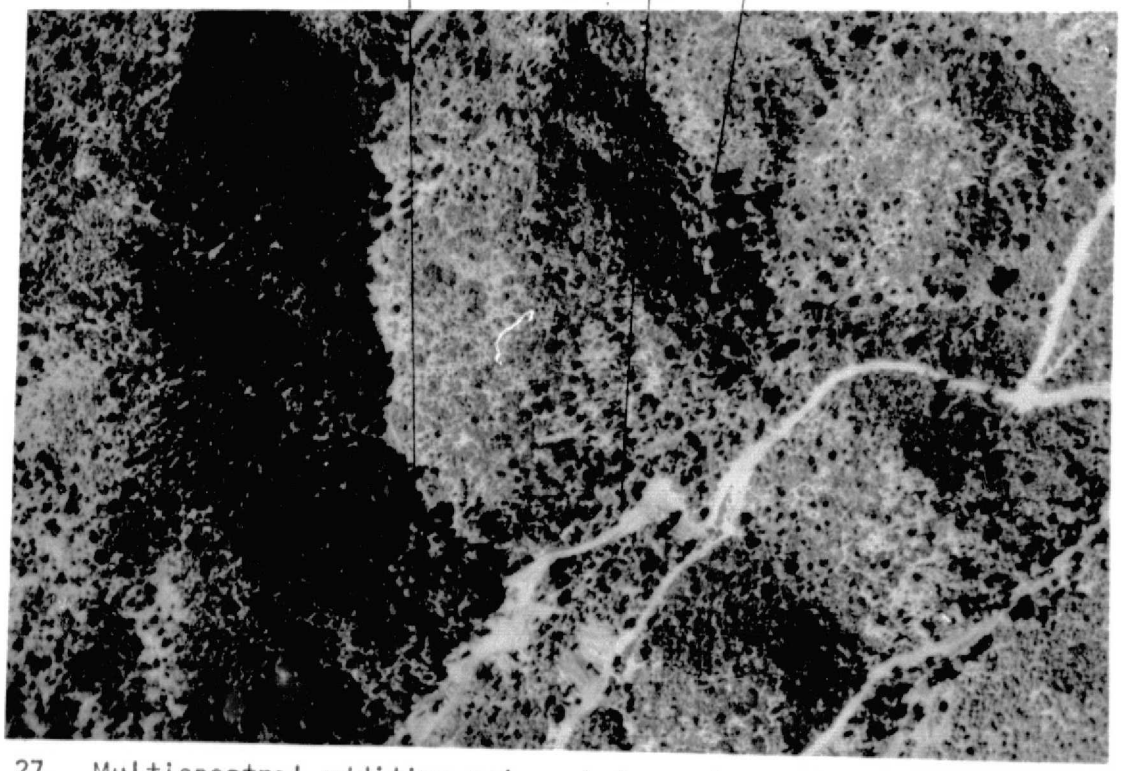

Figure 27. Multispectral additive color photograph of the Copper Creek core zone.

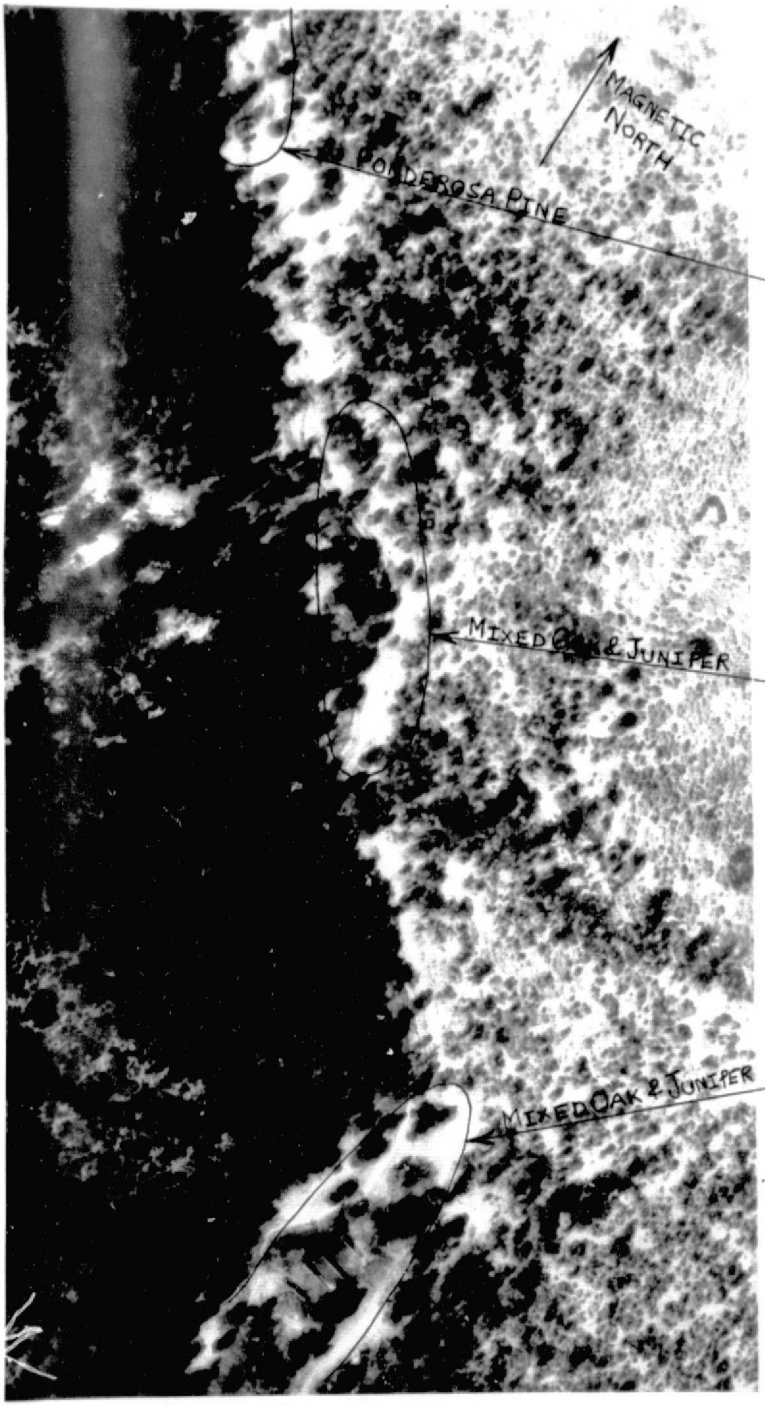

Figure 28. Ground truth - Copper Creek intermediate area of mineralization.

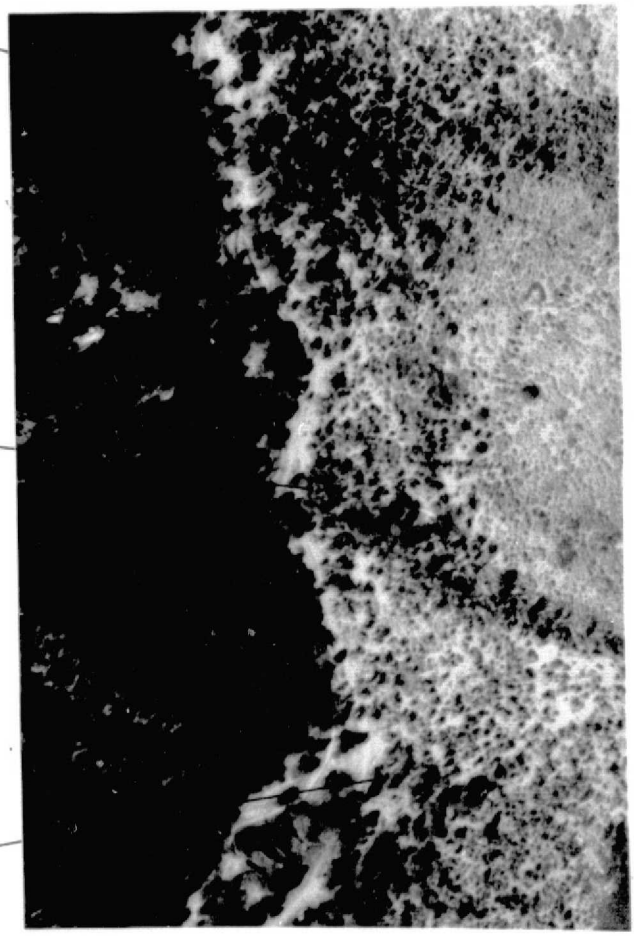

Figure 29. Multispectral additive color photograph of the Copper Creek intermediate mineralization area.

the image was made using a spot brightness meter with high magnification optics. The open gate brightness was also measured. These two measurements were then converted into density of the image. These data are shown in Table 6.

A systematic analysis was made of the density measurements of all 14 trees for each possible pair of multispectral bands shown in Table 6. The results of this analysis are shown in Figures 30, 31, and 32. As can be seen from these figures, the anomalous trees tended to be separated from background trees in only two pairs of multispectral wavelength bands (585-680 nm vs. 406-480 nm and 585-680 nm vs. 505-558 nm). In all other pairs of multispectral wavelength bands, the anomalous and background groups of Ponderosa Pine image densities overlapped.

Using figures 30 and 31, two linear decision rules were established to separate anomalous from background Ponderosa Pine. These were:

Rule #1 (585-680 nm vs. 406-480 nm)

Anomalous → $y > .98 + .66x$

Background → $y < .98 + .66x$

where: x = 585-680 nm band image density

y = 406-480 nm band image density

Rule #2 (585-680 nm vs. 505-558 nm)

Anomalous → $y > .69 + .66x$

Background → $y < .69 + .66x$

where: x = 585-680 nm band image density

y = 505-558 nm band image density

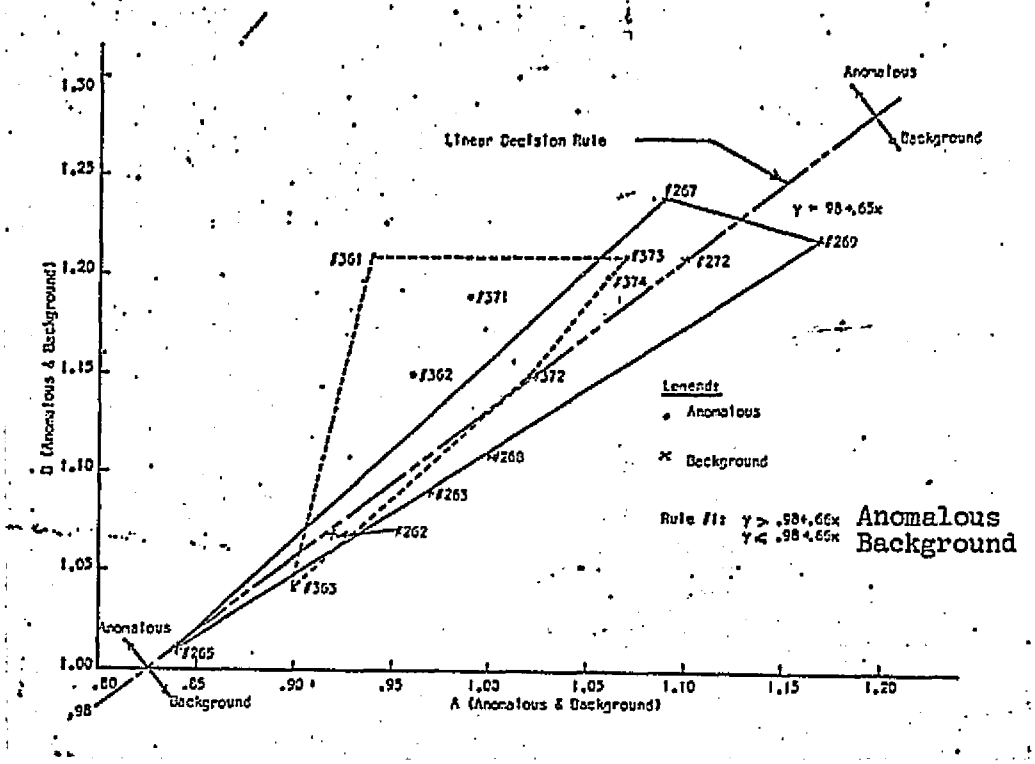

Figure 30. Multispectral image density in 585-680 nm band (A) vs. 406-480 nm band (B) of anomalous and background Ponderosa Pine.

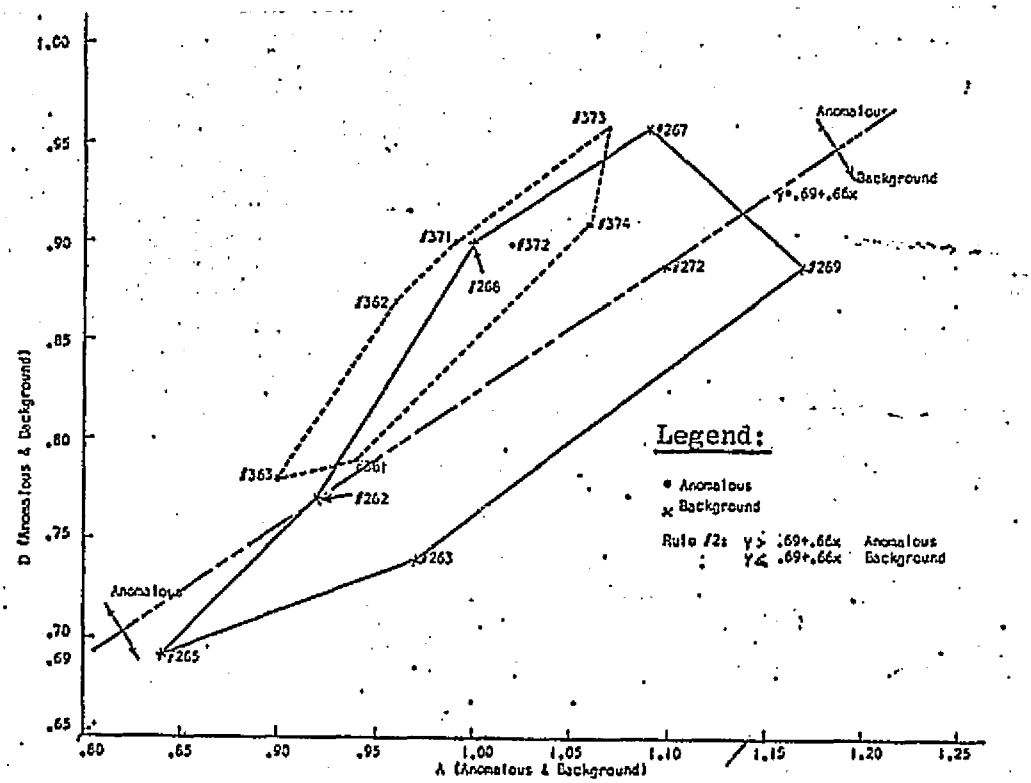

Figure 31. Multispectral image density of anomalous and background Ponderosa Pine in 585-680 nm band (A) vs. 505-558 nm band (D).

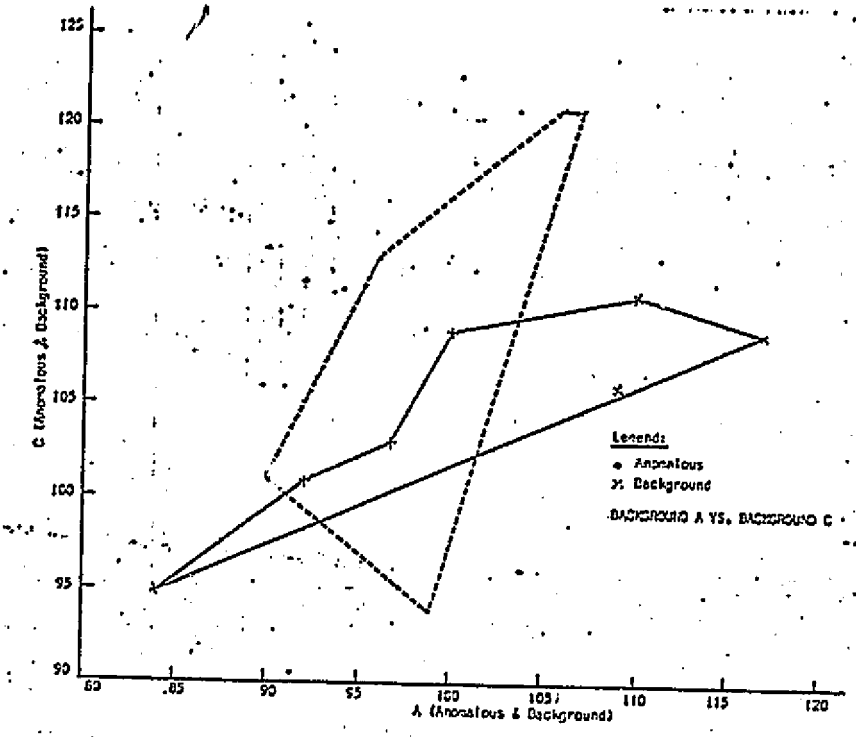

585-640 nm (A) vs. 810-855 nm (C)

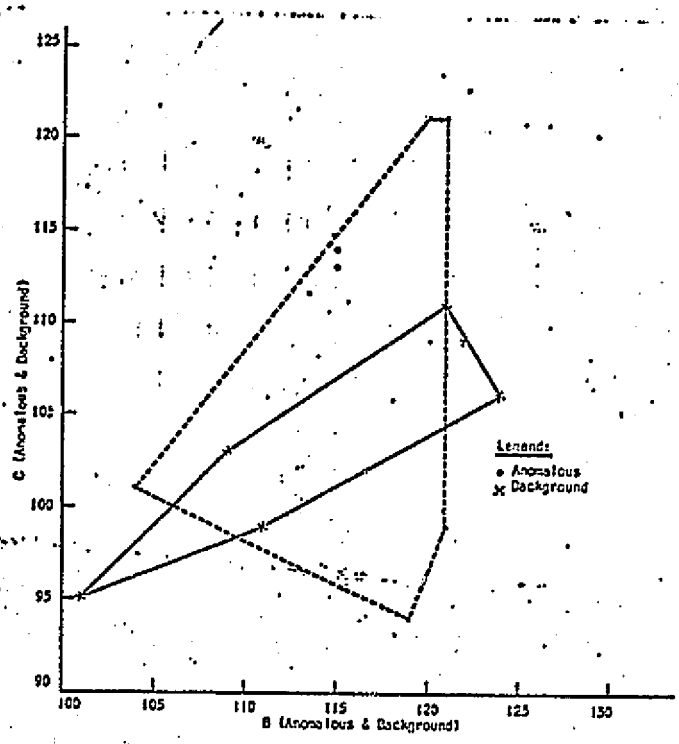

406-480 nm (B) vs. 810-855 nm (C)

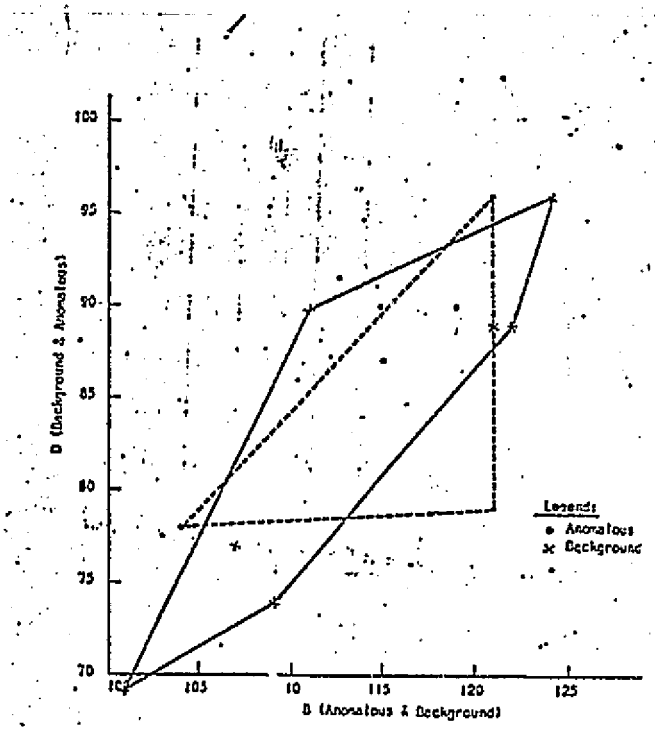

406-480 nm (B) vs. 505-558 nm (D)

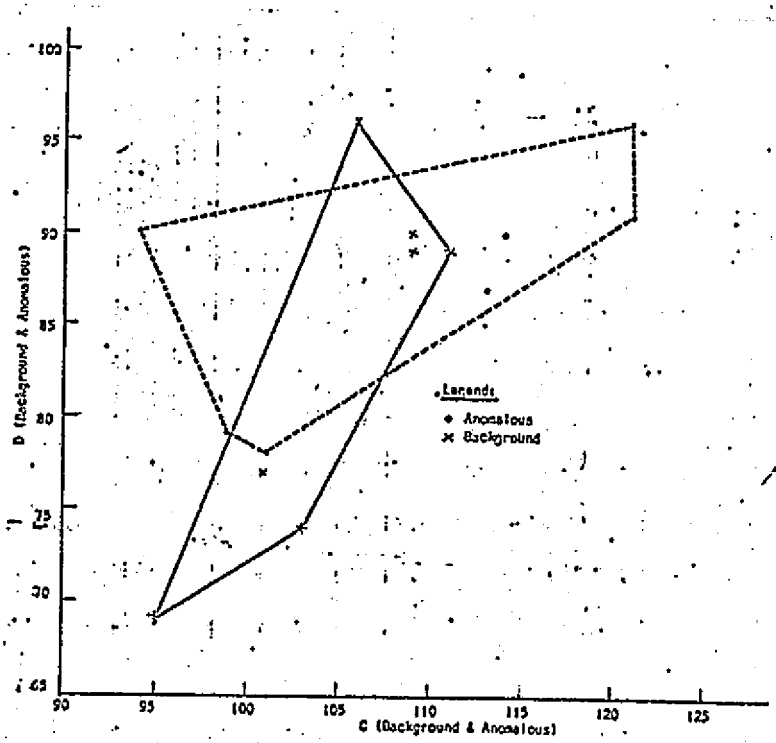

810-855 nm (C) vs. 505-558 nm (D)

Figure 32. Four pairs of multispectral image densities of anomalous and background Ponderosa Pine.

Using these two decision rules, the tree classifications were achieved as shown below by tree number (200 series - background, 300 series - anomalous).

Linear Decision Rule #1

		Actually is	
		Background	Anomalous
Classified as	Background	#262, #263, #265, #268, #269, #272	#363, #372
	Anomalous	#267	#361, #362, #371, #373, #374

Linear Decision Rule #2

		Actually is	
		Background	Anomalous
Classified as	Background	#262, #263, #265, #269, #272	None
	Anomalous	#267, #268	#361, #362, #363, #371, #372, #373, #374

The intersecting background tree classifications using both decision rules #1 and #2 are:

(Background 1 ∧ Background 2) = (#262, #263, #265, #269, #272)

The intersecting anomalous tree classifications using both decision rules #1 and #2 are:

(Anomalous 1 $\wedge$ Anomalous 2) = (#267, #361, #362, #371, #373, #374)

The trees eliminated are:

(#268, #363, #372)

Jointly using the two decision rules,

1. All background trees are correctly classified
2. Five out of six trees classified as anomalous are anomalous
3. Two anomalous and one background tree are eliminated from classification.

Anomalous Tree No.	Cu(ppm)	Density			
		A (Band 3)	B (Band 1)	C (Band 4)	D (Band 2)
363	375	.90	1.04	1.01	.78
362	500	.96	1.15	1.13	.87
361	1,000	.94	1.21	.99	.79
371		.99	1.19	.94	.90
372	Core Zone	1.02	1.15	1.14	.90
373	No Data	1.07	1.21	1.21	.96
374		1.06	1.20	1.21	.91
	Average:	.99	1.17	1.09	.87

Background Tree No.	Cu(ppm)	Density			
		A (Band 3)	B (Band 1)	C (Band 4)	D (Band 2)
272	87	1.10	1.21	1.11	.89
269	125	1.17	1.22	1.09	.89
268	162	1.00	1.11	1.09	.90
267	120	1.09	1.24	1.06	.96
265	237	.84	1.01	.95	.69
263	125	.97	1.09	1.03	.74
262	152	.92	1.07	1.01	.77
	Average:	1.01	1.13	1.05	.83

Table 6. Density measurements of anomalous and background Ponderosa Pine at the Copper Creek site.

Section 6

Conclusions

A computer analysis of the percent relative reflectance differences of Pinion Pine growing in anomalous and background areas of mineralization in the Copper Basin test site showed that the variation in measured spectral reflectance of these trees exceeded the reflectance differences which could be associated with mineralization. This lack of homogeneity in the data may be attributed to either the natural variability in the spectral reflectance of Pinion Pine or to the techniques used to collect the data in 1972.

The same computer analysis of the reflectance spectra of Ponderosa Pine, Alligator Bark Juniper, and Emory Oak (obtained in 1972) in the Copper Creek test site confirmed that all three of these species growing in areas of anomalous mineralization have reduced spectral reflectance.

A visual comparison of multispectral photography obtained using six different filter sets showed that the best filters to use for detecting biogeochemical differences was the following prime filter set:

406-480 nm

505-558 nm

585-680 nm

810-855 nm

Complete coverage of both test sites was obtained using this filter set.

At the Copper Creek test site, a graphical analysis of the mineral content of ashed samples of Ponderosa Pine, Alligator Bark Juniper, and Emory Oak compared to the geochemical analysis of soil samples showed that:

-- Copper in the trees was not related to copper in the B soil horizon (about one foot below the surface).

-- Copper in the trees was related to distance from the drill hole (and from the inferred subsurface mineralization locus).

-- Ponderosa Pine was the best indicator specie having a copper content of 1000 ppm over the inferred mineralization locus which was five times that existing 560 feet away from the inferred locus of subsurface mineralization.

The multispectral image of mineralized trees appearing on the additive color viewer screen exhibited a difference in color saturation which could not be visually detected in a photo interpretation of subsequent frames of imagery.

A quantitative analysis of multispectral photography acquired using the prime filter set showed that the image densities of Ponderosa Pine tree crowns growing in areas of anomalous mineralization and areas of normal background mineralization had minimum intersection in a three-dimensional Euclidian vector space made up of the 585-680 nm band, the 406-480 nm band, and the 505-558 nm band.

When considered in terms of the six possible two-dimensional Cartesian vector spaces which could be constructed from the four multispectral bands, only two spaces had the convex hull of anomalous Ponderosa Pine coordinates with minimum intersection with the convex hull of background Ponderosa Pine coordinates. These spaces were defined by the 585-680 nm and 406-480 nm bands and the 585-680 nm and 505-558 nm bands. In the other four possible two-dimensional spaces (viz., 406-480 nm and 810-855 nm), the minimum convex set containing all the anomalous tree coordinates (the convex hull) excessively overlapped the convex hull of background Ponderosa Pine.

Two linear decision rules were developed for the two-dimensional Cartesian vector spaces in which anomalous Ponderosa Pine tended to be separate from background Ponderosa Pine. These rules were:

Rule #1:

(585-680 nm (x) vs. 406-480 nm (y))

$y > .98 + .66x \rightarrow$ Anomalous

$y < .98 + .66x \rightarrow$ Background

Rule #2:

(585-680 nm (x) vs. 505-558 nm (y))

$y > .69 + .66x \rightarrow$ Anomalous

$y < .69 + .66x \rightarrow$ Background

Applying these decision rules successively resulted in:

-- The six trees classified as being background were all actually trees growing in the background area.

-- Five out of six trees classified as being anomalous actually grew in the anomalous area.

-- One background and two anomalous trees were not classified.

Section 7

Bibliography

The following literature is referenced herein:

Yost, E. and S. Wenderoth (1967), "Multispectral Color Aerial Photography", PHOTOGRAMMETRIC ENGINEERING, pp. 1020.

Yost, E. and S. Wenderoth (1968), "Additive Color Aerial Photography", Manual of Color Aerial Photography, John Smith (editor), American Society of Photogrammetry.

Yost, E. and S. Wenderoth (1969); "Ecological Applications of Multispectral Color Aerial Photography", Remote Sensing in Ecology, P. Johnson (editor), University of Georgia Press.

Canney, F.C., S. Wenderoth, and E. Yost (1970), "Relationship between Vegetation Reflectance Spectra and Soil Geochemistry: New Data from Cathcart Mountain, Maine", NASA Third Annual Earth Resources Program Review, Manned Spacecraft Center, Houston, Texas.

APPENDIX A

Copper Creek Test Site

Tree and Soil Sample Locations

Copper Content of Trees (in Ash)

Soil Sample Copper Content

COPPER CREEK SAMPLES (JUNIPER)

Sample	Cu	Mo
P211	73	17
P214	88	19
P215	75	11
CC51	84	33
CC52	66	20

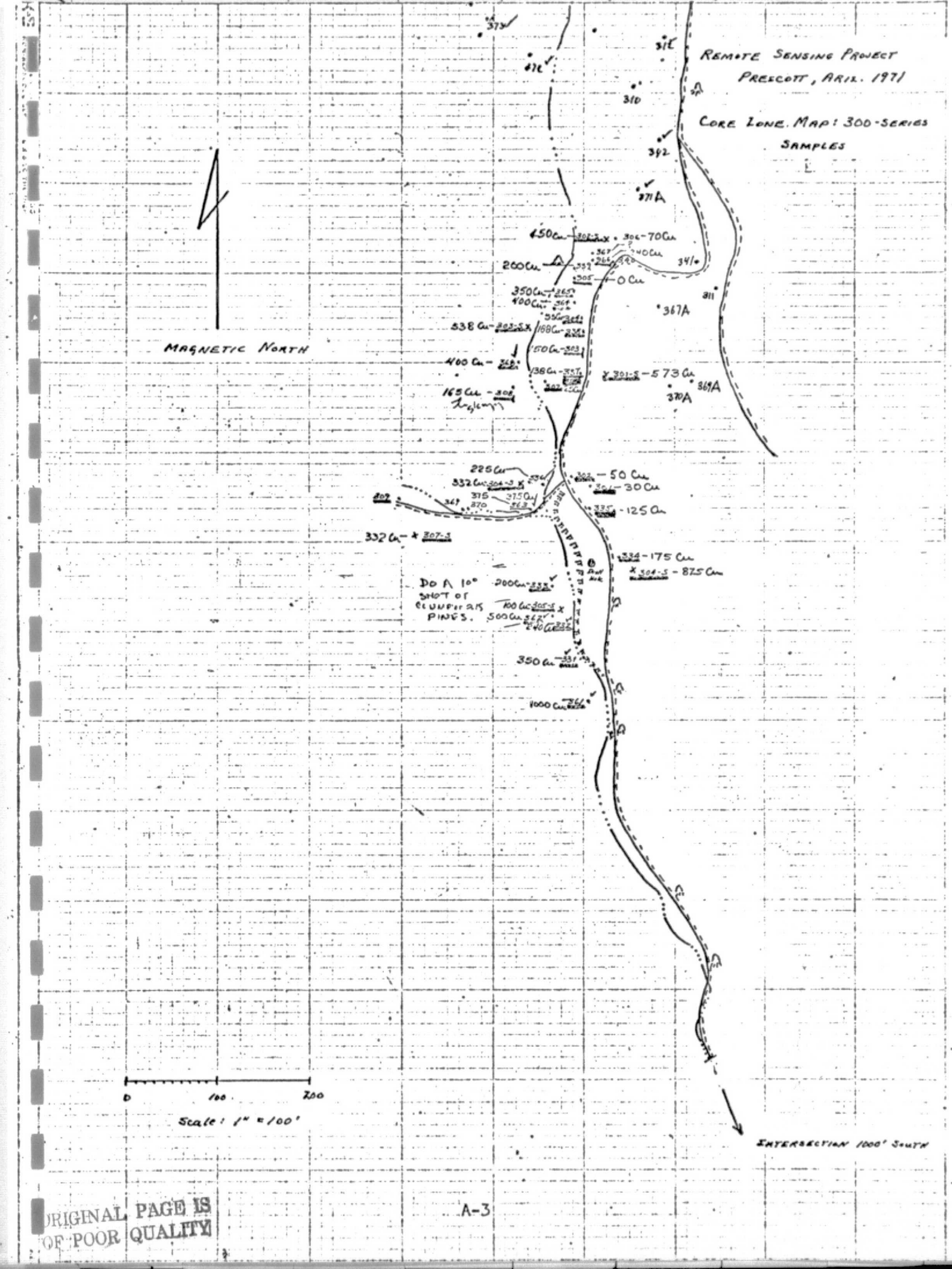

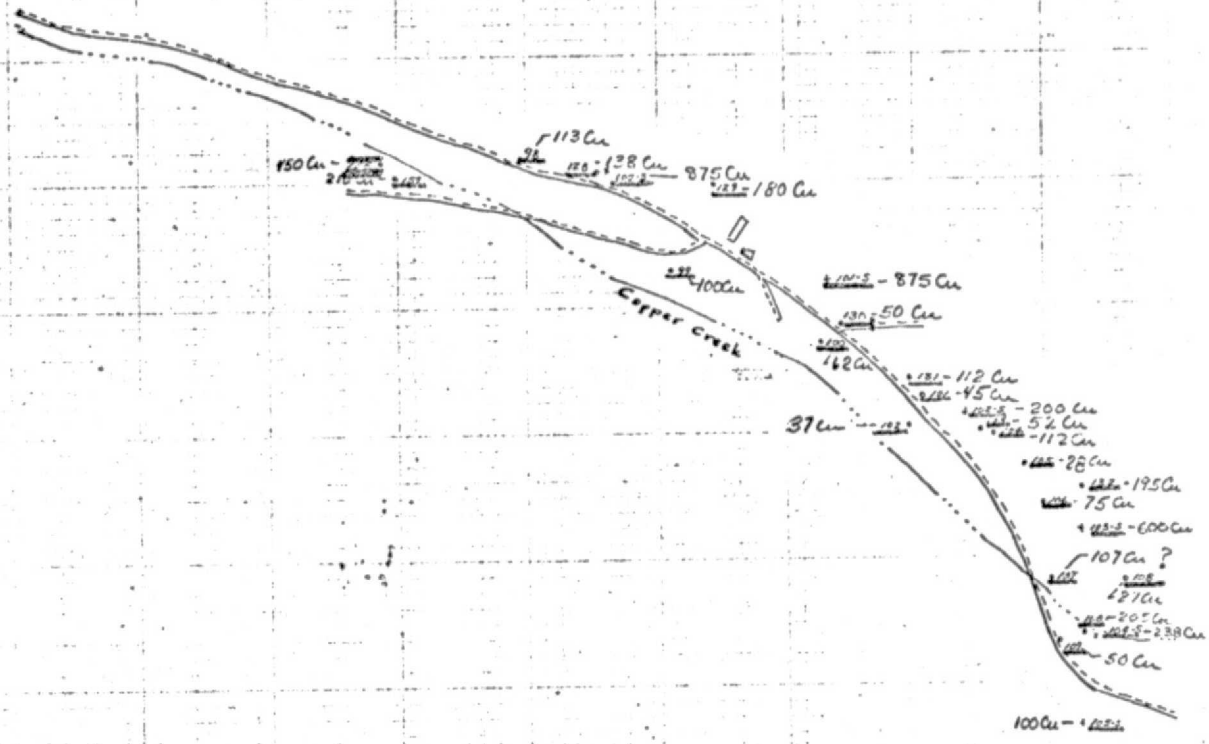

JUNIPER	OAK	PINE
98	128	158
99	129	159
100	130	160
101	131	161
102	132	162
103 ✓	133	163
104 ✓	134	164
105 ✓	135	165
106 ✓	136	166
107	137	167
108 ✓	138	168 ✓
109		169
110		
111		
112		
113		
114		
115 ✓		
116		

page 2 of 3.

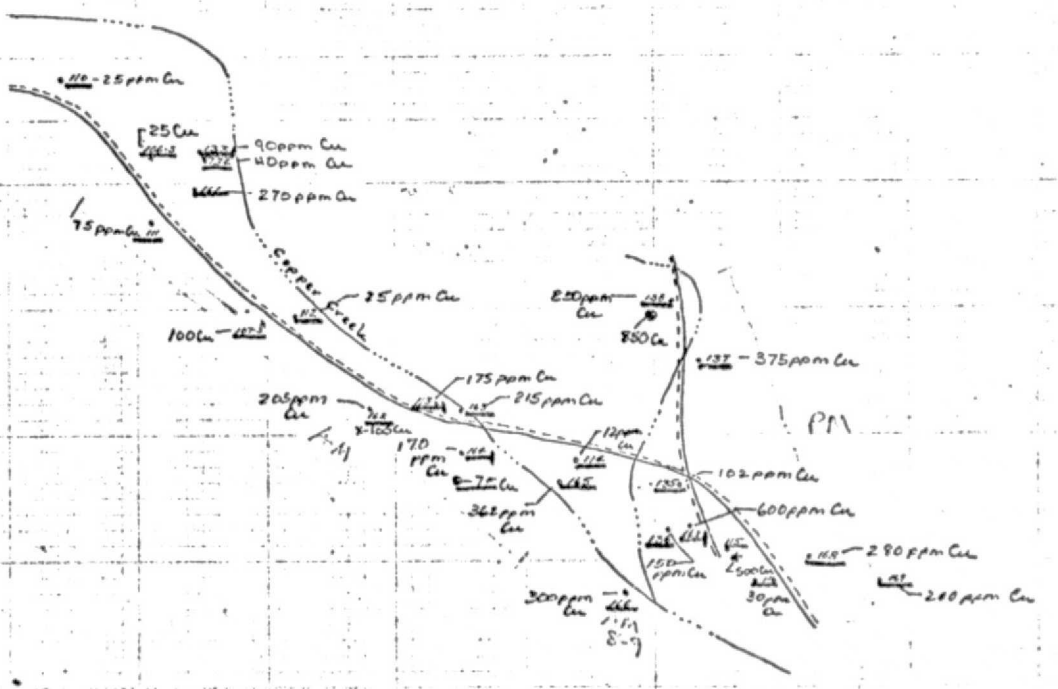

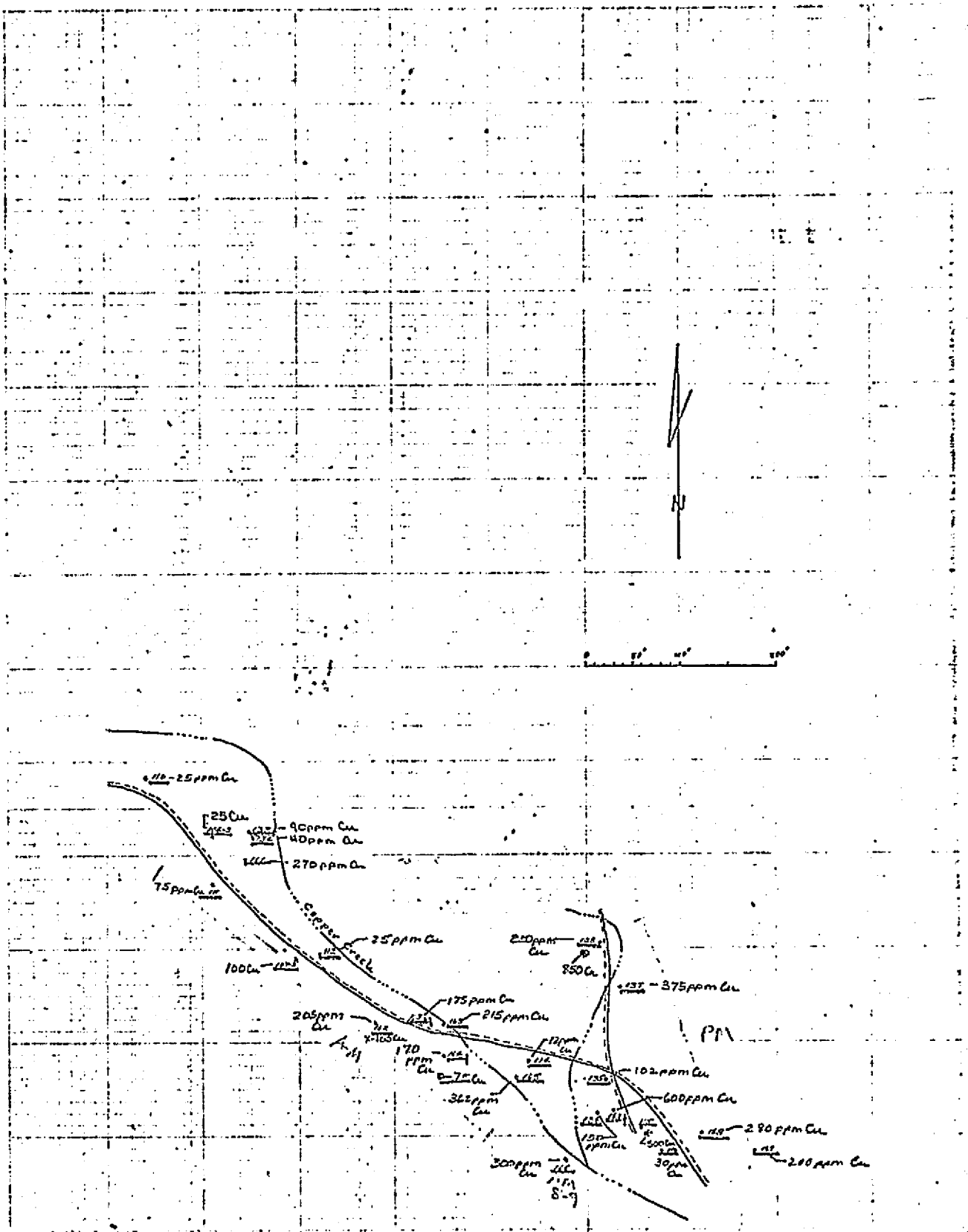

Remote Sensing Project

Prescott, Ariz. 1971

Geobotanical Sample Map

Mineralized Zone

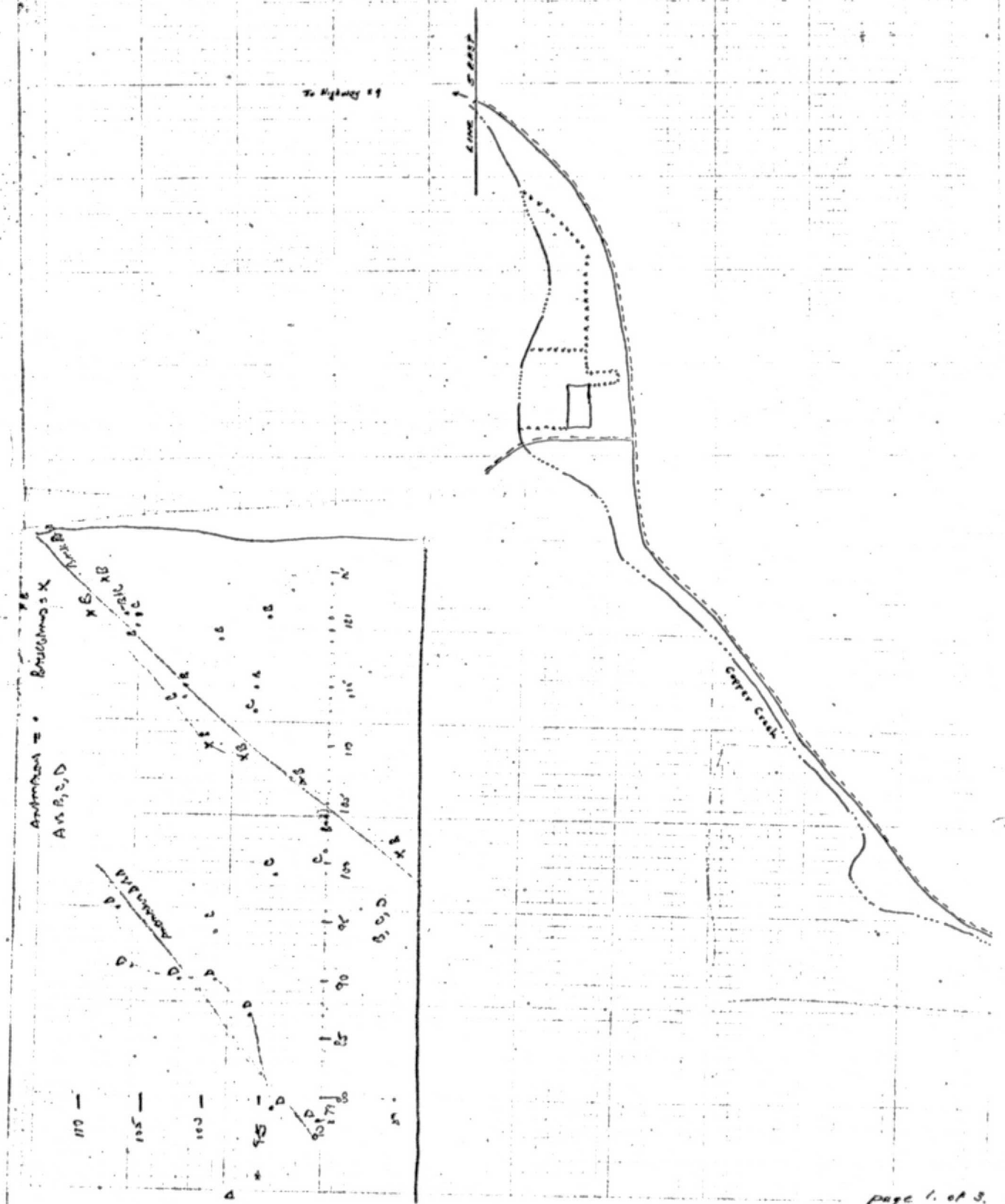

page 1. of 3.

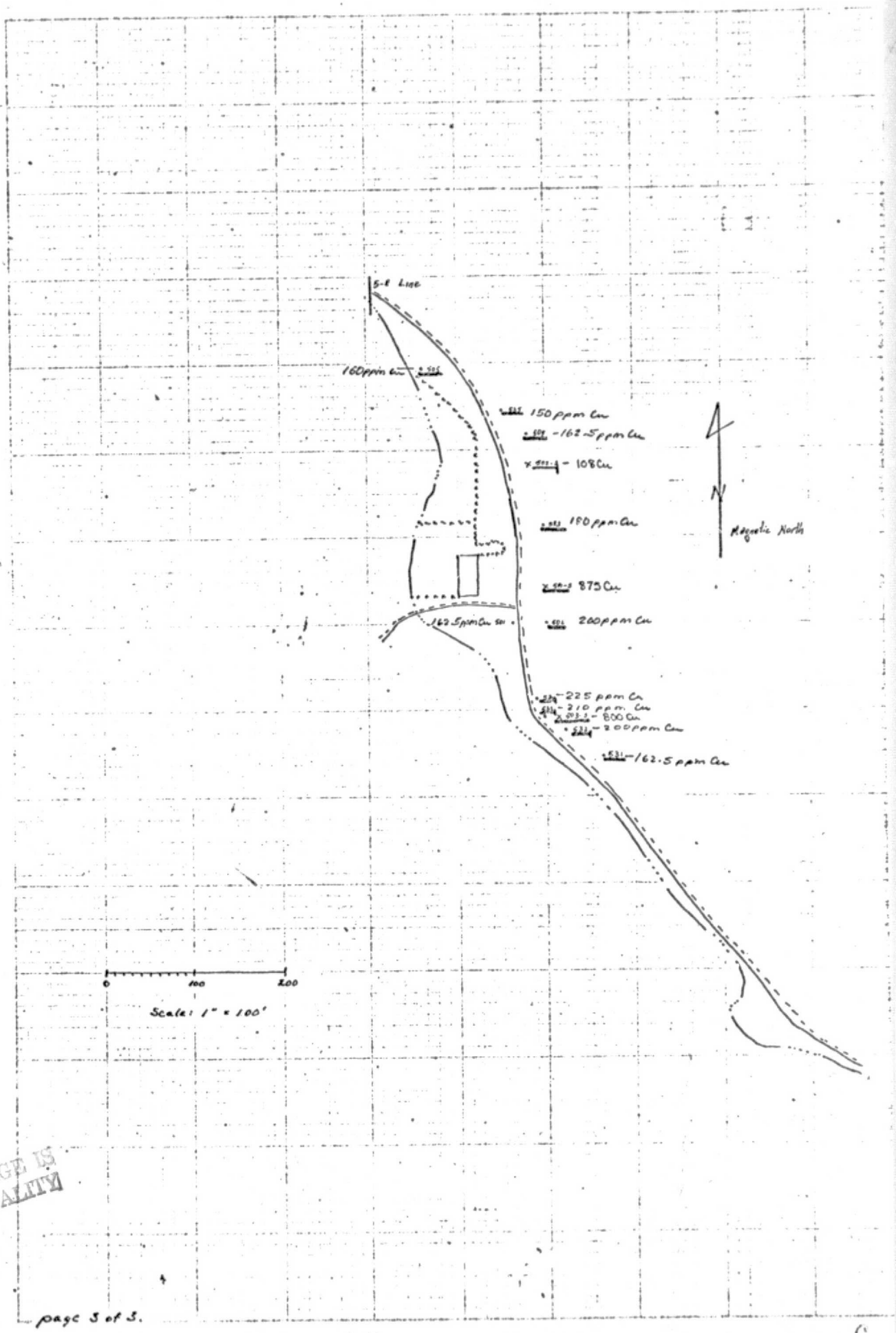

page 3 of 3.

C

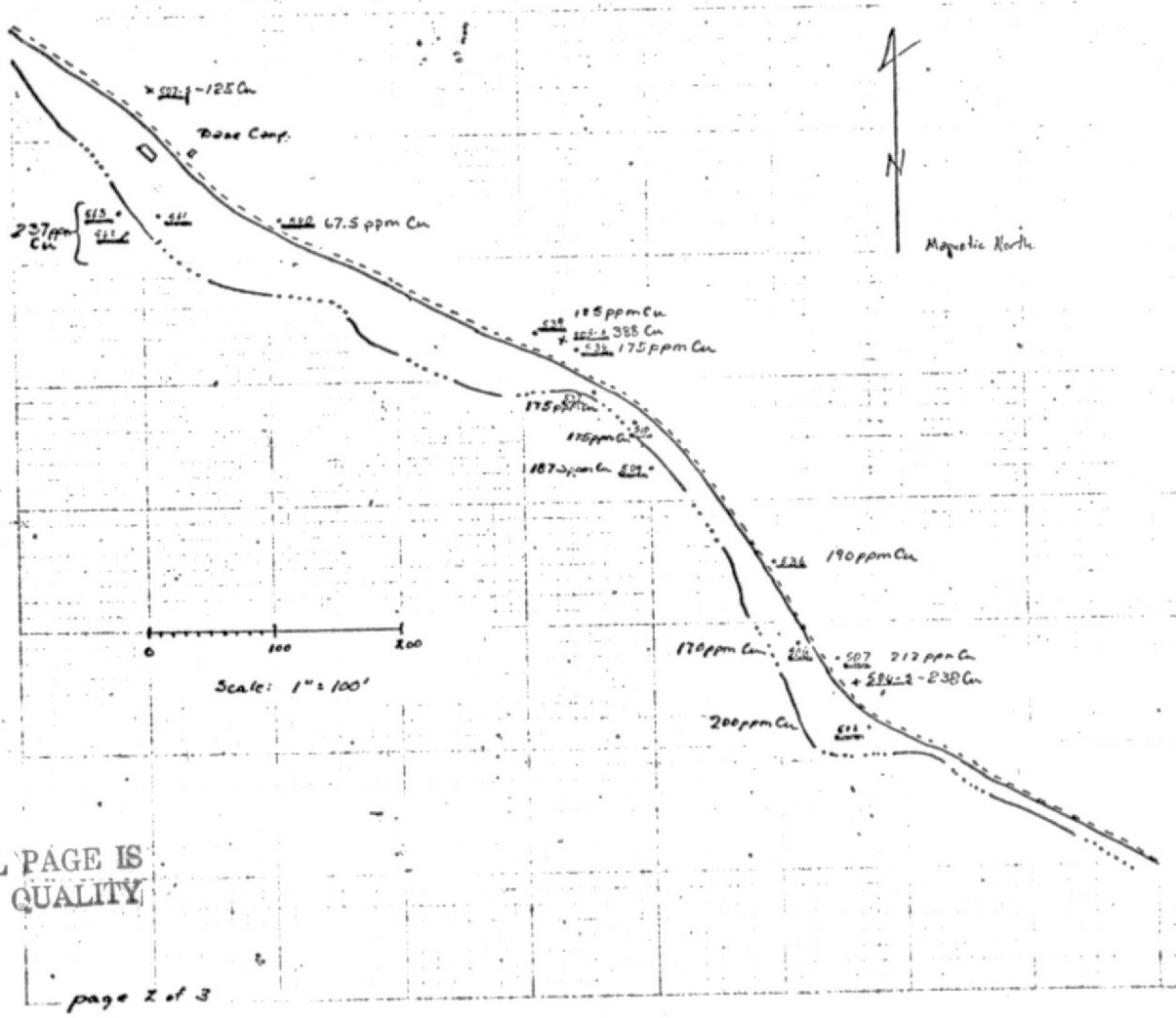

ORIGINAL PAGE IS
OF POOR QUALITY

page 2 of 3

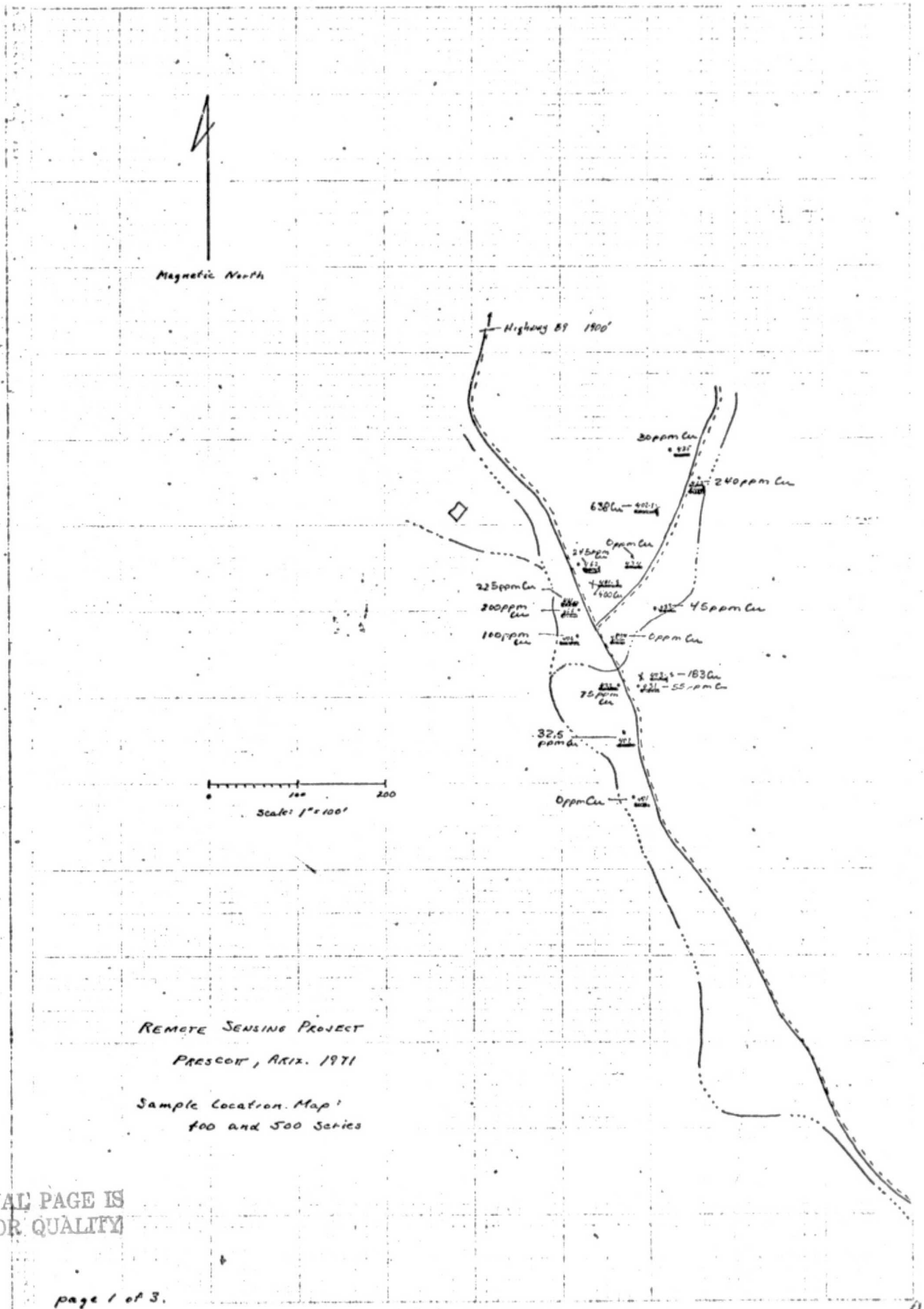

REMOTE SENSING PROJECT

PRESCOTT, ARIZ. 1971

Sample Location Map:
400 and 500 Series

page 1 of 3.

REMOTE SENSING PROJECT
PRESCOTT, ARIZONA 1971

GEOBOTANICAL SAMPLE MAP
'BACKGROUND' AREA

OAK		PINE		JUNIPER	
231	NO	261	✓	201	✓
232	✓	262	✓	202	
233	✓	263	✓	203	✓
234	✓	264	NO	204	✓
235	✓	265	✓	205	✓
236	✓	266	✓	206	✓
237	✓	267	✓	207	
238	✓	268	✓	208	
239		269	✓	209	✓
240	✓	270	✓	210	✓
241	✓	271	✓	211	✓
		272	✓	212	✓
		273		213	✓
		274		214	✓
		275		215	✓
				216	
				217	
				218	

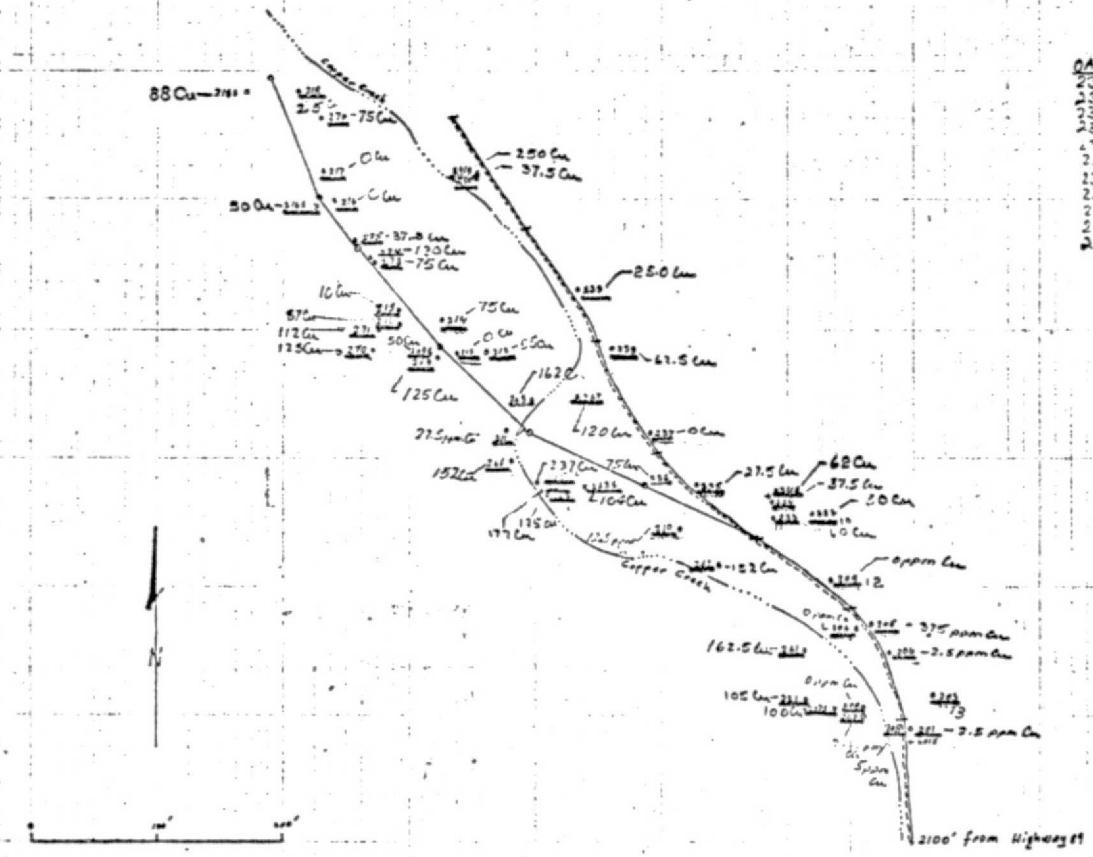

APPENDIX B

Copper Basin Test Site

Tree and Soil Sample Locations

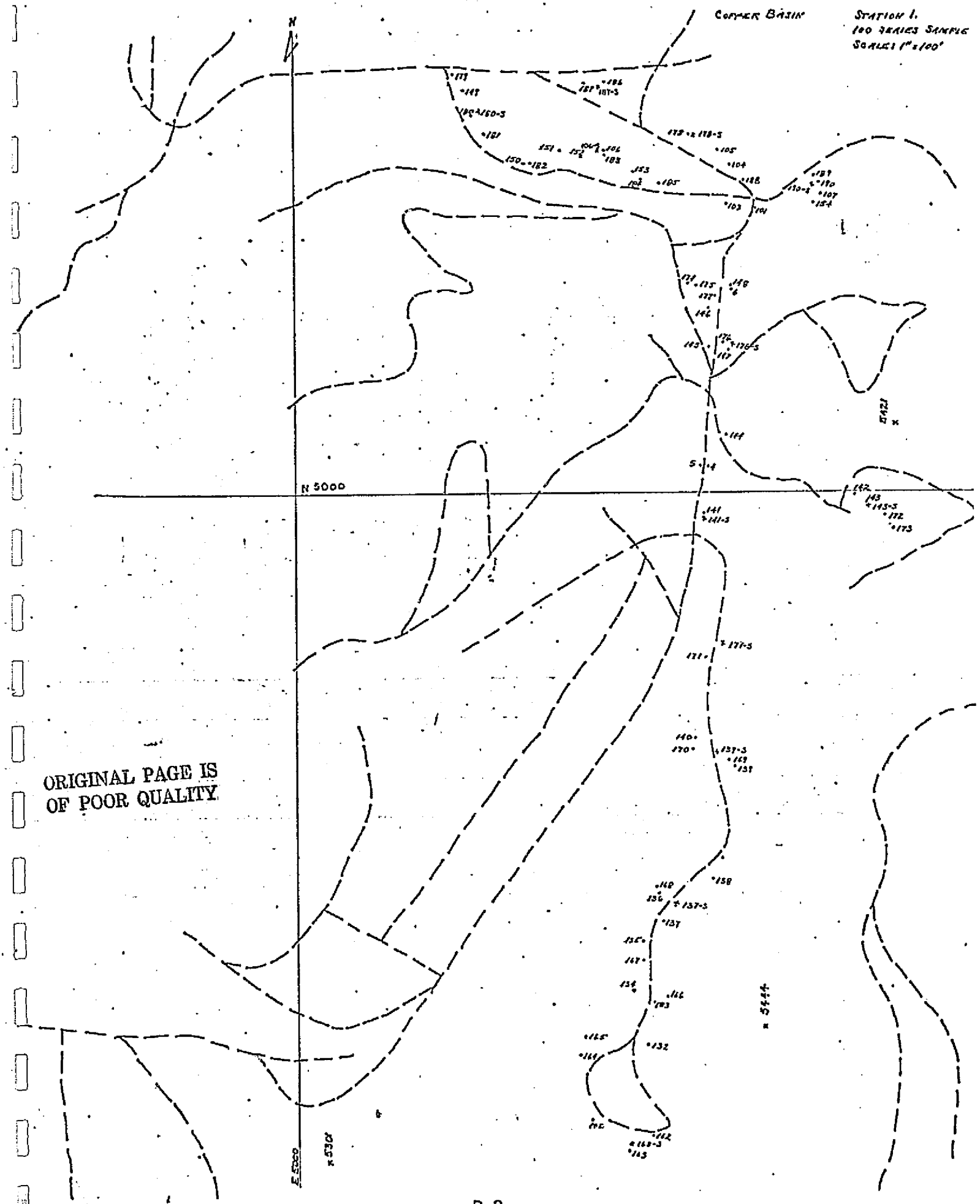

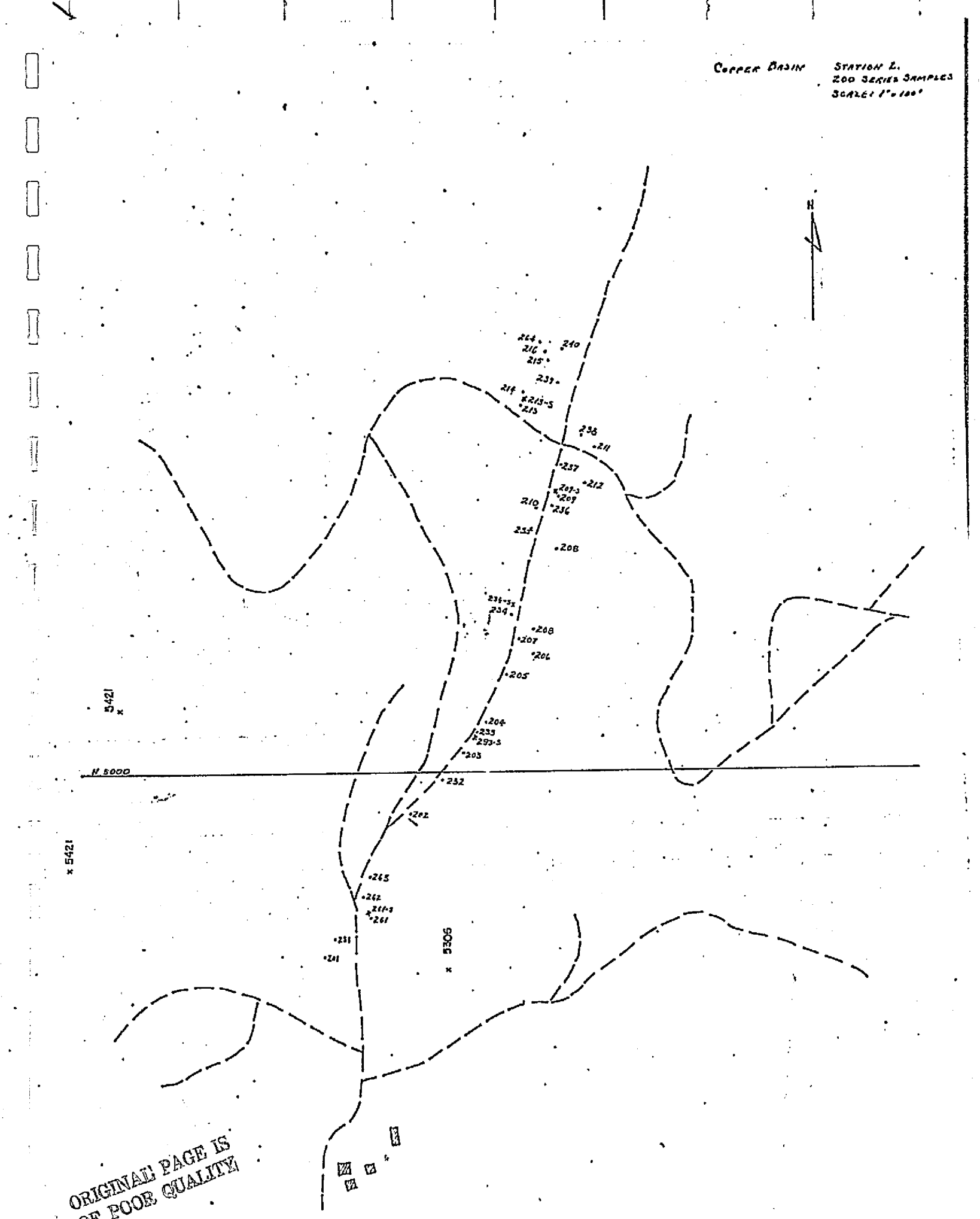

ORIGINAL PAGE IS
OF POOR QUALITY

COPPER BASIN

STATION 3, SHEET 1
300 SERIES SAMPLES
SCALE: 1" = 100'

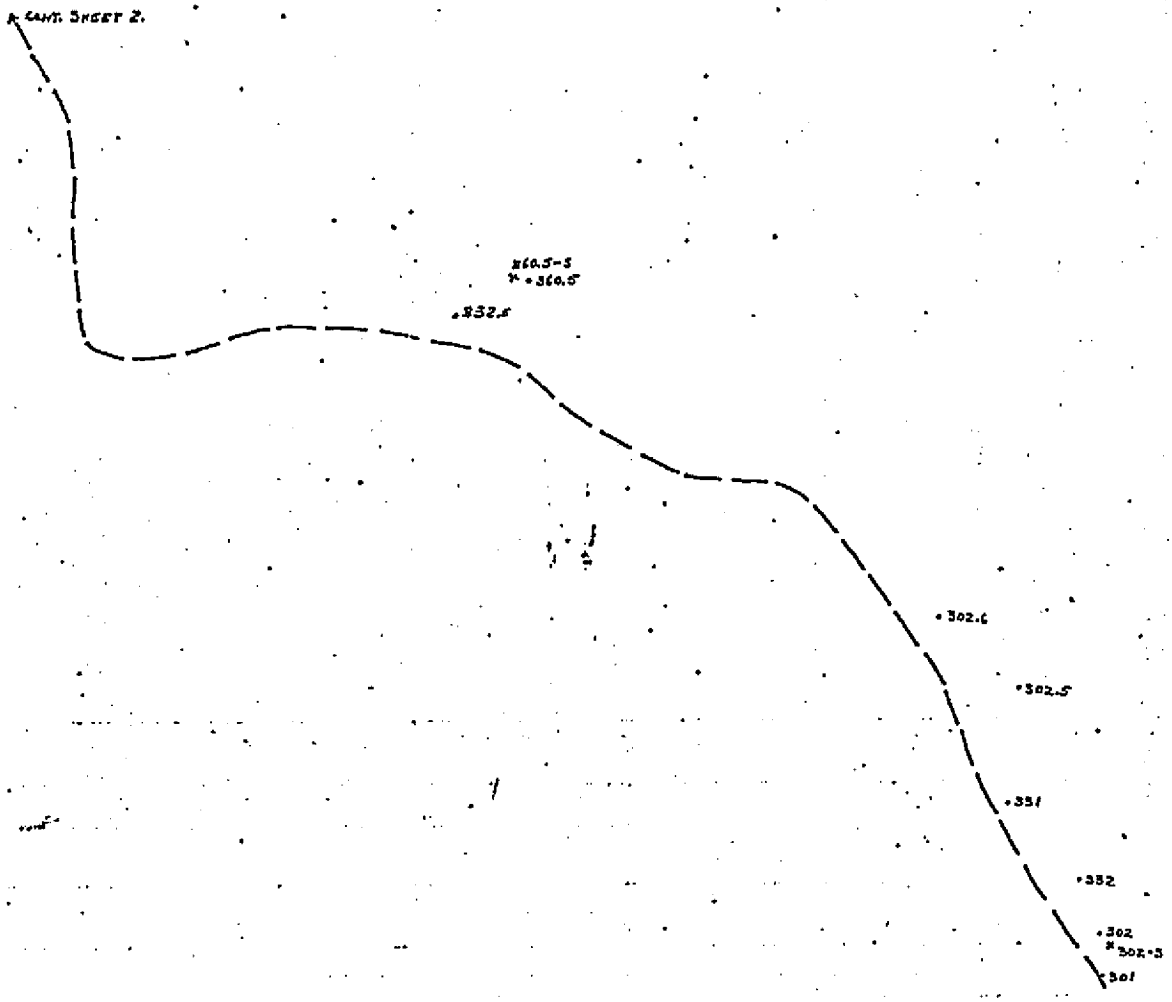

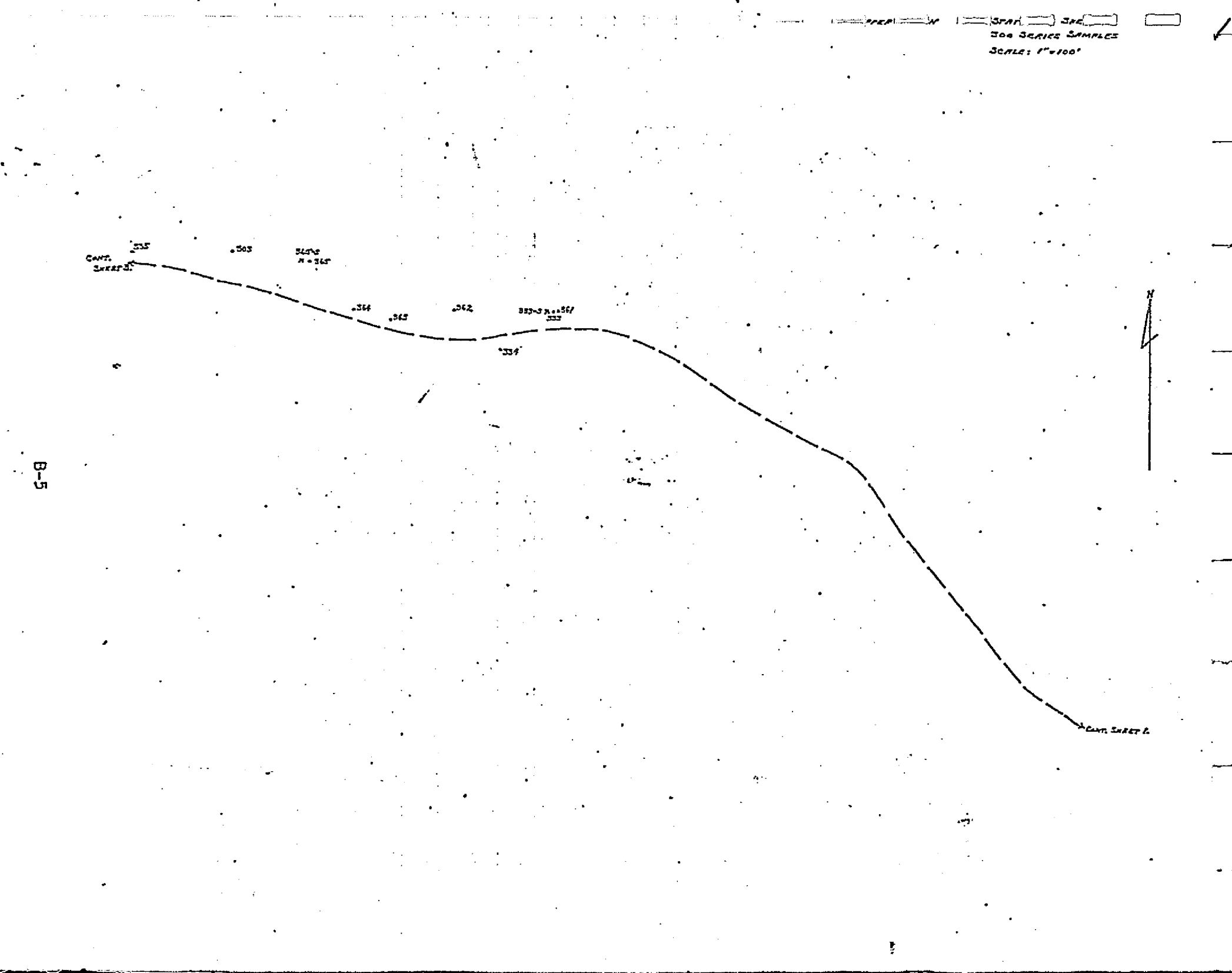
300 SERIES SAMPLES
SCALE: 1"=100'
N
CONT. SHEET B
CONT. SHEET B

COPPER BASIN

SECTION B, SHEET 3.
300 SERIES SAMPLES
SCALE, 1" = 100'

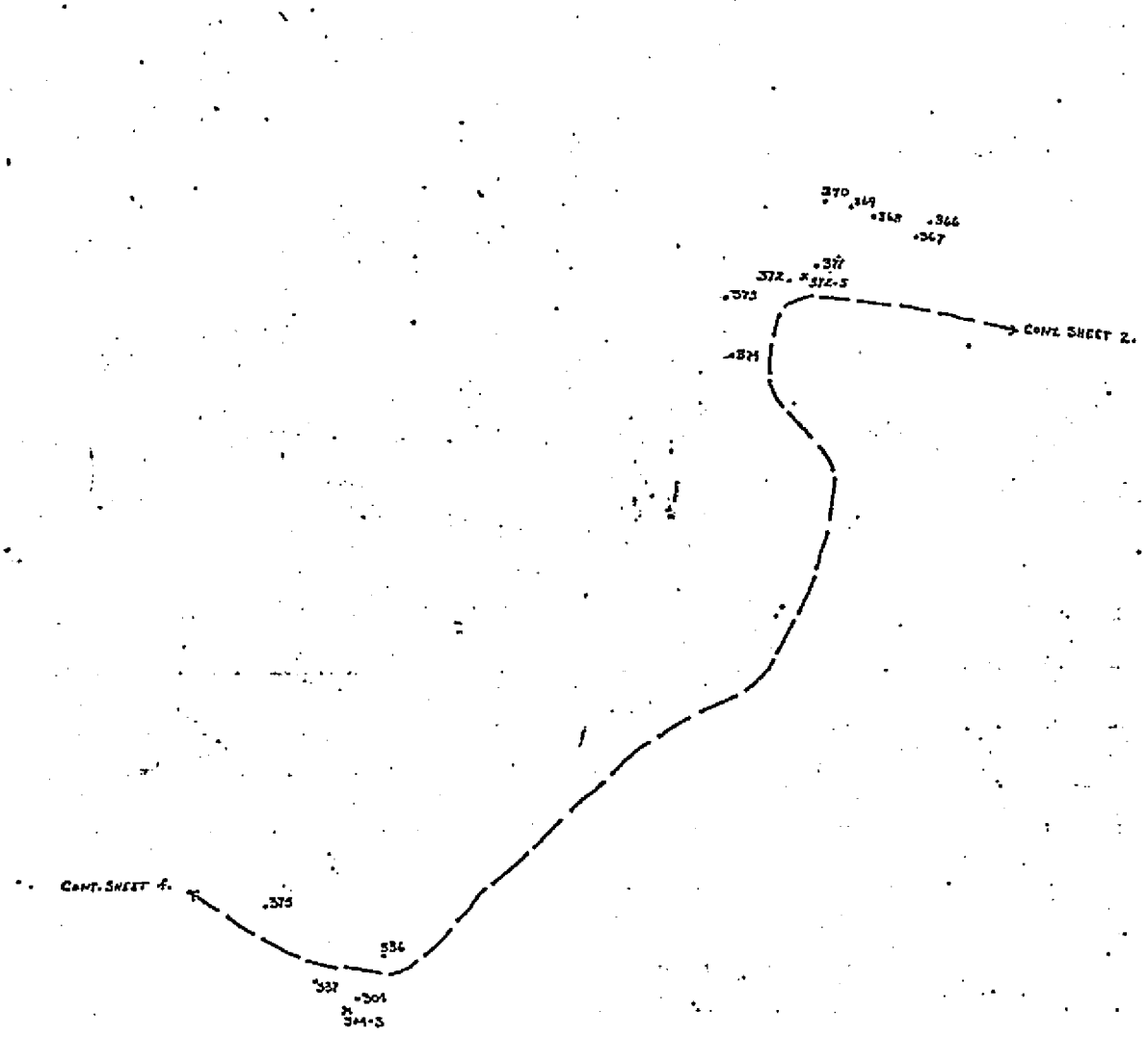

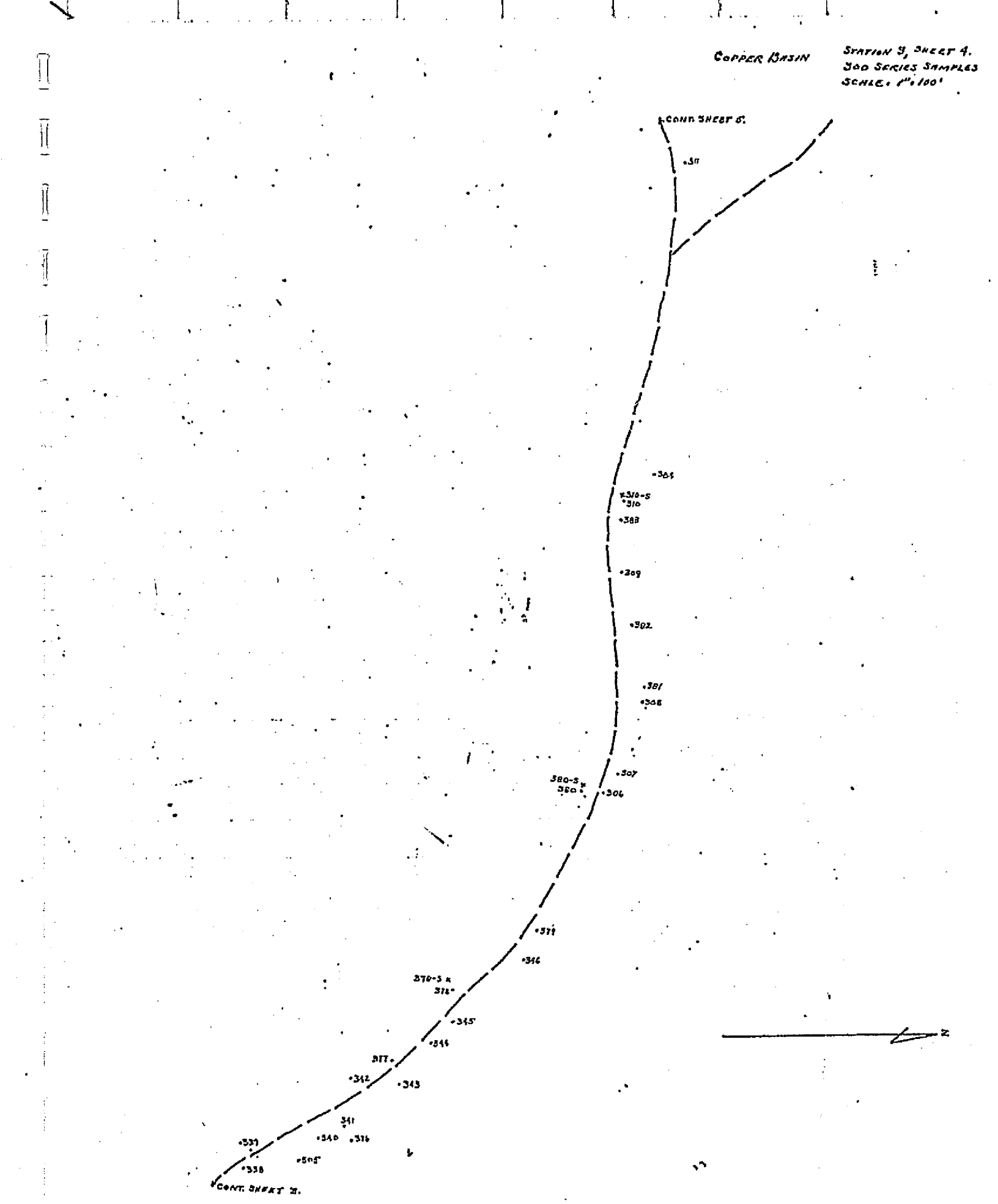
COPPER BASIN
STATION 3, SHEET 4.
300 SERIES SAMPLES
SCALE: 1" = 100'
CONN. SHEET 5.
311
314
310-S
310
308
309
302
301
306
307
380-S
380
306
319
316
378-S
378
345
344
377
342
343
341
339
340
336
305
338
CONT. SHEET 3.
N

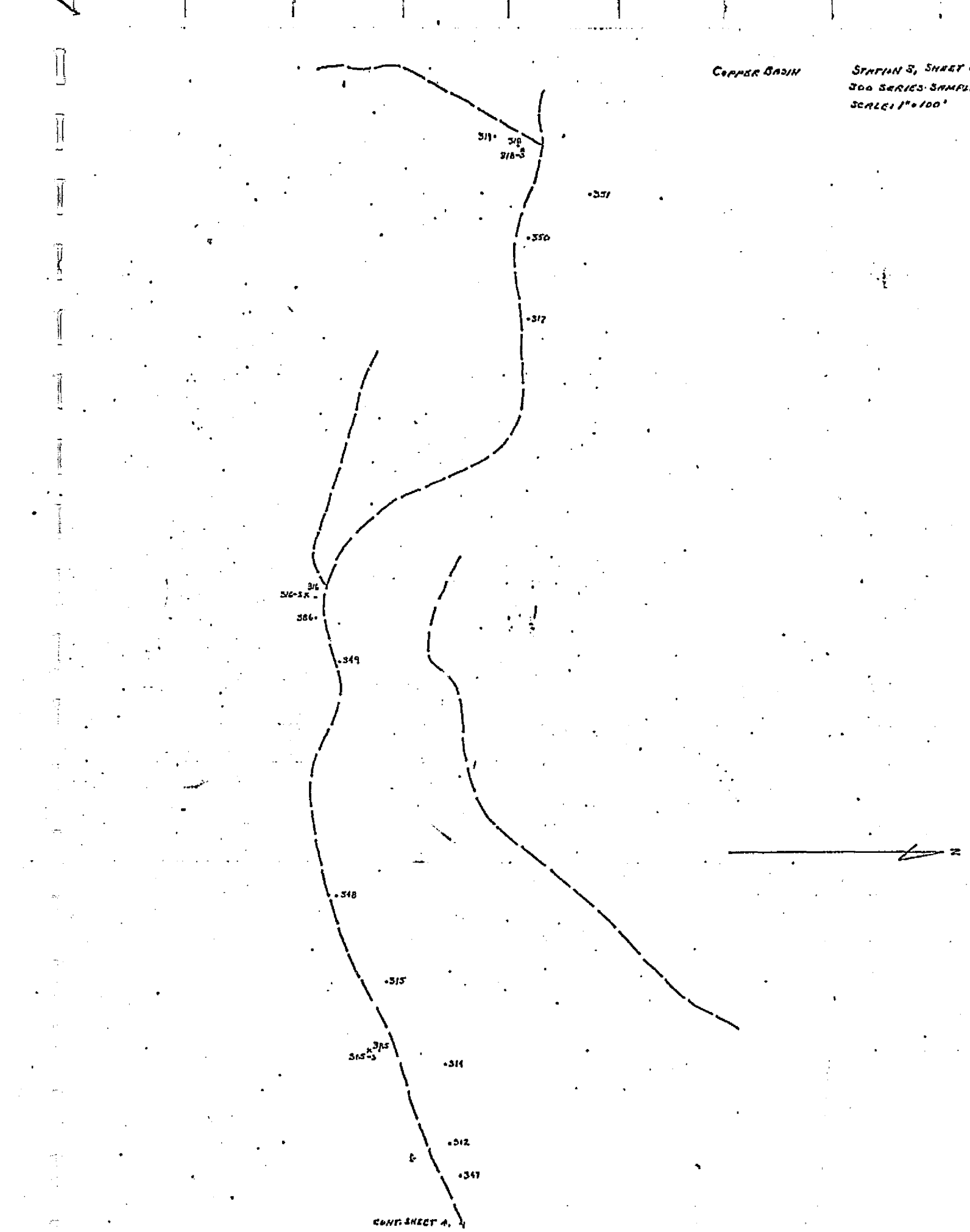
COPPER BASIN
STATION 3, SHEET 3.
300 SERIES SAMPLES
SCALE: 1"=100'
318-3
351
350
317
316-3
349
348
315
315-3
314
312
347
CONT. SHEET 4.

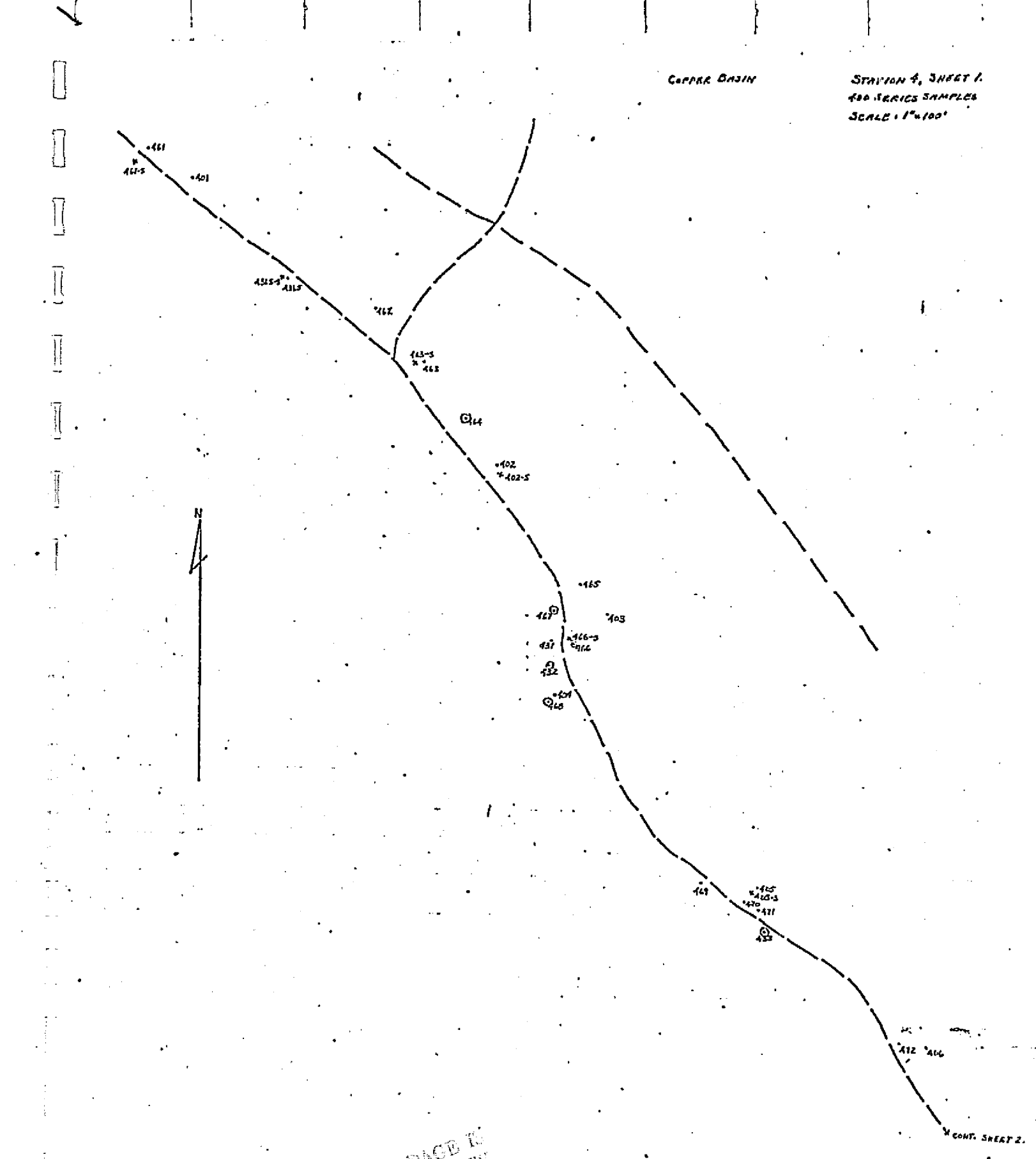

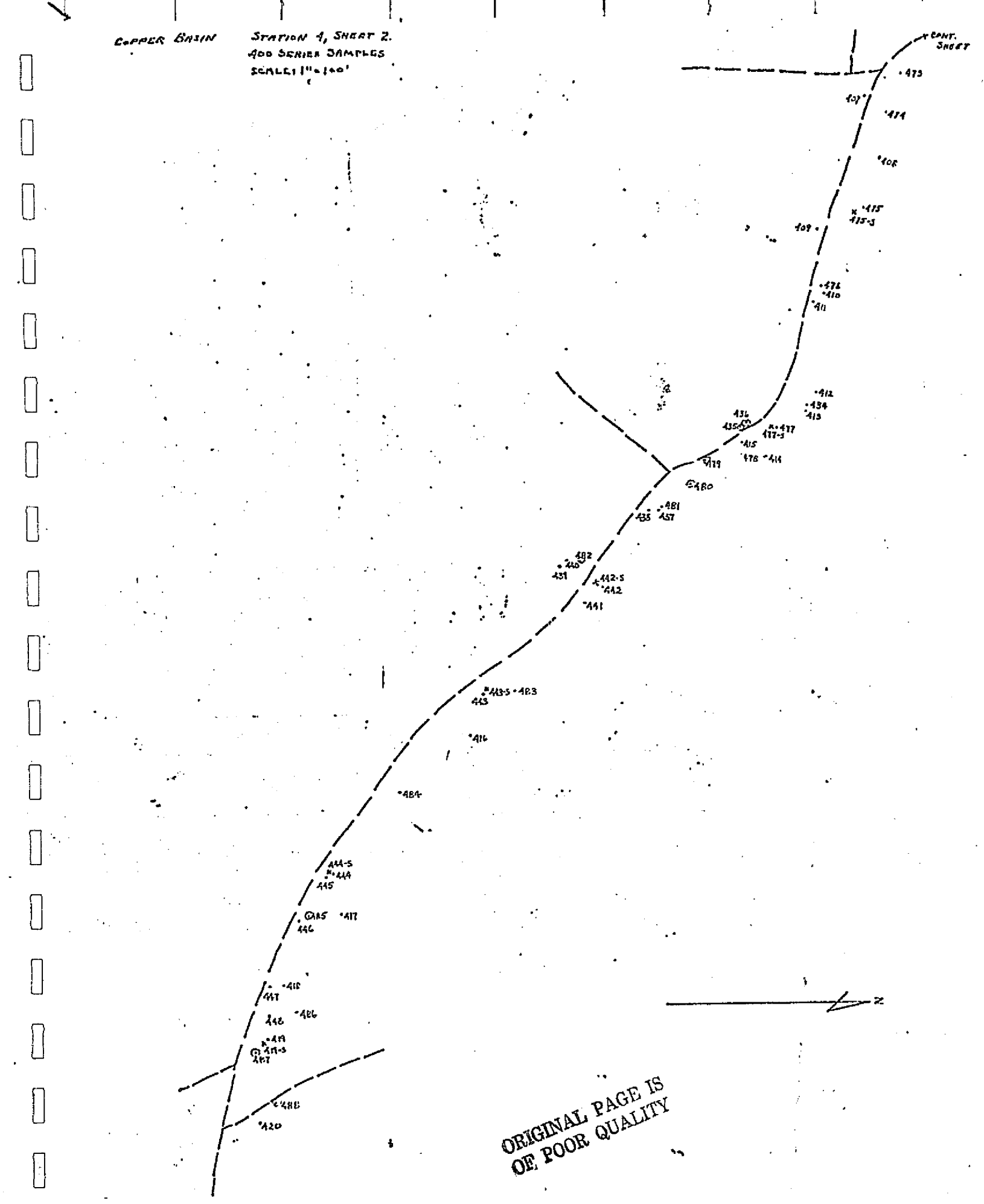

ORIGINAL PAGE IS
OF POOR QUALITY

COPPER BASIN

STATION 5, SHEET 1.
600 SERIES SAMPLES
SCALE: 1" = 100'

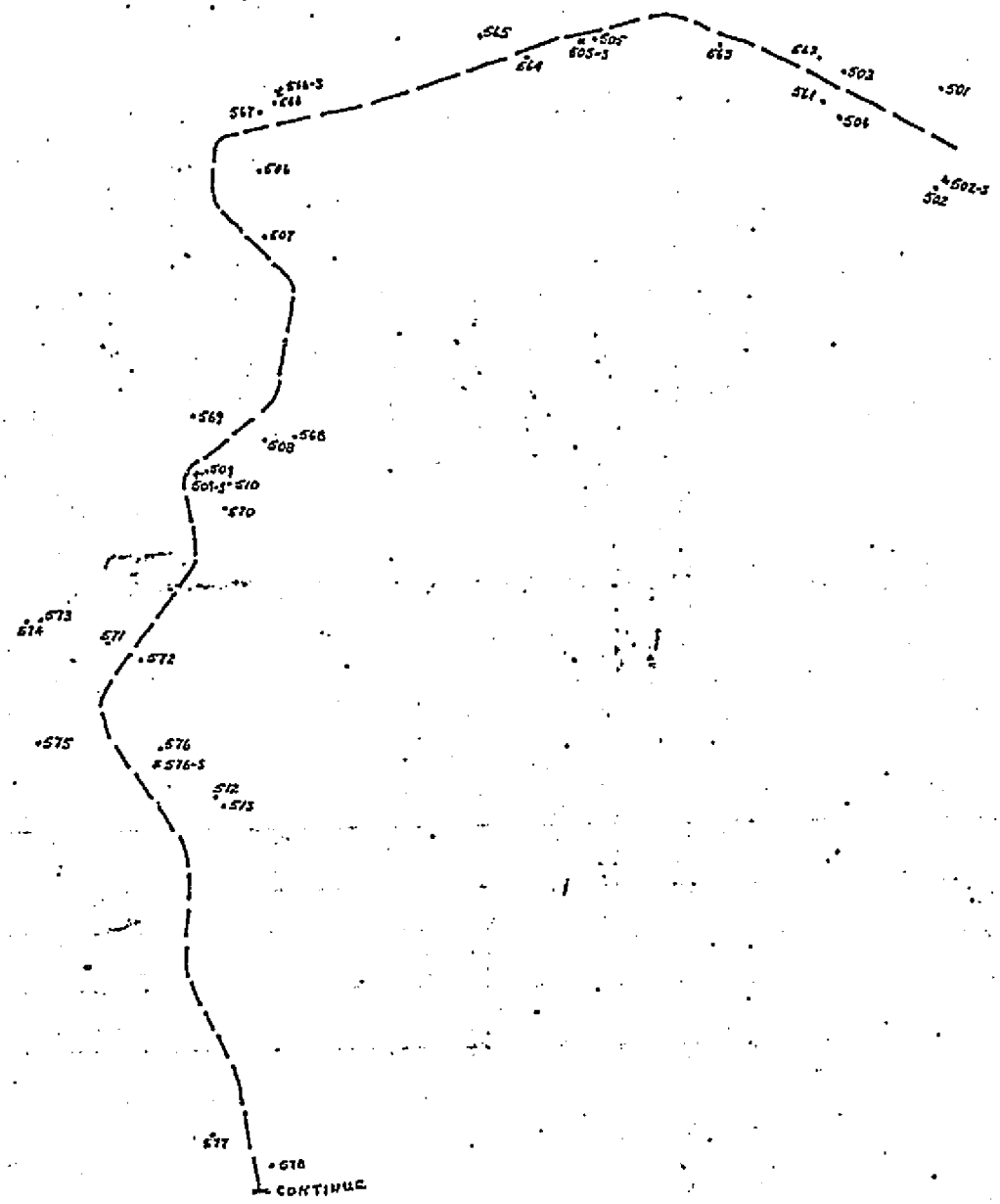

COPPER BASIN

STATION 5, SHEET 2.
500 SERIES SAMPLES
SCALE: 1"=100'

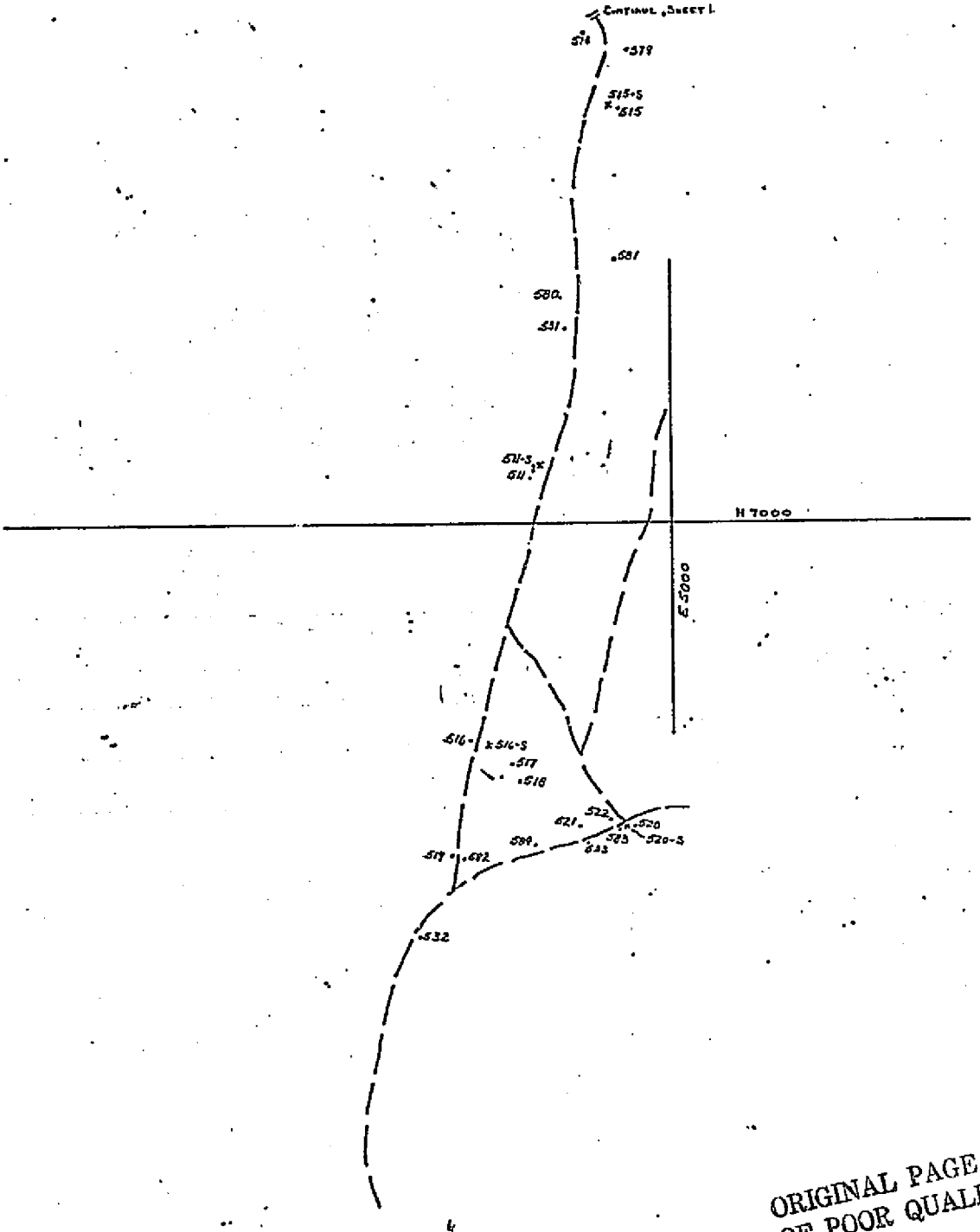

ORIGINAL PAGE IS
OF POOR QUALITY

APPENDIX C

Copper Basin Test Site

Tree and Soil Sample

Geochemical Data

PLANT ASHES - COPPER BASIN

Station 1

Sample	Cu	Mo
101	54.7	20
102	152	46
103	267	22
104	226	128
105	211	78
106	231	63
107	126	264
131	1130	67
132	558	38
133	2160	138
134	>3240	217
135	1560	124
136	1540	94
137	1360	39
138	2470	120
139	1205	117
140	1420	192
141	1425	107
142	1560	68
143	723	48
144	>2560	77
145	>2860	137
146	2400	386
147	>2660	96
148	1860	93
149	920	52
150	1590	84
151	1190	43
152	>2280	41
153	2010	79
154	>7000	126
161	472	17
162	334	7
163	285	17
164	1580	104
165	>2360	32
166	1310	28
167	400	18
168	1710	70
169	327	62
170	858	98
171	1190	39
172	321	14
173	314	12
174	834	25
175	1160	21

PLANT ASHES - COPPER BASIN

Station 1 - Continued

Sample	Cu	Mo
176	1500	34
177	1410	40
178	508	25
179	880	22
180	346	28
181	247	27
182	1088	50
183	723	61
184	436	90
185	1780	198
186	1480	15
187	1060	149
188	1610	-44
189	945	96
190	3230	126

PLANT ASHES - COPPER BASIN

Station 2

Sample	Cu	Mo
201	165	86
202	145	71
203	137	34
204	96	46
205	102	67
206	66	39
207	131	39
208A	314	210
208B	145	161
209	141	62
210	224	72
211	158	86
212	118	101
213	122	61
214	173	93
215	215	83
216	134	29
231	45	72
232	522	37
233	1980	89
234	310	37
235	302	40
236	426	54
237	142	25
238	1300	56
239	711	35
240	263	24
261	462	60
262	984	64
263	864	26
264	1288	121

PLANT ASHES - COPPER BASIN

Station 3

Sample	Cu	Mo
301	86	6
302	47	14
302.5	113	40
302.6	521	45
303	78	97
304	82	37
305	95	107
306	77	0
307	109	33
308	100	50
309	68	14
310	89	7
311	124	37
312	109	41
313	129	17
314	52	50
315	98	49
316	139	111
317	>2840	342
318	356	82
319	150	42
331	247	62
332	215	9
332.5	253	106
333	386	26
334	243	37
335	236	42
336	265	9
337	149	13
338	202	43
339	592	42
340	352	92
341	433	46
342	387	33
343	516	12
344	460	18
345	321	9
346	292	15
347	399	60
348	262	52
349	645	50
350	75	20
351	2820	186
360.5	243	4
361	142	4
362	279	0

Station 3 - Continued

Sample	Cu	Mo
363	159	69
364	204	N.D.
365	261	13
366	173	6
367	413	0
368	429	0
369	187	0
370	210	0
371	134	18
372	339	36
373	544	8
374	81	24
375	177	12
376	175	0
377	263	22
378	179	3
379	144	23
380	195	21
381	230	43
382	248	34
383	160	31
384	226	47
385	286	147
386	540	0

PLANT ASHES - COPPER BASIN

Station 4

Sample	Cu	Mo
401	149	53
402	128	32
403	102	86
404	76	39
405	115	40
406	102	9
407	111	55
408	66	23
409	119	12
410	120	13
411	43	32
412	154	112
413	195	95
414	229	65
415	194	166
416	236	101
417	303	382
418	164	216
419	256	241
420	891	114
431	190	13
431.5	201	77
432	92	0
433	107	7
434	>2580	278
435	>2390	101
436	>2650	111
437	3320	194
438	>3560	320
439	781	68
440	1420	31
441	921	124
442	180	41
443	>2650	190
444	>2890	260
445	>3170	676
446	331	50
447	1300	356
448	2620	338
461	264	15
462	218	12
463	252	29
464	193	12
465	206	52
466	188	79

PLANT ASHES - COPPER BASIN

Station 4 - Continued

Sample	Cu	Mo
467	186	12
468	119	42
469	237	14
470	422	15
471	225	18
472	177	23
473	280	46
474	406	31
475	302	15
476	340	30
477	445	30
478	438	156
479	2220	47
480	835	12
481	608	87
482	780	65
483	745	64
484	718	104
485	1275	105
486	501	11
487	987	99
488	1200	62

PLANT ASHES - COPPER BASIN

Station 5

Sample	Cu	Mo
501	82	37
502	79	30
503	82	0
504	86	0
505	78	38
506	64	13
507	133	15
508	181	0
509	93	20
510	53	13
511	69	59
512	123	160
513	63	38
514	99	144
515	83	43
516	89	94
517	101	60
518	141	84
519	92	84
520	53	101
521	127	208
522	119	47
531	109	12
532	1514	165
561	343	174
562	155	36
563	333	32
564	415	7
565	81	37
566	183	32
567	77	7
568	374	7
569	142	28
570	414	36
571	69	14
572	228	0
573	218	39
574	150	0
575	198	112
576	161	30
577	127	29
578	228	45
579	122	33
580	242	50
581	216	110

PLANT ASHES - COPPER BASIN

Station 5 - Continued

Sample	Cu	Mo
582	557	62
583	408	41
584	508	49

SOILS DATA (ppm)

	Nitrate	P	Ammonia	Sulfate	Chloride	Nitrite	Mo	Cu
Station 1								
163-S	350	3.5	14	<1050	140	<7	126	20
137-S	245	<3.5	14	<1050	140	<7	138	630
139-S	210	<3.5	14	<1050	210	<7	225	35
171-S	350	<3.5	14	<1050	210	<7	90	300
141-S	525	3.5	14	<1050	210	<7	30	480
193-S	70	3.5	14	<1050	140	7	72	11.5
176-S	175	<3.5	14	4200	210	<7	156	90
190-S	350	<3.5	14	<1050	210	<7	147	180
178-S	70	3.5	175	2100	210	<7	216	420
106-S	175	<3.5	14	1050	280	<7	126	480
187-S	875	<3.5	14	<1050	280	<7	138	512
180-S	245	<3.5	14	<1050	210	<7	198	.500
Station 2								
261-S	350	7	14	<1050	140	<7	105	780
233-S	245	<3.5	14	<1050	210	7	72	500
234-S	175	<3.5	14	<1050	350	<7	20	300
209-S	350	<3.5	14	<1050	140	<7	20	500
213-S	70	3.5	14	<1050	140	<7	15	30
Station 3								
302-S	175	3.5	14	<1050	210	<7	0	5
360.5-S	350	<3.5	14	<1050	280	<7	6	5
333-S	210	<3.5	14	<1050	140	<7	72	15
365-S	70	<3.5	14	1050	280	<7	90	75
372-S	35	<3.5	14	<1050	280	<7	117	340
309-S	70	<3.5	14	<1050	140	<7	0	15
378-S	210	<3.5	14	<1050	140	<7	51	500
380-S	175	<3.5	14	<1050	280	<7	15	22.5
310-S	70	<3.5	14	<1050	140	<7	51	45
385-S	140	<3.5	14	<1050	140	<7	177	5
316-S	280	<3.5	14	<1050	140	<7	20	55
318-S	175	<3.5	14	<1050	210	<7	51	80

SOILS DATA (ppm)

	Nitrate	P	Ammonia	Sulfate	Chloride	Nitrite	Mo	Cu
Station 4								
461-S	175	<3.5	14	<1050	210	<7	126	47.5
431.5-S	70	<3.5	14	<1050	280	<7	72	70
463-S	175	<3.5	14	<1050	140	<7	15	15
402-S	70	<3.5	14	<1050	210	<7	117	55
466-S	70	<3.5	14	<1050	140	<7	30	30
405-S	105	<3.5	14	<1050	140	<7	72	32.5
475-S	70	<3.5	14	<1050	420	<7	117	360
477-S	350	<3.5	14	<1050	140	<7	138	540
442-S	245	<3.5	14	<1050	140	<7	186	840
443-S	280	<3.5	14	<1050	210	<7	126	25
444-S	105	<3.5	14	1750	210	<7	168	390
419-S	175	<3.5	14	<1050	140	<7	117	930
Station 5								
520-S	105	<3.5	14	<1050	140	<7	72	37.5
516-S	175	<3.5	14	<1050	140	<7	207	2500
511-S	70	<3.5	14	<1050	140	<7	126	390
515-S	175	<3.5	14	<1050	140	<7	90	400
576-S	245	<3.5	14	<1050	140	<7	117	42.5
509-S	280	<3.5	14	<1050	140	<7	30	70
566-S	175	<3.5	14	<1050	140	<7	156	500
505-S	70	<3.5	14	<1050	175	<7	0	230
502-S	105	<3.5	14	<1050	140	<7	15	5

APPENDIX D

Copper Creek Average Ponderosa Pine Spectra

Scan #101
(Background Area)

Tree #	Cu(ppm)
262	152
263	125
265	237
266	152
267	120
268	162
269	125
272	87

Tree Avg. 145 ppm in ash
Soil Avg. 76 ppm

Scan #259
(Intermediate Area)

Tree #	Cu(ppm)
461	225
462	245

Tree Avg. 235 ppm in ash
Soil Avg. 407 ppm

Scan #229
(Intermediate Area)

Tree #	Cu(ppm)
561	No data
562	237
563	237

Tree Avg. 237 ppm in ash
Soil Avg. 422 ppm

Scan #179
(Intermediate Area)

Tree #	Cu(ppm)
160	205
162	205
164	170
165	362

Tree Avg. 236 ppm in ash
Soil Avg. 376 ppm

Scan #387
(Core Zone)

Tree #	Cu(ppm)
361	1000
362	500
363	375
368	400
371	No data, Core zone
372	No data, Core zone

Tree Avg. 569 ppm in ash
Soil Avg. 456 ppm

Note: All tree mineralization data are ppm in ashed sample.

SCAN # 101 Average spectra of trees 262, 263, 265, 266, 267, 268, 269, 272

PERCENT DIRECTIONAL REFLECTANCE

PDR (X100)	WVL (NM)	0 10 20 30 40 50 60 70 80 90 100
350	400	+
369	412	+
382	425	+
396	437	+
398	450	+
395	462	+
399	475	+
403	487	+
402	500	+
434	512	+
516	525	+
602	537	+
686	550	+
728	562	+
715	575	+
669	587	+
639	600	+
627	612	+
605	625	+
605	637	+
601	650	+
589	662	+
734	675	+
1039	687	+
1555	700	*
2207	712	*
2790	725	*
3676	737	*
3836	750	*
3911	762	*
3955	775	*
4000	787	*
4043	800	*
4090	812	*
4129	825	*
4171	837	*
4189	850	*
4212	862	*
4216	875	*
4222	887	*
4237	900	*
4247	912	*
4228	925	*
4182	937	*
4105	950	*
4041	962	*
4063	975	*
4096	987	*
4187	1000	*
4284	1025	*
4485	1050	*
4633	1075	*

(X100) (NM)

Ponderosa Pine

SCAN # 259 Average spectra of trees 461, 462

PERCENT DIRECTIONAL REFLECTANCE

PDR (X100)	WVL (NM)	0 10 20 30 40 50 60 70 80 90 100
336	400	+
347	412	+
359	425	+
368	437	+
362	450	+
350	462	+
353	475	+
354	487	+
353	500	+
381	512	+
450	525	+
529	537	+
616	550	+
658	562	+
649	575	+
619	587	+
603	600	+
594	612	+
589	625	+
604	637	+
615	650	+
610	662	+
706	675	+
983	687	+
1474	700	*
2136	712	*
2704	725	*
3553	737	*
3758	750	*
3837	762	*
3874	775	*
3913	787	*
3958	800	*
3979	812	*
4009	825	*
4043	837	*
4073	850	*
4090	862	*
4119	875	*
4158	887	*
4214	900	*
4332	912	*
4365	925	*
4332	937	*
4220	950	*
4141	962	*
4162	975	*
4198	987	*
4208	1000	*
4285	1025	*
4434	1050	*
4496	1075	*

(X100) (NM) 0 10 20 30 40 50 60 70 80 90 100

C.2

Ponderosa Pine

SCAN # 229 Average spectra of trees 561, 562, 563

PERCENT DIRECTIONAL REFLECTANCE

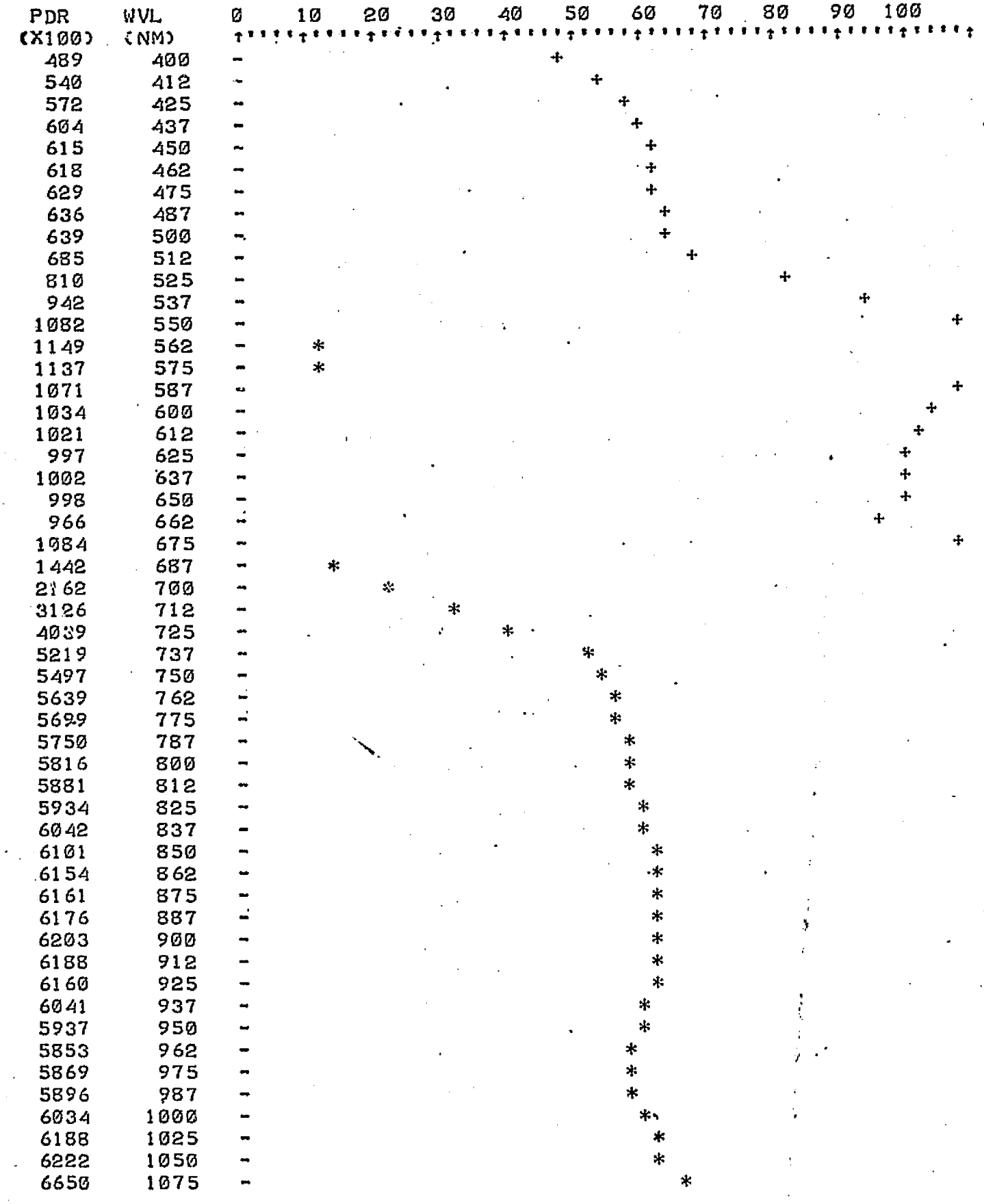

SCAN # 179 Average spectra of trees 160, 162, 164, 165

PERCENT DIRECTIONAL REFLECTANCE

PDR (X100)	WVL (NM)	0 10 20 30 40 50 60 70 80 90 100
331	400	+
343	412	+
352	425	+
355	437	+
348	450	+
346	462	+
348	475	+
349	487	+
350	500	+
377	512	+
448	525	+
528	537	+
601	550	+
633	562	+
609	575	+
562	587	+
533	600	+
519	612	+
506	625	+
525	637	+
532	650	+
525	662	+
590	675	+
827	687	+
1296	700	*
1948	712	*
2560	725	*
3402	737	*
3612	750	*
3705	762	*
3745	775	*
3787	787	*
3829	800	*
3851	812	*
3878	825	*
3921	837	*
3944	850	*
3950	862	*
3994	875	*
4009	887	*
4070	900	*
4092	912	*
4101	925	*
4066	937	*
3966	950	*
3885	962	*
3874	975	*
3918	987	*
4006	1000	*
4094	1025	*
4211	1050	*
4357	1075	*
(X100)	(NM)	0 10 20 30 40 50 60 70 80 90 100

Ponderosa Pine

SCAN # 387 Average spectra of trees 361, 362, 363, 368, 371, 372

PERCENT DIRECTIONAL REFLECTANCE

PDR (X100)	WVL (NM)	0 10 20 30 40 50 60 70 80 90 100
158	400	+
166	412	+
175	425	+
187	437	+
199	450	+
220	462	+
224	475	+
229	487	+
241	500	+
267	512	+
316	525	+
380	537	+
437	550	+
464	562	+
445	575	+
402	587	+
376	600	+
363	612	+
350	625	+
371	637	+
398	650	+
418	662	+
474	675	+
621	687	+
924	700	+
1385	712	*
1814	725	*
2440	737	*
2616	750	*
2718	762	*
2777	775	*
2824	787	*
2880	800	*
2912	812	*
2947	825	*
2974	837	*
3001	850	*
3010	862	*
3029	875	*
3026	887	*
3059	900	*
3077	912	*
3076	925	*
3055	937	*
2975	950	*
2951	962	*
2964	975	*
3018	987	*
3109	1000	*
3208	1025	*
3259	1050	*
3319	1075	*

(X100) (NM) 0 10 20 30 40 50 60 70 80 90 100

APPENDIX E

Copper Creek

Average Alligator Bark Juniper Spectra

Scan #79

Tree #	Cu(ppm)
201	3
206	0
210	13
213	0
214	75
215	10
Average	17 ppm

Scan #241

Tree #	Cu(ppm)
401	0
402	33
403	0
405	200
Average	58 ppm

Scan #319

Tree #	Cu(ppm)
501	163
502	200
503	180
505	150
506	200
Average	179 ppm

Scan #176

Tree #	Cu(ppm)
110	25
112	25
114	12
Average	21 ppm

Scan #402

Tree #	Cu(ppm)
312	Core Zone - No Cu measurement available.

SCAN # 79 Average spectra of trees 201, 206, 210, 213, 214, 215

PERCENT DIRECTIONAL REFLECTANCE

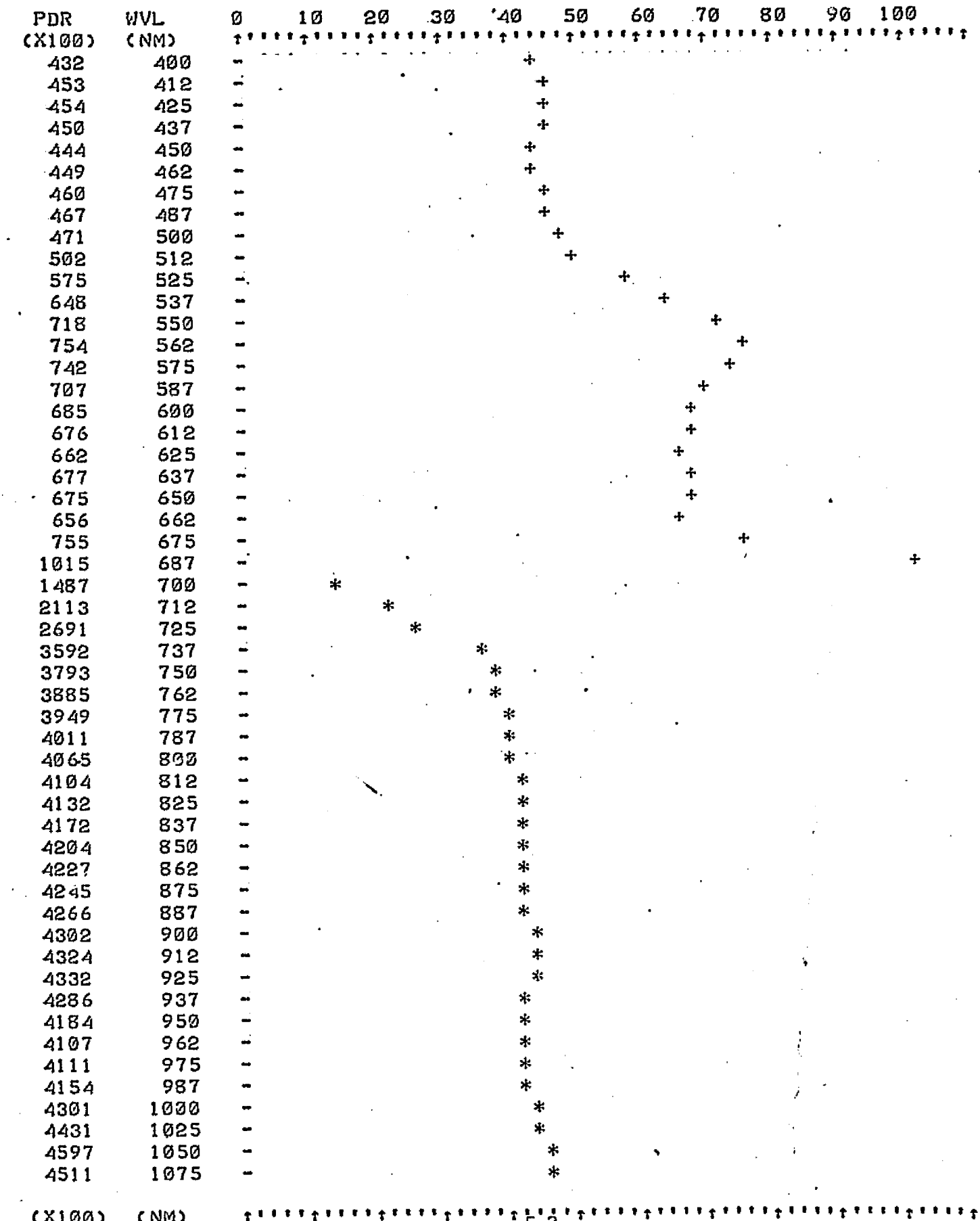

Alligator Bark Juniper

SCAN # 241 Average spectra of trees 401, 402, 403, 405 Av. Cu 58 ppm

PERCENT DIRECTIONAL REFLECTANCE

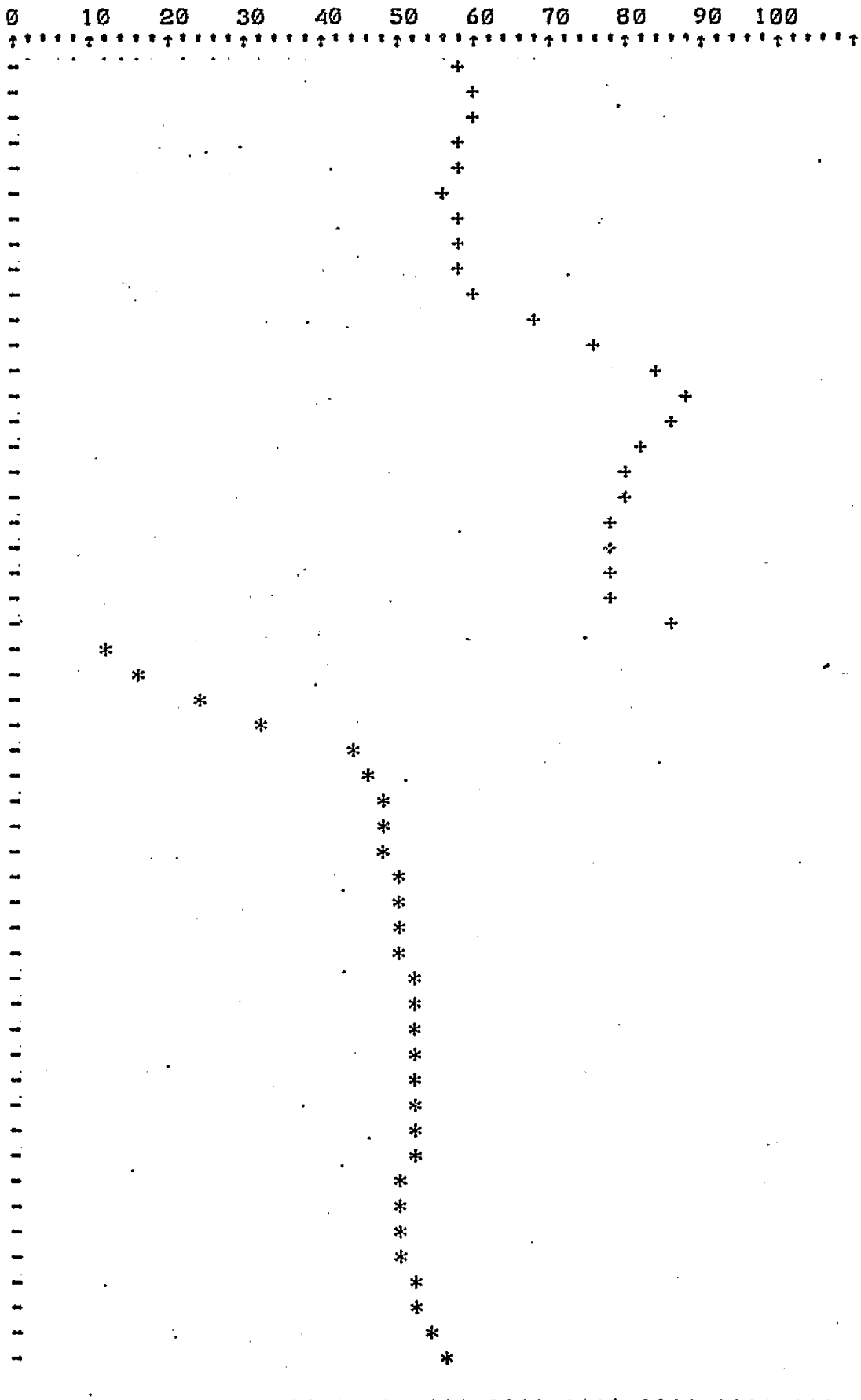

PDR (X100)	WVL (NM)
573	400
595	412
596	425
589	437
575	450
567	462
574	475
578	487
575	500
606	512
680	525
756	537
839	550
880	562
867	575
826	587
797	600
792	612
779	625
788	637
786	650
774	662
865	675
1153	687
1686	700
2419	712
3127	725
4360	737
4613	750
4735	762
4808	775
4855	787
4916	800
4959	812
5003	825
5058	837
5102	850
5136	862
5149	875
5145	887
5233	900
5281	912
5263	925
5202	937
5064	950
4962	962
4954	975
5005	987
5147	1000
5292	1025
5482	1050
5550	1075

(X100) (NM)

Alligator Bark Juniper

SCAN # 319 Average spectra of trees 501, 502, 503, 505, 506 Av. Cu 179 ppm

PERCENT DIRECTIONAL REFLECTANCE

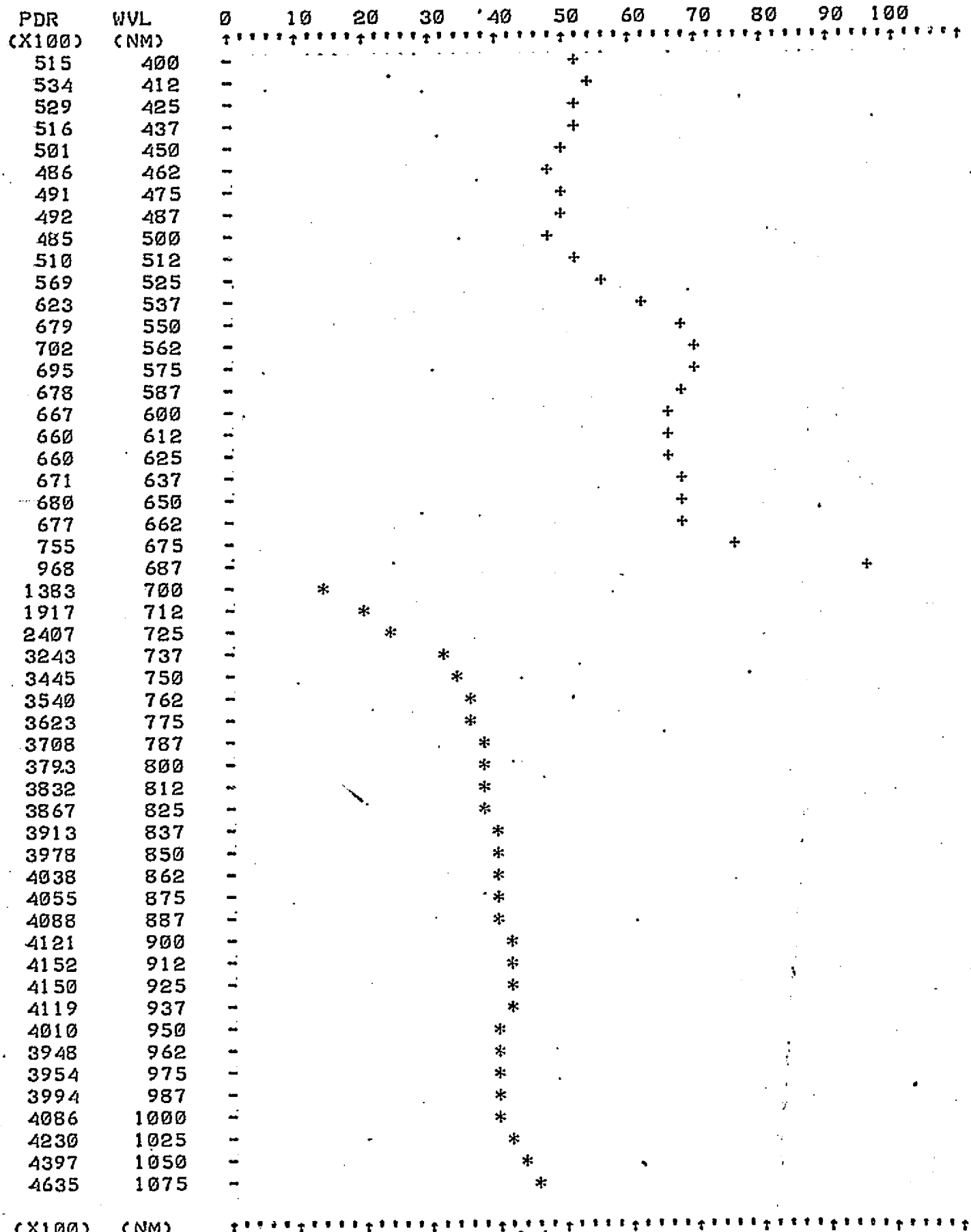

PDR (X100)	WVL (NM)
515	400
534	412
529	425
516	437
501	450
486	462
491	475
492	487
485	500
510	512
569	525
623	537
679	550
702	562
695	575
678	587
667	600
660	612
660	625
671	637
680	650
677	662
755	675
968	687
1383	700
1917	712
2407	725
3243	737
3445	750
3540	762
3623	775
3708	787
3793	800
3832	812
3867	825
3913	837
3978	850
4038	862
4055	875
4088	887
4121	900
4152	912
4150	925
4119	937
4010	950
3948	962
3954	975
3994	987
4086	1000
4230	1025
4397	1050
4635	1075

(X100) (NM)

Alligator Bark Juniper

SCAN # 176 Average spectra of trees 110, 112, 114 Av. Cu 21 ppm

PERCENT DIRECTIONAL REFLECTANCE

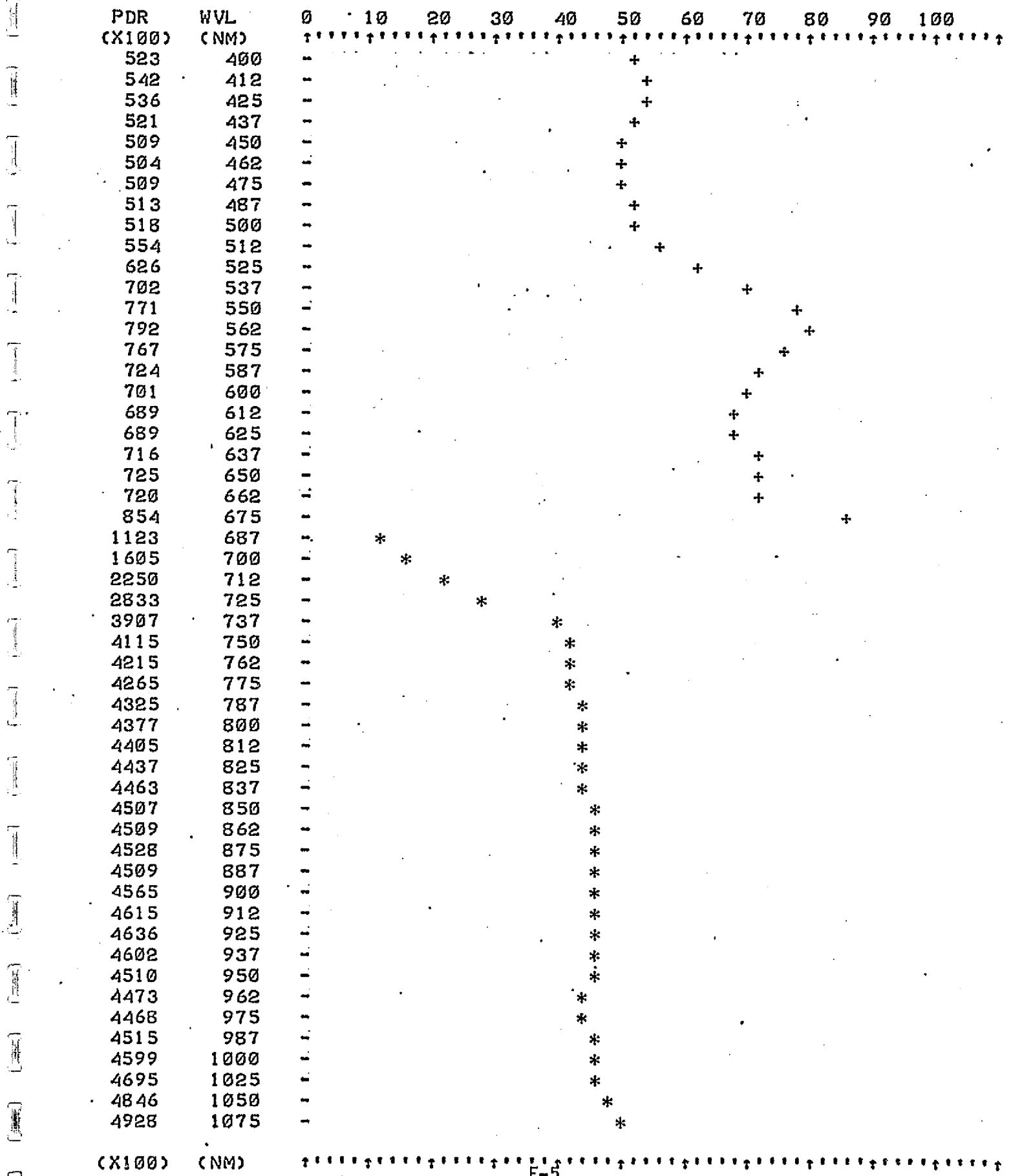

SCAN # 402 Average spectra of tree 312

Core Zone - Unknown ppm Cu

PERCENT DIRECTIONAL REFLECTANCE

PDR (X100)	WVL (NM)
160	400
178	412
180	425
188	437
209	450
242	462
256	475
269	487
294	500
344	512
421	525
507	537
565	550
588	562
559	575
515	587
496	600
484	612
458	625
478	637
521	650
535	662
600	675
795	687
1164	700
1654	712
1895	725
2490	737
2704	750
2781	762
2771	775
2801	787
2885	800
2894	812
2971	825
3013	837
2992	850
2956	862
2961	875
2945	887
2878	900
2832	912
2823	925
2818	937
2739	950
2644	962
2616	975
2633	987
2844	1000
3194	1025
3321	1050
3210	1075

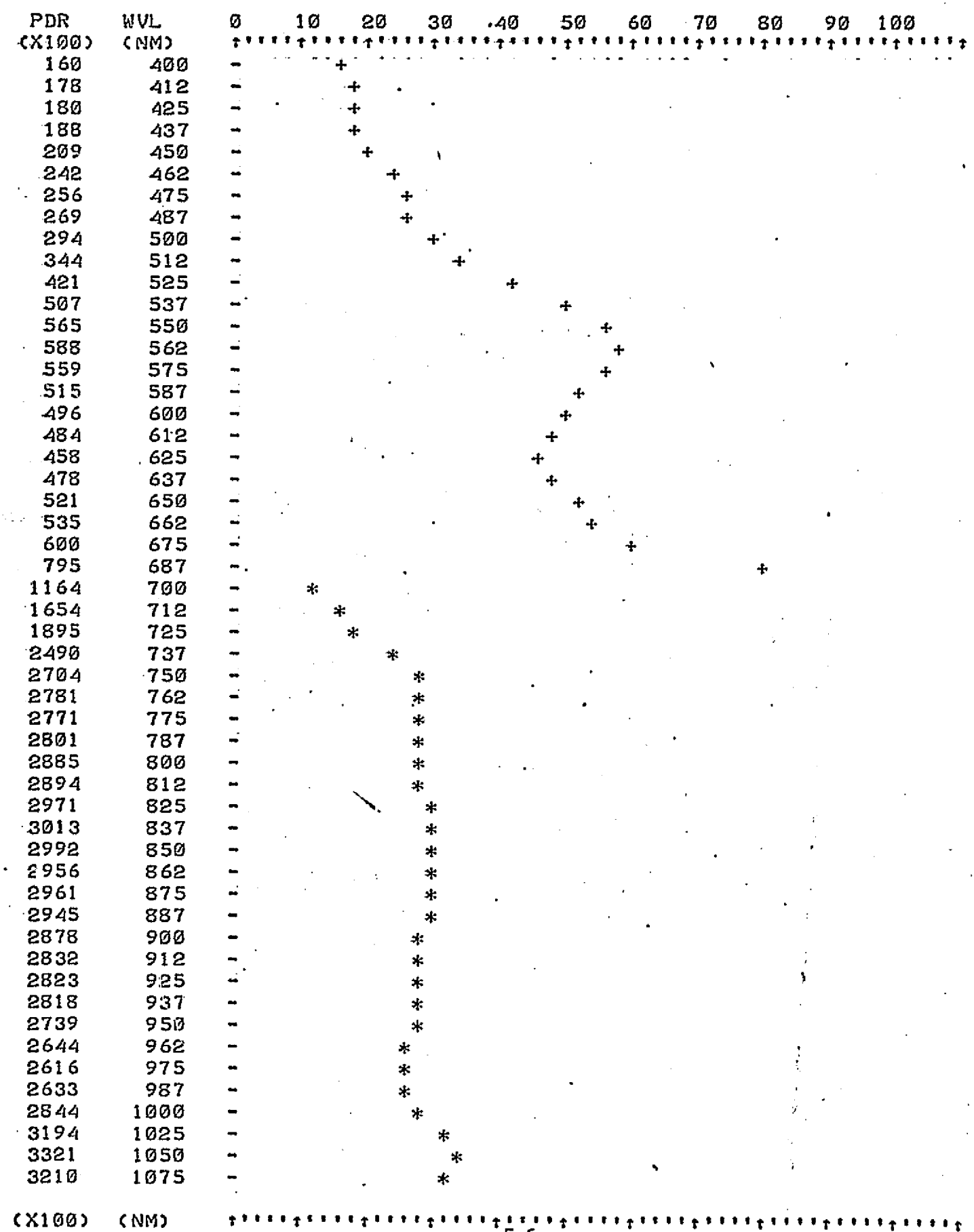

APPENDIX F

Copper Creek Average Emory Oak Spectra

Scan #103

Tree #	Cu(ppm)
234	38
235	28
236	75
237	0
238	63
239	25
240	38
241	250
Average	36 ppm

Scan #248

Tree #	Cu(ppm)
431	55
432	75
433	45
Average	58 ppm

Scan #220

Tree #	Cu(ppm)
531	163
532	200
533	210
534	225
538	175
539	125
Average	183 ppm

Scan # 212

Tree #	Cu(ppm)
133	90
134	40
137	375
138	250
Average	188 ppm

Scan #378

Tree #	Cu(ppm)
332	240
333	200
336	225
341	No data (Core Zone)
Average	222 ppm

Emory Oak

#SCAN # 103 Average spectra of trees 234, 235, 236, 237, 238, 239, 240, 241

PERCENT DIRECTIONAL REFLECTANCE

PDR (X100)	WVL (NM)	0 10 20 30 40 50 60 70 80 90 100
382	400	+
396	412	+
399	425	+
392	437	+
377	450	+
366	462	+
367	475	+
371	487	+
368	500	+
387	512	+
435	525	+
491	537	+
555	550	+
588	562	+
580	575	+
552	587	+
539	600	+
536	612	+
537	625	+
557	637	+
574	650	+
582	662	+
655	675	+
876	687	+
1304	700	*
1887	712	*
2441	725	*
3427	737	*
3644	750	*
3742	762	*
3797	775	*
3850	787	*
3905	800	*
3931	812	*
3971	825	*
4017	837	*
4067	850	*
4107	862	*
4122	875	*
4143	887	*
4220	900	*
4284	912	*
4335	925	*
4353	937	*
4314	950	*
4297	962	*
4314	975	*
4354	987	*
4408	1000	*
4451	1025	*
4549	1050	*
4638	1075	*

(X100) (NM)

SCAN # 248 Average spectra of trees 431, 432, 433

PERCENT DIRECTIONAL REFLECTANCE

PDR (X100)	WVL (NM)	0 10 20 30 40 50 60 70 80 90 100
373	400	+
388	412	+
392	425	+
389	437	+
374	450	+
360	462	+
362	475	+
366	487	+
364	500	+
384	512	+
444	525	+
513	537	+
595	550	+
634	562	+
625	575	+
593	587	+
575	600	+
569	612	+
559	625	+
572	637	+
585	650	+
583	662	+
657	675	+
888	687	+
1329	700	*
1928	712	*
2476	725	*
3328	737	*
3529	750	*
3615	762	*
3645	775	*
3694	787	*
3736	800	*
3770	812	*
3795	825	*
3860	837	*
3942	850	*
4003	862	*
4017	875	*
4029	887	*
4076	900	*
4134	912	*
4222	925	*
4253	937	*
4210	950	*
4197	962	*
4221	975	*
4213	987	*
4253	1000	*
4286	1025	*
4381	1050	*
4472	1075	*

(X100) (NM) 0 10 20 30 40 50 60 70 80 90 100

Emory Oak

SCAN # 220 Average spectra of trees 531, 532, 533, 534, 538, 539

PERCENT DIRECTIONAL REFLECTANCE

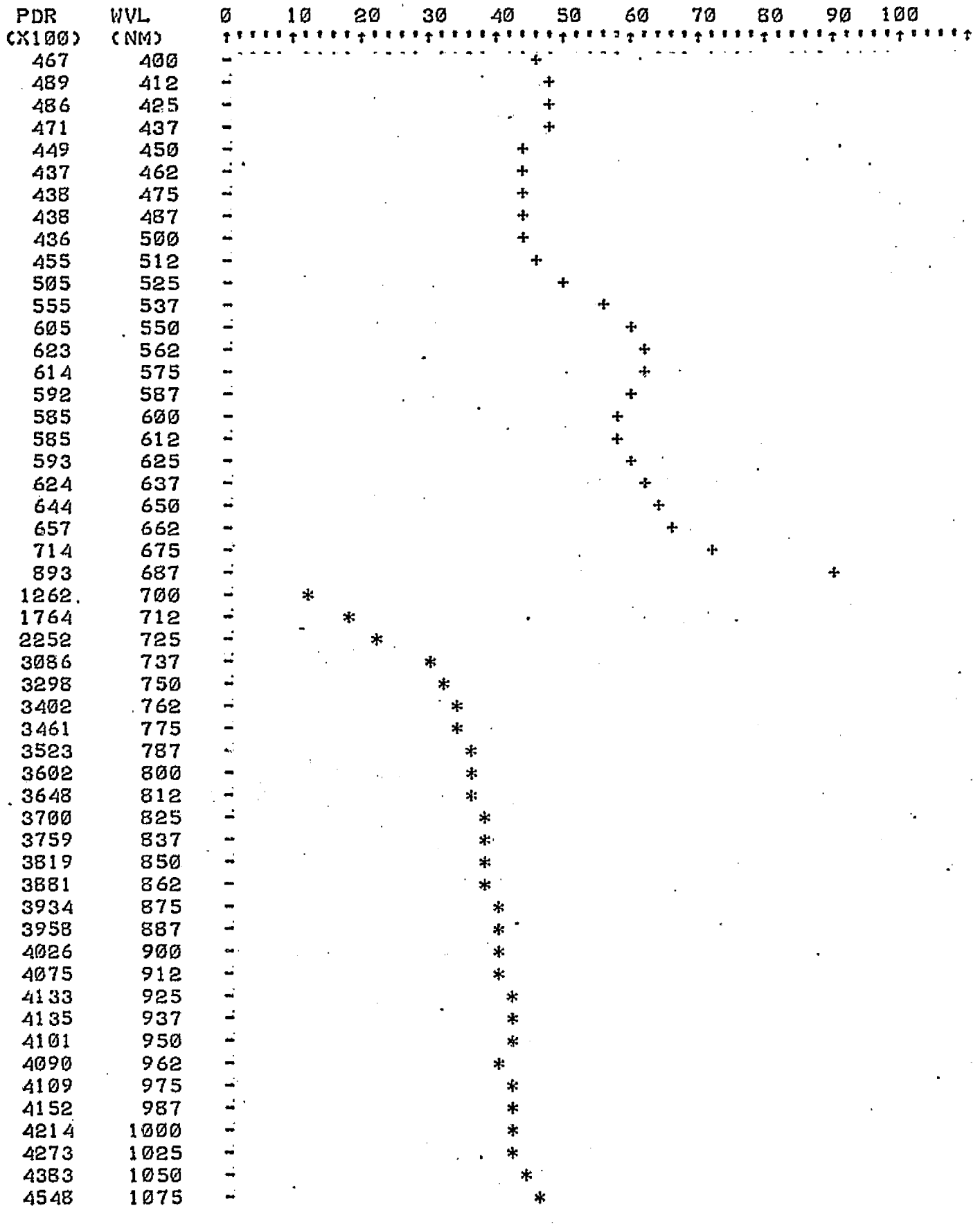

PDR (X100)	WVL (NM)
467	400
489	412
486	425
471	437
449	450
437	462
438	475
438	487
436	500
455	512
505	525
555	537
605	550
623	562
614	575
592	587
585	600
585	612
593	625
624	637
644	650
657	662
714	675
893	687
1262.	700
1764	712
2252	725
3086	737
3298	750
3402	762
3461	775
3523	787
3602	800
3648	812
3700	825
3759	837
3819	850
3881	862
3934	875
3958	887
4026	900
4075	912
4133	925
4135	937
4101	950
4090	962
4109	975
4152	987
4214	1000
4273	1025
4383	1050
4548	1075

(X100) (NM)

Emory Oak

SCAN # 212 Average spectra of trees 133, 134, 137, 138

PERCENT DIRECTIONAL REFLECTANCE

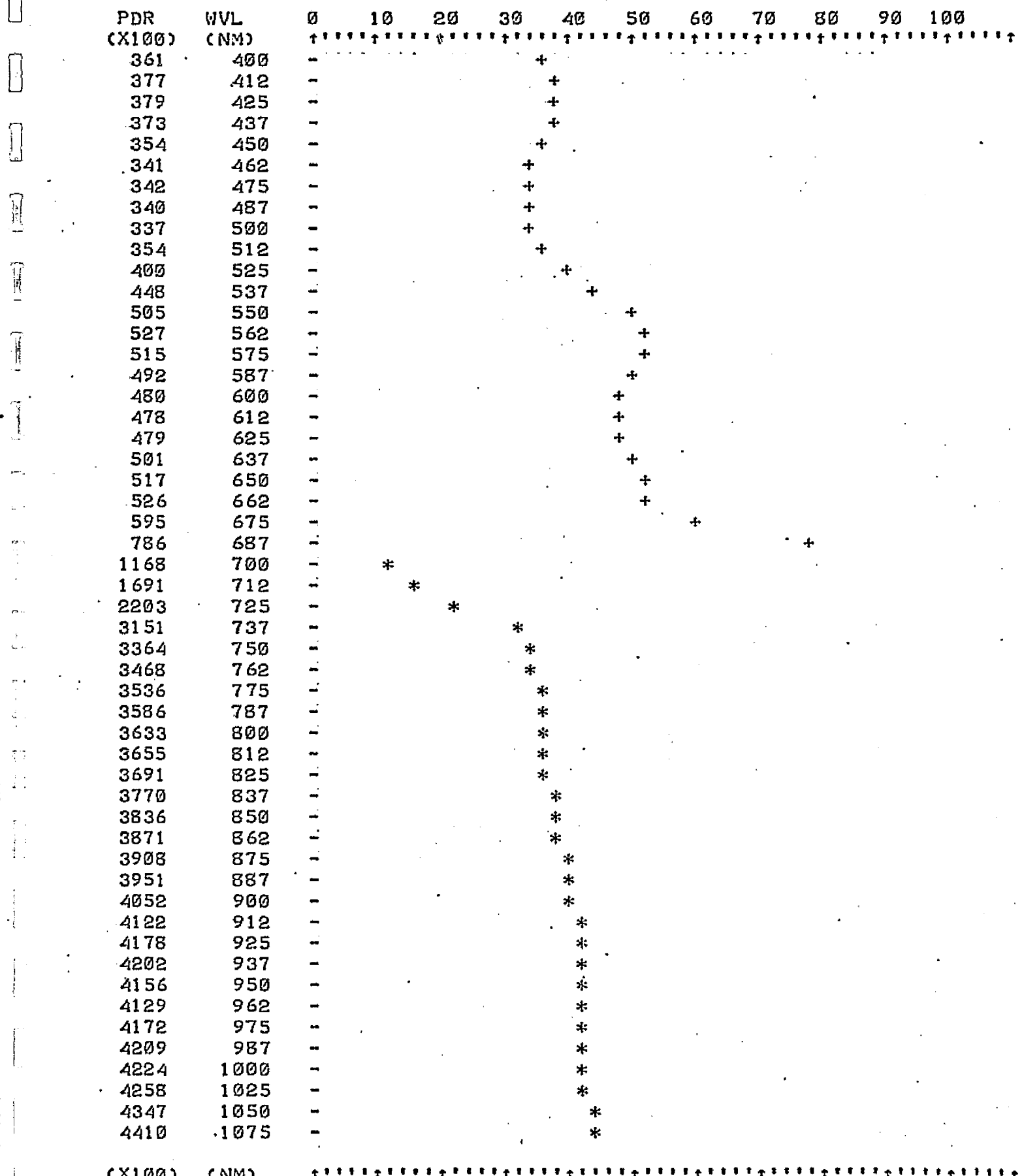

Emory Oak

SCAN # 378 Average spectra of trees 332, 333, 336, 341

PERCENT DIRECTIONAL REFLECTANCE

PDR (X100)	WVL (NM)
273	400
289	412
295	425
299	437
306	450
332	462
340	475
346	487
365	500
400	512
450	525
527	537
595	550
631	562
602	575
546	587
520	600
508	612
498	625
525	637
570	650
598	662
640	675
803	687
1149	700
1655	712
2133	725
2825	737
3017	750
3129	762
3194	775
3276	787
3344	800
3379	812
3405	825
3454	837
3477	850
3477	862
3508	875
3520	887
3573	900
3606	912
3614	925
3620	937
3616	950
3602	962
3614	975
3654	987
3780	1000
3886	1025
3923	1050
4029	1075

(X100) (NM)

APPENDIX G

Copper Basin Manzanita Spectra

Manzanita No.	Scan No.	Cu (ppm)	Mo (ppm)	Remarks
431	1411	190	13	Background; Data looks erratic
431.5	1374	201	77	Background; Data looks fair
432	1514	92	0	Background; Data looks fair
433	1509	107	7	Background; Data looks fair
435	1505	2390	101	Anomalous; Data looks fair
436	1501	2650	111	Anomalous; Data looks fair

††† Background Manzanita #431 - Copper Basin, Cu 190 ppm, Mo 13 ppm

†AVERAGE OF SCANS # [1411] 1412 1413

PERCENT DIRECTIONAL REFLECTANCE

PDR (%X10)	WVL (NM)
34	400
33	412
34	425
37	437
41	450
43	462
43	475
45	487
45	500
49	512
51	525
60	537
64	550
71	562
70	575
75	587
72	600
79	612
80	625
86	637
84	650
81	662
71	675
85	687
164	700
221	712
264	725
303	737
308	750
323	762
337	775
331	787
343	800
347	812
351	825
343	837
355	850
361	862
373	875
364	887
378	900
361	912
382	925
370	937
351	950
366	962
331	975
366	987
389	1000
337	1025
370	1050
490	1075

(%X10) (NM)

††† Background Manzanita #431.5 - Copper Basin, Cu 201 ppm, Mo 77 ppm

†AVERAGE OF SCANS # [1374] 1375 1376

PERCENT DIRECTIONAL REFLECTANCE

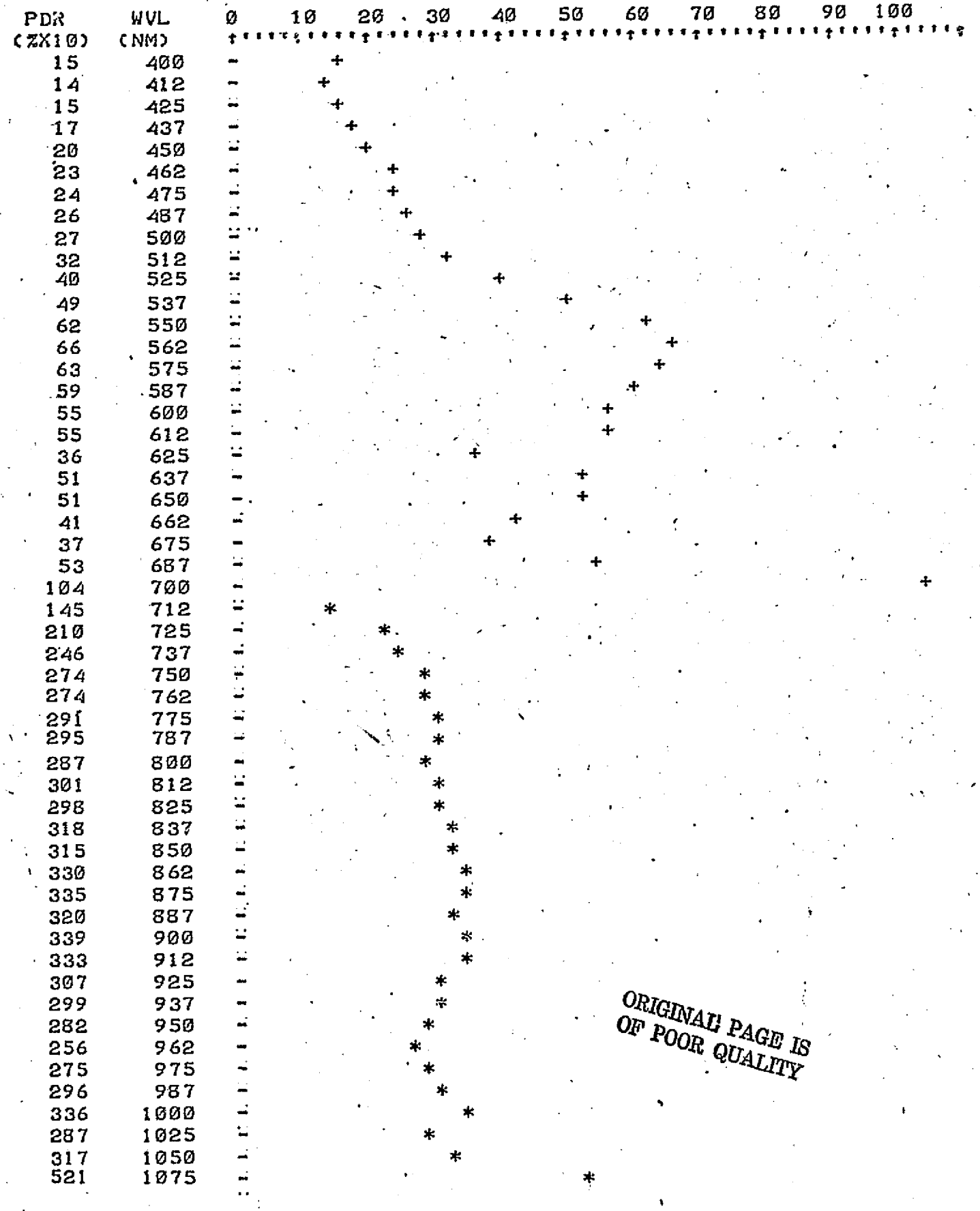

††† Background Manzanita #432, Copper Basin - Cu 92 ppm, Mo 0 ppm

†AVERAGE OF SCANS # 1514 1515

PERCENT DIRECTIONAL REFLECTANCE

PDR (%X10)	WVL (NM)
29	400
27	412
29	425
35	437
41	450
49	462
52	475
53	487
54	500
58	512
66	525
76	537
86	550
91	562
94	575
92	587
91	600
92	612
96	625
93	637
95	650
76	662
98	675
116	687
234	700
341	712
428	725
461	737
531	750
564	762
532	775
525	787
571	800
594	812
556	825
631	837
585	850
588	862
621	875
603	887
596	900
576	912
569	925
601	937
646	950
591	962
588	975
540	987
639	1000
632	1025
450	1050
614	1075

(%X10) (NM)

††† Background Manzanita #433 – Copper Basin, Cu 107 ppm, Mo 7 ppm

AVERAGE OF SCANS # 1509 1510 1511 1512

PERCENT DIRECTIONAL REFLECTANCE

PDR (%X10)	WVL (NM)
35	400
37	412
33	425
46	437
53	450
59	462
60	475
63	487
67	500
70	512
84	525
95	537
103	550
114	562
116	575
104	587
107	600
106	612
100	625
101	637
95	650
93	662
83	675
99	687
171	700
235	712
295	725
358	737
384	750
398	762
397	775
415	787
429	800
448	812
457	825
456	837
455	850
459	862
469	875
496	887
466	900
488	912
491	925
486	937
483	950
468	962
494	975
510	987
468	1000
523	1025
521	1050
524	1075

(%X10) (NM)

††† Anomalous Manzanita #435 – Copper Basin, Cu > 2390 ppm, Mo 101 ppm

AVERAGE OF SCANS # 1505 1506 1507

PERCENT DIRECTIONAL REFLECTANCE

PDR (%X10)	WVL (NM)
84	400
78	412
82	425
96	437
113	450
126	462
135	475
139	487
144	500
153	512
173	525
206	537
244	562
245	587
230	600
228	612
220	625
219	637
206	650
193	662
189	675
231	687
430	700
559	712
653	725
729	737
764	750
778	762
791	775
793	787
820	800
814	812
829	825
820	837
847	850
834	862
832	875
841	887
852	900
849	912
809	925
796	937
773	950
770	962
736	975
742	987
765	1000
809	1025
842	1050
791	1075

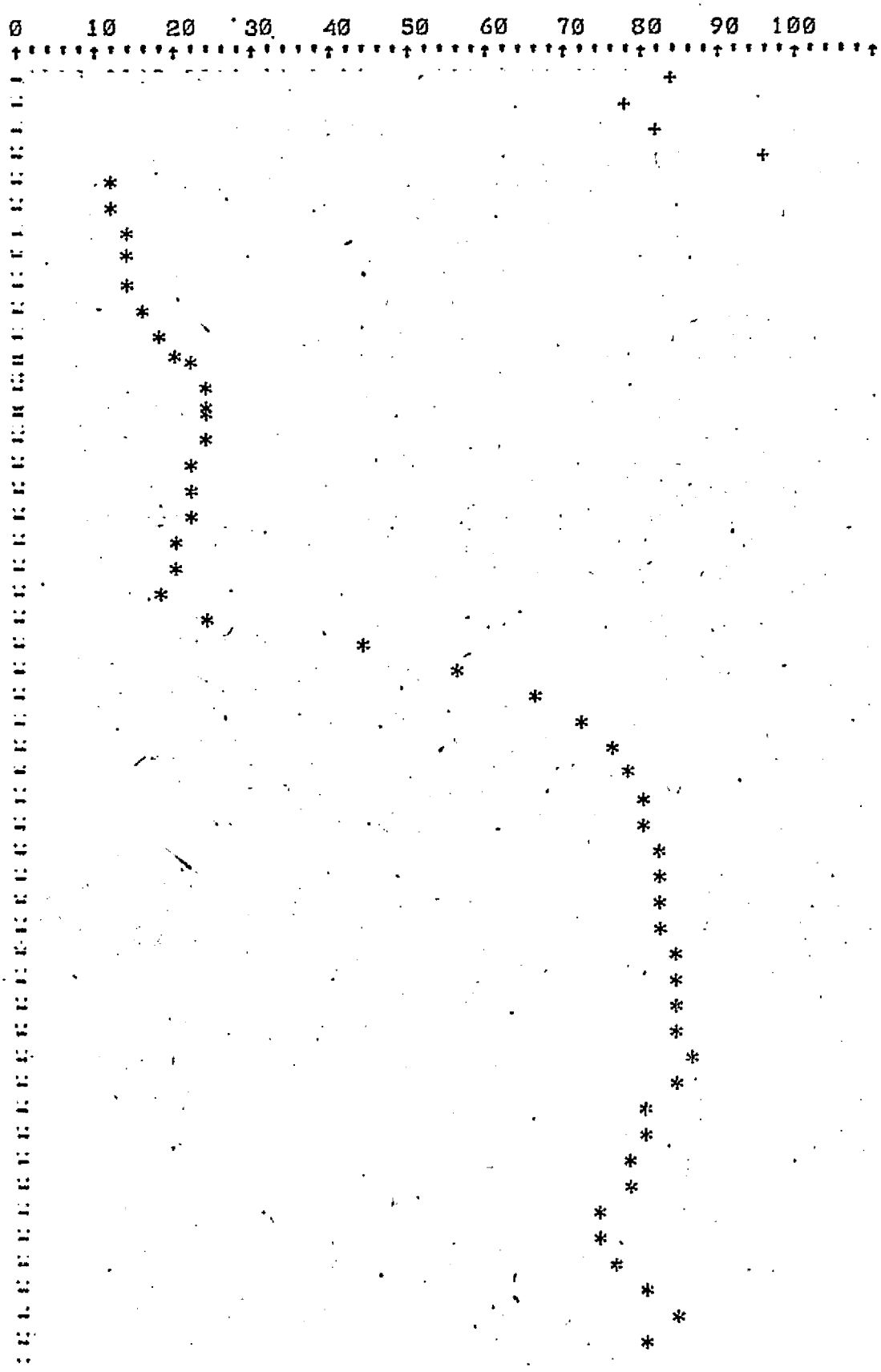

(%X10) (NM)

††† Anomalous Manzanita #436 - Copper Basin, Cu > 2650 ppm, Mo 111 ppm

AVERAGE OF SCANS # 1501 1502 1503

PERCENT DIRECTIONAL REFLECTANCE

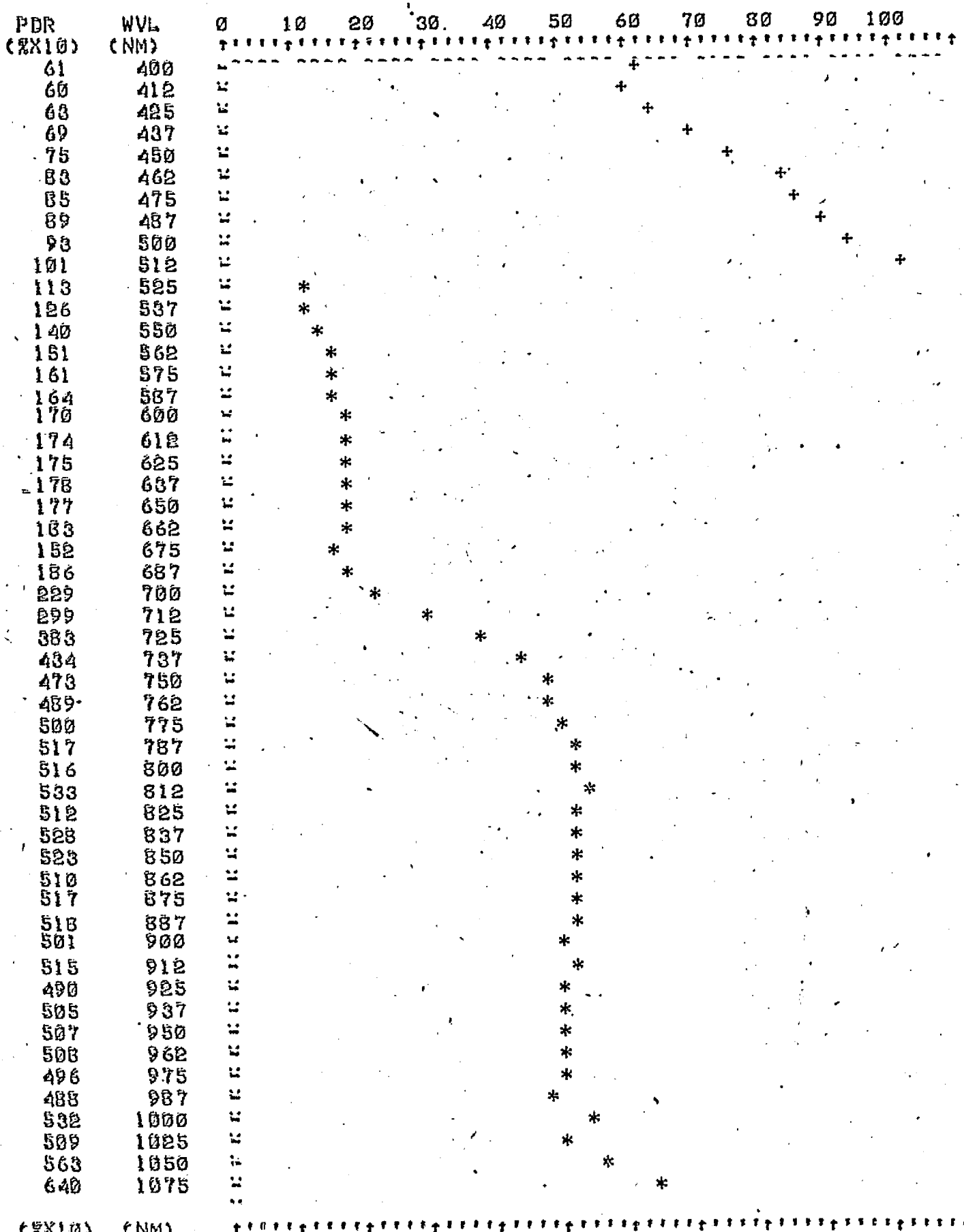

APPENDIX H

Copper Basin Pinion Pine Spectra

Pinion Pine No.	Scan No.	Cu (ppm)	Mo (ppm)	Remarks
461	1368	264	15	Background; cloudy conditions.
462	1387	218	12	Background; good data.
463	1393	252	29	Background; good data, poor tree.
464	1497	193	12	Background; good data.
465	1408	206	52	Background; cloudy conditions.
466	1469*	188	70	Background; fair data.
467	1481*	186	12	Background; good data.
468	1465	199	42	Background; fair data.
472	1477*	177	23	Background; good data.
479	1439	2220	47	Anomalous; fair data.
480	1485*	835	12	Anomalous; good data.
482	1489*	780	65	Anomalous; good data.
485	1473*	1275	105	Anomalous; good data.
487	1493*	987	99	Anomalous; good data.
488	1456	1200	62	Anomalous; Fair data.

*Spectra taken under similar conditions.

††† Background Pinion Pine #461, Copper Basin - Cu 264 ppm, Mo 15 ppm

JAVERAGE OF SCANS # 1368 1369 1370

PERCENT DIRECTIONAL REFLECTANCE

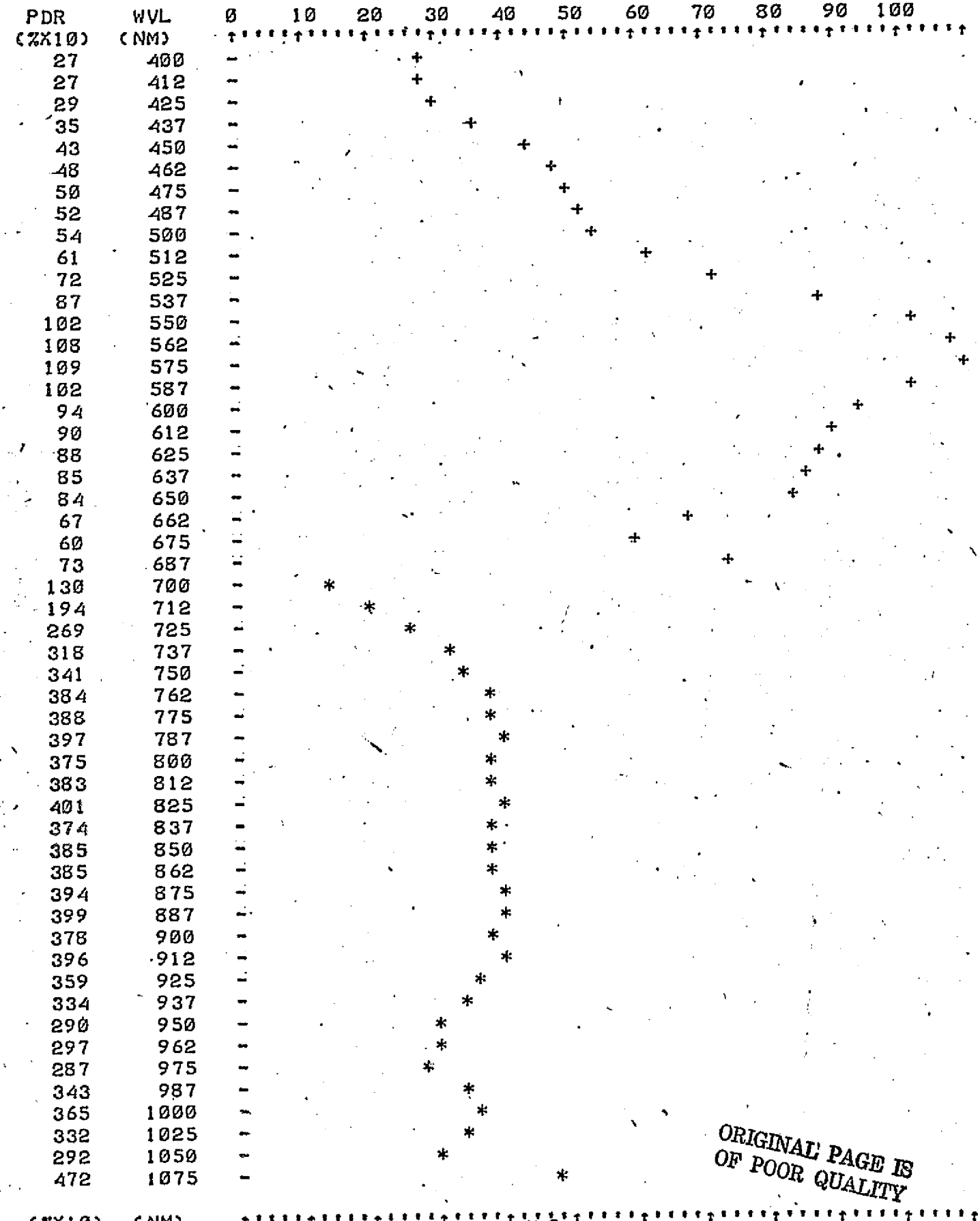

††† Background Pinion Pine #462, Copper Basin - Cu 218 ppm, Mo 12 ppm

AVERAGE OF SCANS # 1387 1388 1389

PERCENT DIRECTIONAL REFLECTANCE

PDR (%X10)	WVL (NM)
52	400
52	412
55	425
65	437
70	450
74	462
79	475
81	487
83	500
92	512
108	525
131	537
151	550
171	562
167	575
164	587
154	600
151	612
135	625
137	637
132	650
118	662
121	675
137	687
289	700
416	712
520	725
556	737
621	750
629	762
676	775
636	787
631	800
641	812
613	825
643	837
637	850
643	862
641	875
654	887
648	900
689	912
636	925
660	937
643	950
641	962
637	975
635	987
633	1000
640	1025
634	1050
582	1075

0 10 20 30 40 50 60 70 80 90 100

(%X10) (NM)

Background Pinion Pine #464, Copper Basin - Cu 193 ppm, Mo 12 ppm

AVERAGE OF SCANS # 1497 1498 1499

PERCENT DIRECTIONAL REFLECTANCE

PDR (%X10)	WVL (NM)
71	400
68	412
71	425
78	437
81	450
84	462
86	475
90	487
89	500
99	512
114	525
130	537
149	550
155	562
156	575
144	587
139	600
136	612
131	625
127	637
123	650
115	662
104	675
118	687
159	700
219	712
288	725
352	737
387	750
396	762
407	775
416	787
407	800
406	812
401	825
406	837
414	850
413	862
418	875
416	887
406	900
415	912
406	925
417	937
407	950
407	962
404	975
404	987
447	1000
457	1025
491	1050
551	1075

(%X10) (NM)

Background Pinion Pine #465, Copper Basin - Cu 206 ppm, Mo 52 ppm

AVERAGE OF SCANS # 1408 1409 1410

PERCENT DIRECTIONAL REFLECTANCE

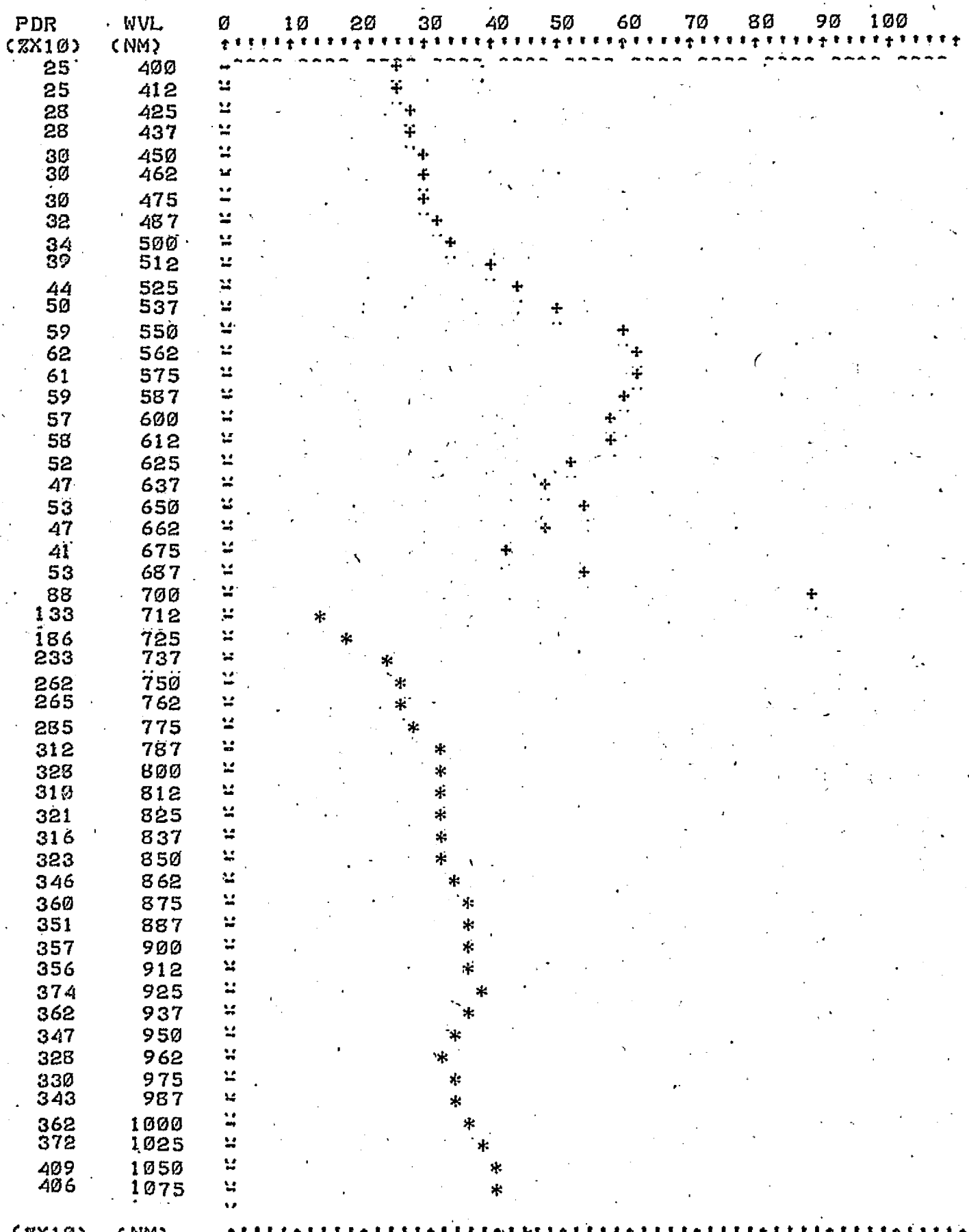

PDR (%X10)	WVL (NM)
25	400
25	412
28	425
28	437
30	450
30	462
30	475
32	487
34	500
39	512
44	525
50	537
59	550
62	562
61	575
59	587
57	600
58	612
52	625
47	637
53	650
47	662
41	675
53	687
88	700
133	712
186	725
233	737
262	750
265	762
285	775
312	787
328	800
310	812
321	825
316	837
323	850
346	862
360	875
351	887
357	900
356	912
374	925
362	937
347	950
328	962
330	975
343	987
362	1000
372	1025
409	1050
406	1075

*** Background Pinion Pine #466, Copper Basin - Cu 188 ppm, Mo 79 ppm

AVERAGE OF SCANS # 1469 1470 1471

PERCENT DIRECTIONAL REFLECTANCE

PDR (%X10)	WVL (NM)
54	400
53	412
59	425
68	437
75	450
78	462
79	475
84	487
86	500
98	512
120	525
142	537
167	550
177	562
176	575
166	587
159	600
152	612
148	625
138	637
131	650
116	662
131	675
158	687
318	700
464	712
600	725
660	737
694	750
746	762
734	775
739	787
752	800
756	812
758	825
754	837
758	850
762	862
764	875
760	887
781	900
772	912
740	925
682	937
710	950
719	962
744	975
698	987
706	1000
709	1025
771	1050
852	1075

Background Pinion Pine # 467, Copper Basin - Cu 186 ppm, Mo 12 ppm

AVERAGE OF SCANS # 1481 1482 1483

PERCENT DIRECTIONAL REFLECTANCE

PDR (%X10)	WVL (NM)
51	400
50	412
53	425
61	437
65	450
67	462
69	475
72	487
74	500
84	512
97	525
114	537
128	550
132	562
132	575
125	587
120	600
119	612
116	625
110	637
105	650
95	662
108	675
122	687
206	700
283	712
357	725
380	737
394	750
414	762
414	775
418	787
411	800
411	812
401	825
400	837
405	850
413	862
412	875
401	887
397	900
405	912
388	925
374	937
398	950
432	962
405	975
413	987
420	1000
439	1025
451	1050
554	1075

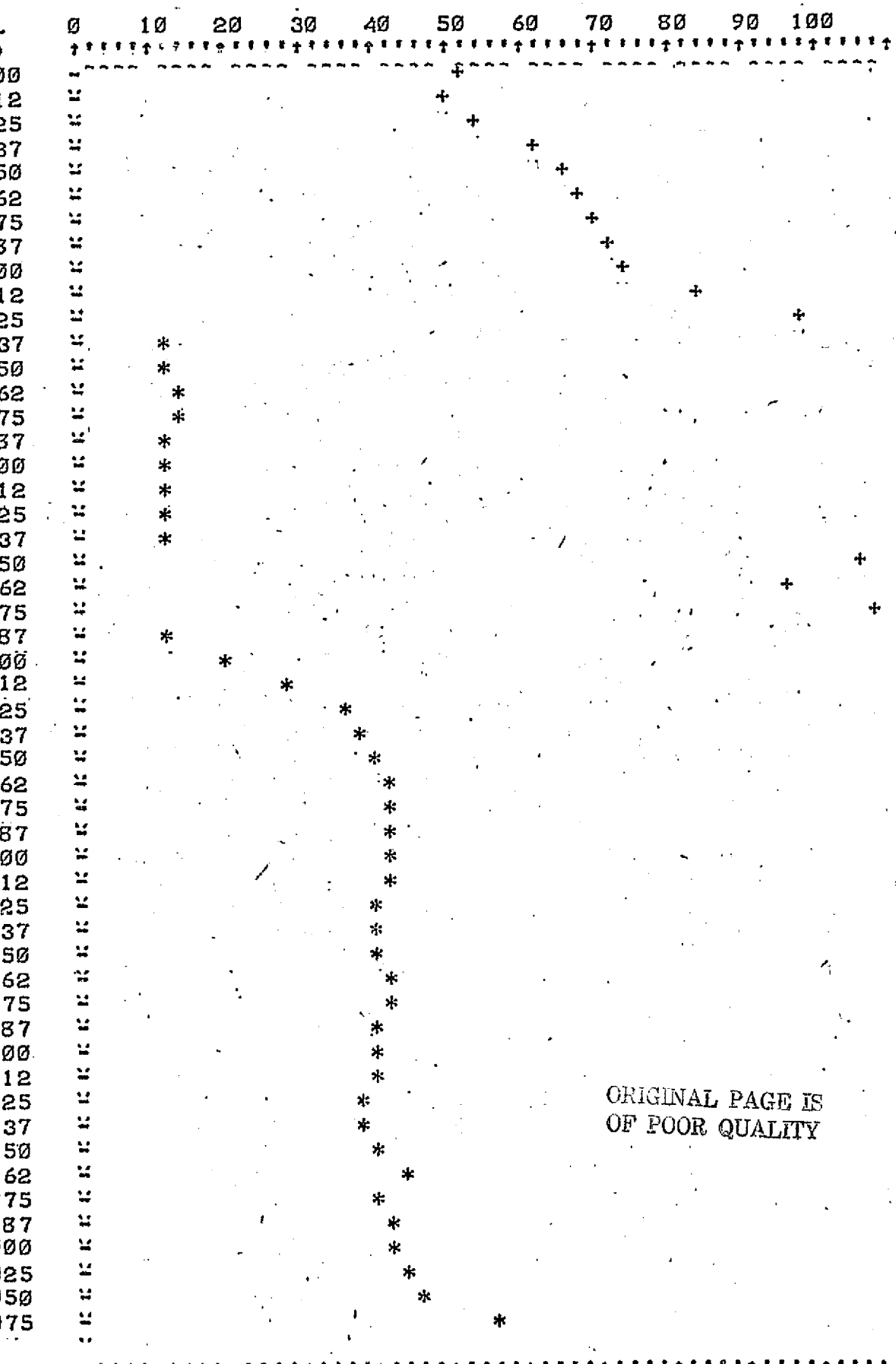

(%X10) (NM)

††† Background Pinion Pine #468, Copper Basin - Cu 199 ppm, Mo 42 ppm

‡AVERAGE OF SCANS # 1465 1466 1467

PERCENT DIRECTIONAL REFLECTANCE

PDR (%X10)	WVL (NM)
38	400
38	412
39	425
54	437
57	450
59	462
60	475
62	487
65	500
72	512
84	525
98	537
112	550
118	562
116	575
115	587
109	600
106	612
104	625
99	637
97	650
90	662
89	675
116	687
215	700
309	712
382	725
430	737
475	750
510	762
531	775
529	787
538	800
542	812
553	825
574	837
569	850
564	862
557	875
549	887
563	900
566	912
587	925
497	937
506	950
563	962
532	975
510	987
575	1000
525	1050
687	1075

(%X10) (NM)

††† Background Pinion Pine #472, Copper Basin - Cu 177 ppm, Mo 23 ppm

†AVERAGE OF SCANS # 1477 1478 1479

PERCENT DIRECTIONAL REFLECTANCE

PDR (%X10)	WVL (NM)
64	400
60	412
64	425
72	437
78	450
80	462
82	475
83	487
88	500
94	512
106	525
122	537
134	550
141	562
140	575
133	587
130	600
126	612
121	625
116	637
112	650
103	662
84	675
83	687
104	700
148	712
188	725
210	737
228	750
249	762
244	775
244	787
254	800
256	812
258	825
258	837
257	850
260	862
256	875
264	887
253	900
256	912
262	925
248	937
250	950
268	962
254	975
258	987
272	1000
279	1025
326	1050
479	1075

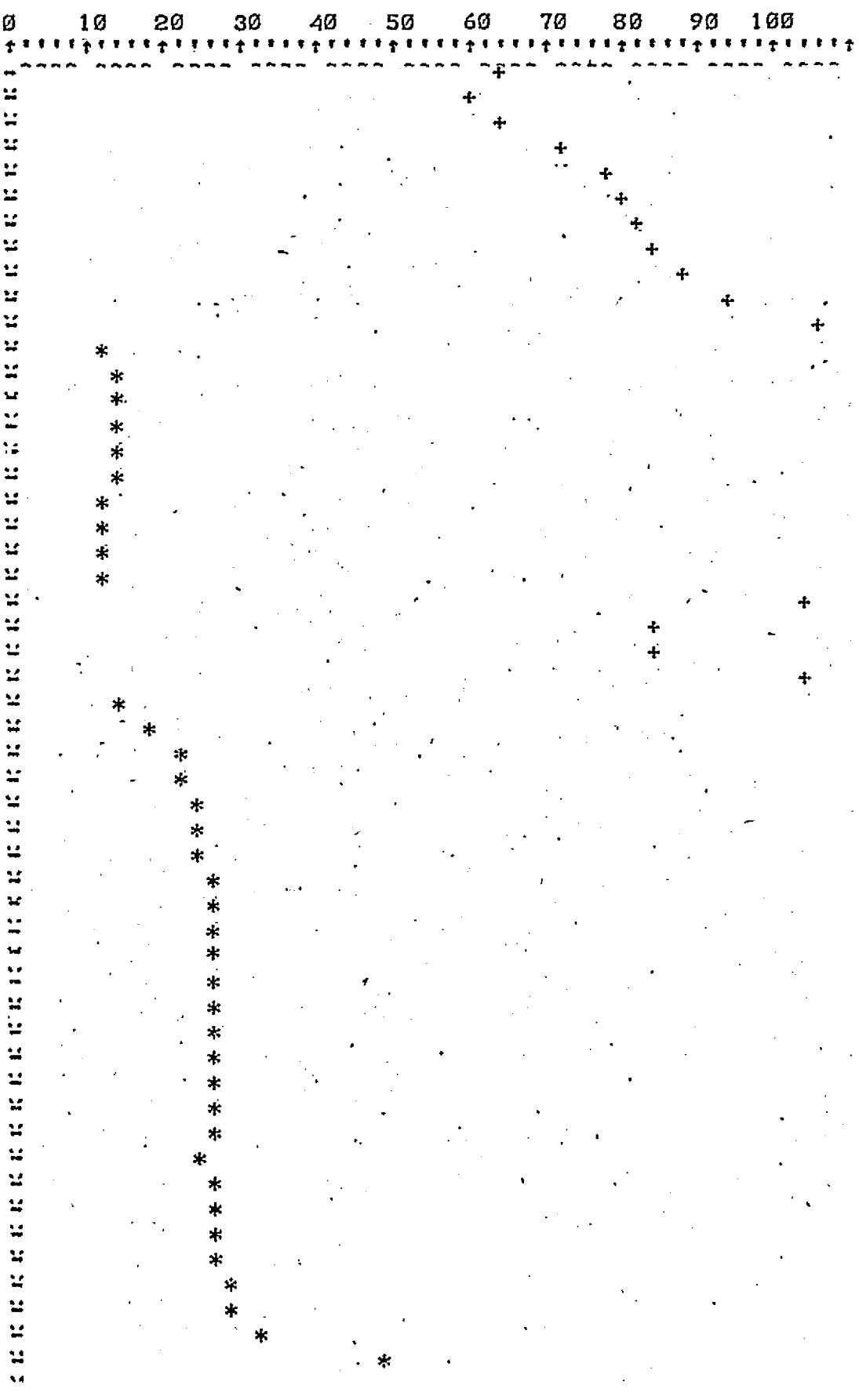

(%X10) (NM)

††† ANomalous Pinion Pine #479, Copper Basin - Cu 2220 ppm, Mo 47 ppm

*AVERAGE OF SCANS # 1439 1441 1442

PERCENT DIRECTIONAL REFLECTANCE

PDR (%X10)	WVL (NM)
33	400
34	412
38	425
44	437
49	450
57	462
59	475
61	487
63	500
67	512
74	525
86	537
95	550
100	562
104	575
101	587
96	600
94	612
93	625
92	637
90	650
78	662
74	675
91	687
143	700
217	712
303	725
368	737
419	750
448	762
449	775
461	787
481	800
454	812
451	825
474	837
460	850
471	862
480	875
514	887
484	900
447	912
506	925
442	937
374	950
293	962
369	975
366	987
379	1000
435	1025
381	1050
570	1075

(%X10) (NM)

††† Anomalous Pinion Pine #480, Copper Basin - Cu 835 ppm, Mo 12 ppm

†AVERAGE OF SCANS # 1485 1486 1487

PERCENT DIRECTIONAL REFLECTANCE

PDR (%X10)	WVL (NM)
41	400
40	412
42	425
47	437
52	450
52	462
53	475
55	487
55	500
61	512
70	525
84	537
98	550
101	562
98	575
94	587
93	600
89	612
91	625
84	637
82	650
72	662
102	675
115	687
243	700
320	712
397	725
448	737
481	750
497	762
502	775
490	787
506	800
513	812
507	825
489	837
504	850
546	862
510	875
500	887
546	900
488	912
483	925
486	937
514	950
512	962
513	975
571	987
518	1000
534	1025
487	1050
629	1075

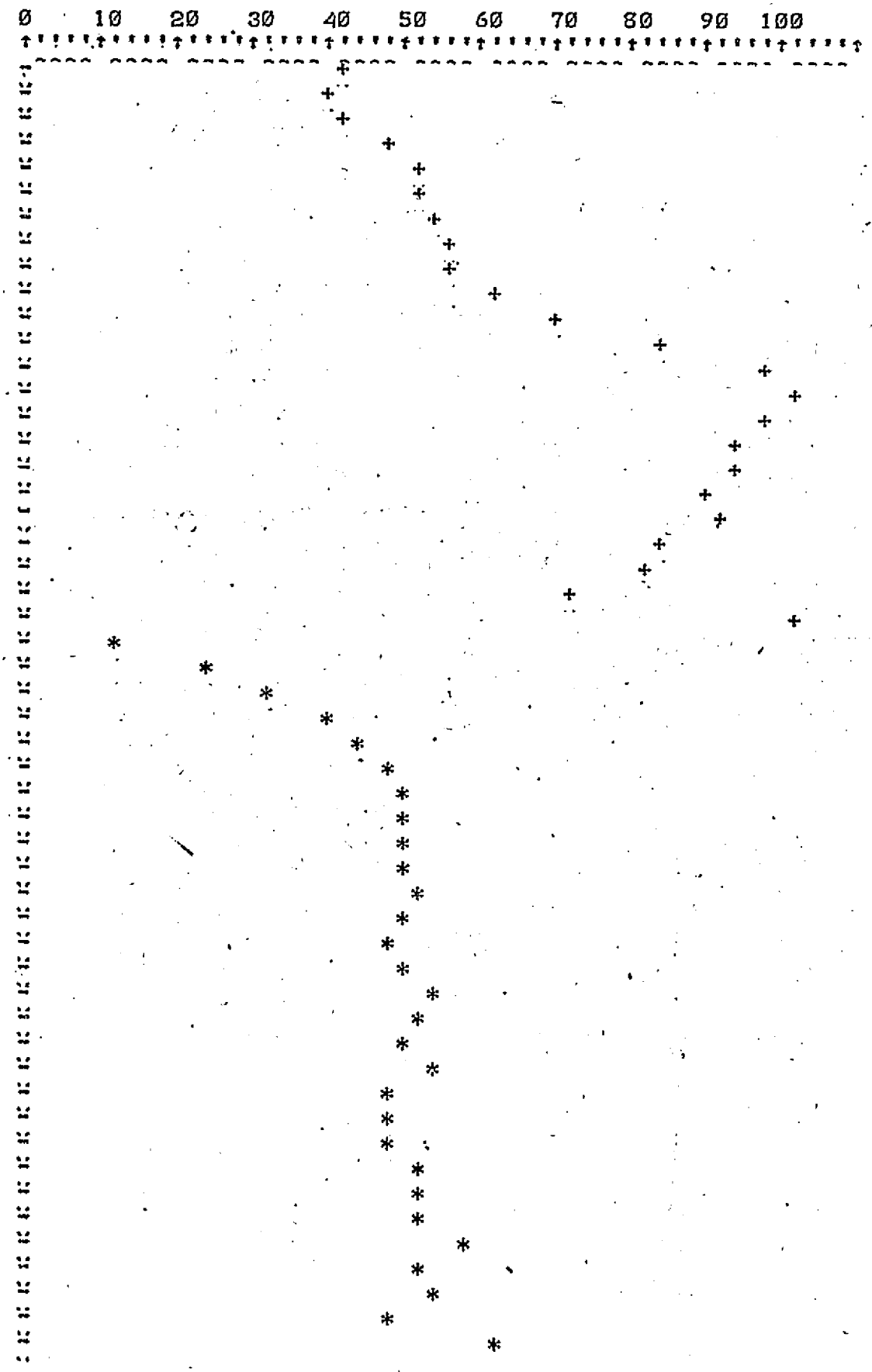

(%X10) (NM)

††† Anomalous Pinion Pine #482, Copper Basin - Cu 780 ppm, Mo 65 ppm

†AVERAGE OF SCANS # [1489] 1490 1491

PERCENT DIRECTIONAL REFLECTANCE

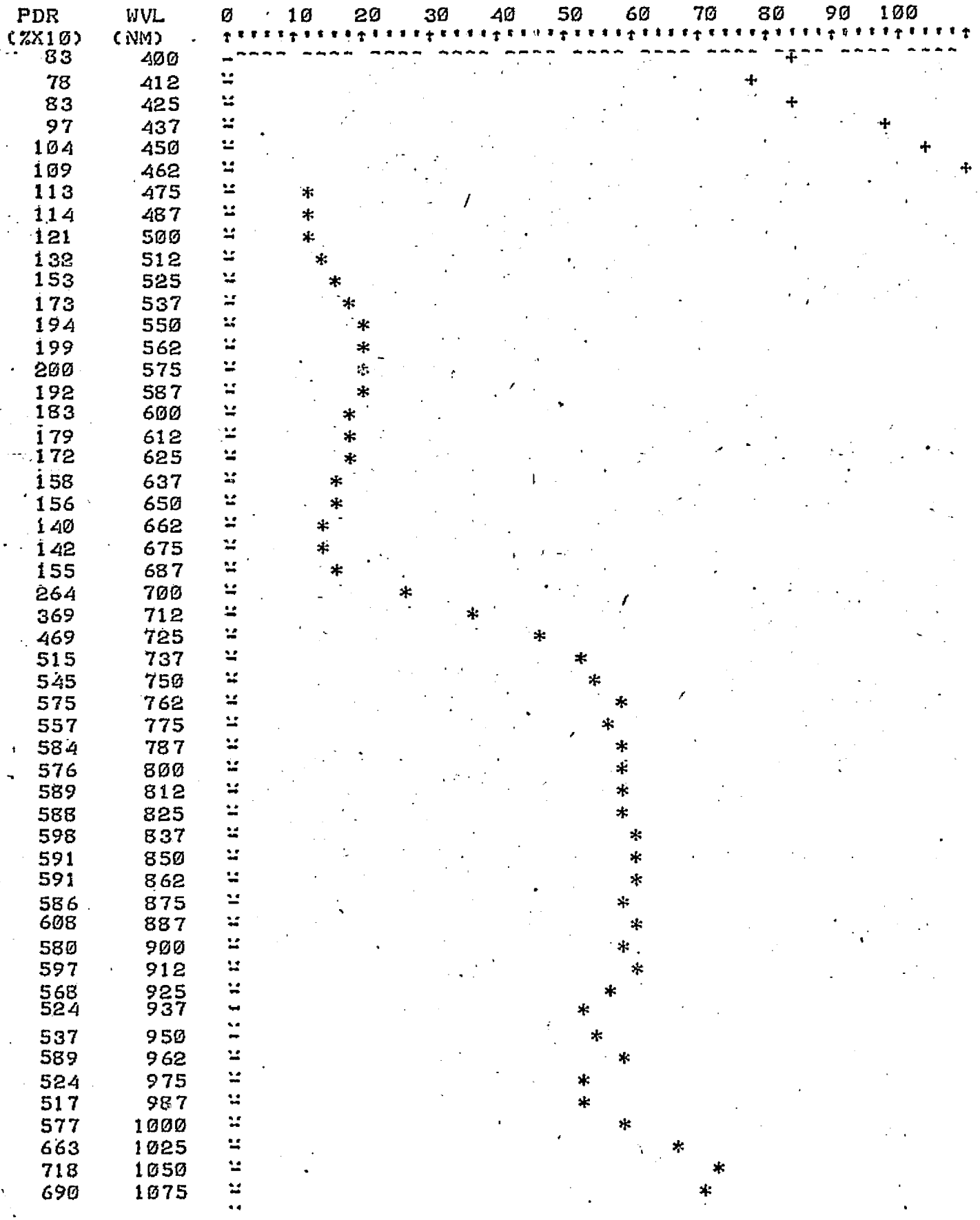

††† Anomalous Pinion Pine #485, Copper Basin - Cu 1275 ppm, Mo 105 ppm

†AVERAGE OF SCANS # 1473 1474 1475

PERCENT DIRECTIONAL REFLECTANCE

PDR (%X10)	WVL (NM)
68	400
64	412
69	425
82	437
90	450
93	462
97	475
99	487
104	500
113	512
131	525
159	537
177	550
187	562
186	575
176	587
165	600
160	612
154	625
145	637
140	650
126	662
156	675
169	687
297	700
390	712
481	725
525	737
549	750
588	762
598	775
612	787
600	800
613	812
632	825
615	837
633	850
628	862
607	875
608	887
611	900
606	912
610	925
560	937
573	950
612	962
597	975
601	987
610	1000
627	1025
677	1050
617	1075

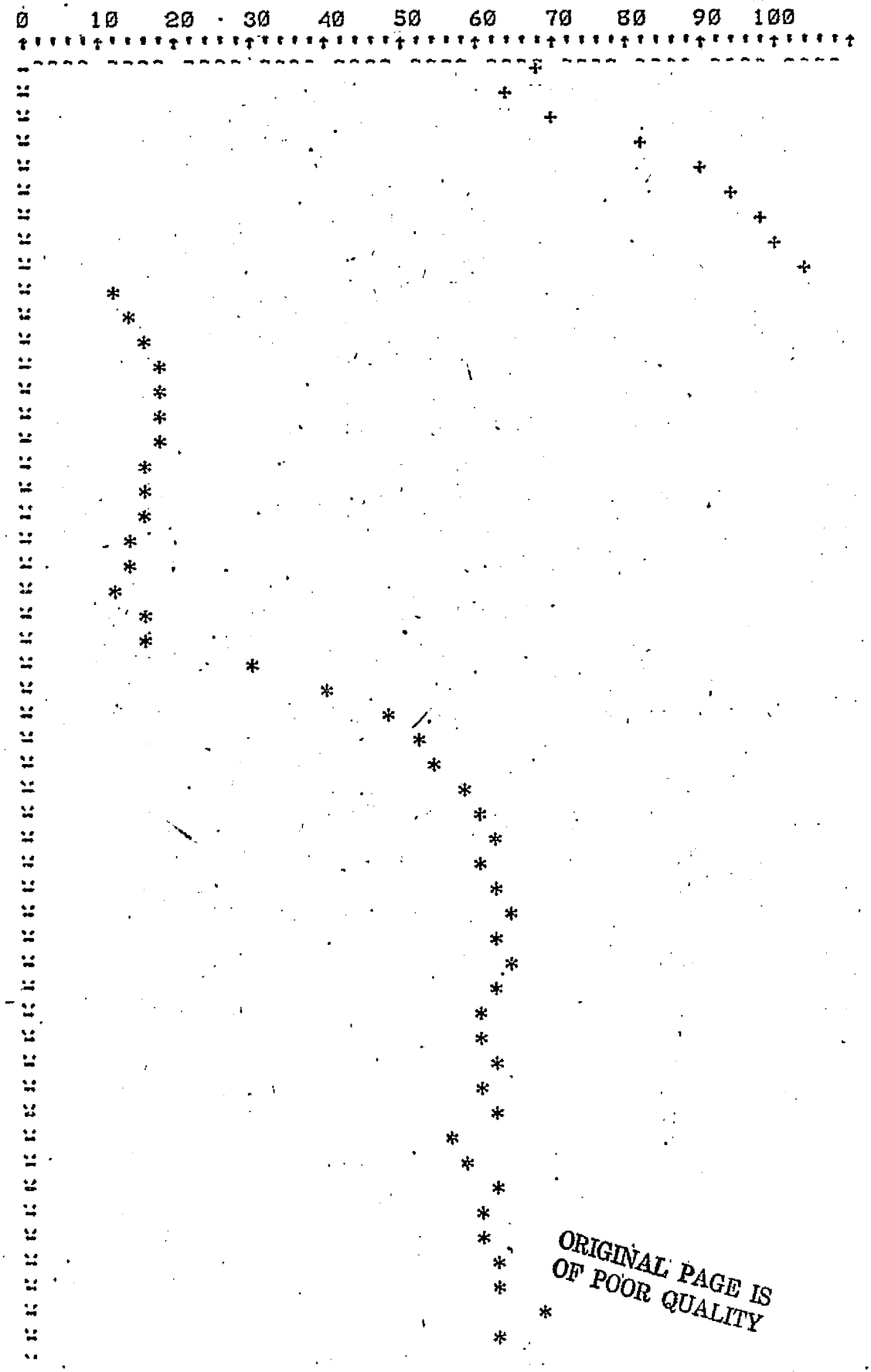

††† Anomalous Pinion Pine $487, Copper Basin - Cu 987 ppm, Mo 99 ppm

#AVERAGE OF SCANS # 1493 1494

PERCENT DIRECTIONAL REFLECTANCE

PDR (%X10)	WVL (NM)
29	400
31	412
33	425
39	437
43	450
46	462
48	475
50	487
52	500
57	512
68	525
79	537
88	550
93	562
92	575
90	587
86	600
85	612
84	625
80	637
78	650
73	662
99	675
122	687
269	700
393	712
505	725
584	737
619	750
657	762
679	775
669	787
664	800
673	812
680	825
675	837
678	850
696	862
696	875
696	887
670	900
679	912
652	925
620	937
653	950
638	962
631	975
621	987
628	1000
640	1025
658	1050
784	1075

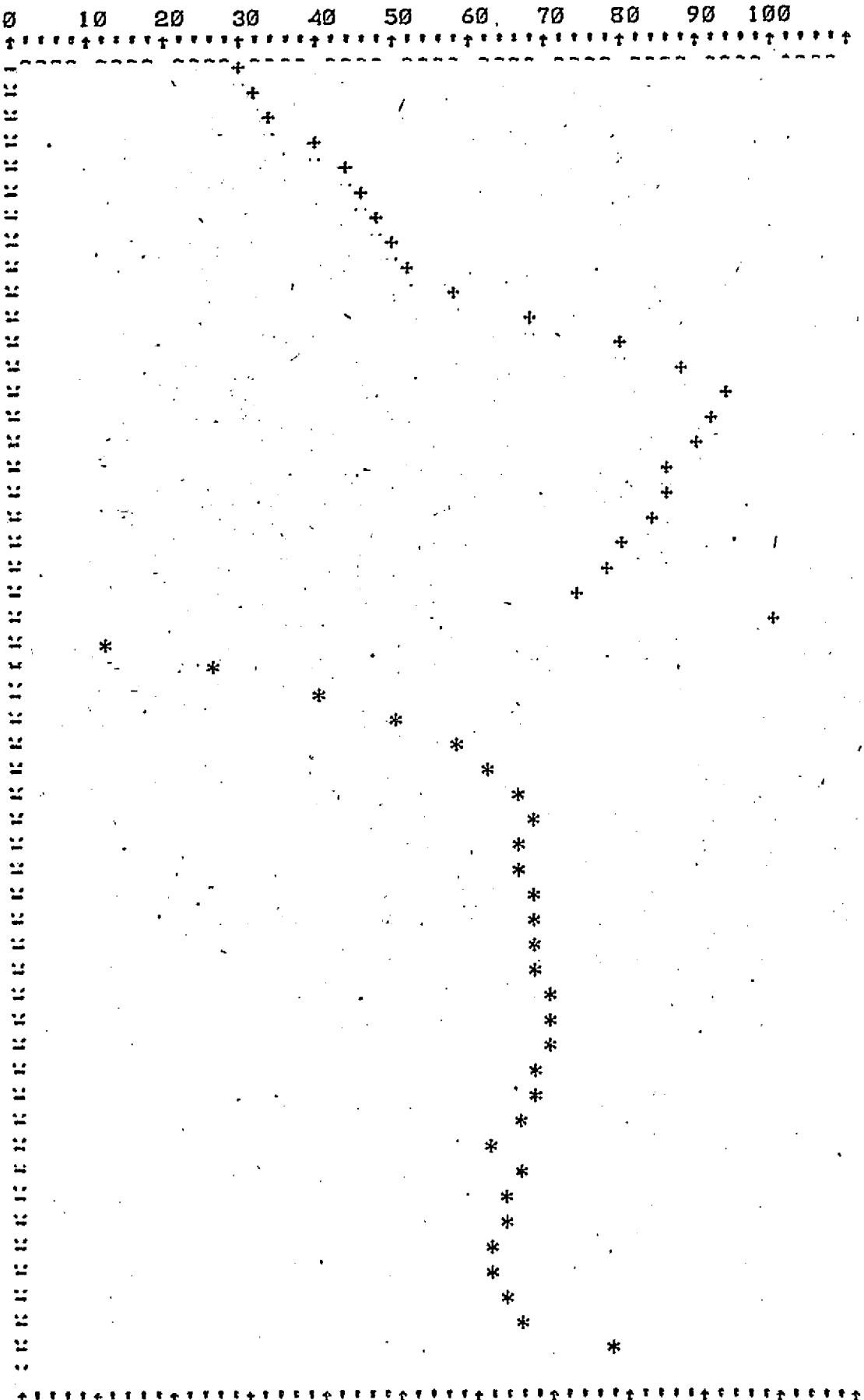

(%X10) (NM)

H=1-5

Anomalous Pinion Pine $488, Copper Basin - Cu 1200 ppm, Mo 62 ppm

AVERAGE OF SCANS # 1456 1457 1458

PERCENT DIRECTIONAL REFLECTANCE

PDR (%X10)	WVL (NM)
33	400
36	412
41	425
44	437
52	450
55	462
55	475
56	487
61	500
64	512
74	525
96	537
103	550
112	562
115	575
109	587
99	600
96	612
86	625
85	637
81	650
87	662
72	675
118	687
159	700
255	712
360	725
456	737
515	750
533	762
572	775
563	787
621	800
554	812
574	825
578	837
570	850
611	862
583	875
522	887
679	900
533	912
595	925
622	937
566	950
557	962
519	975
551	987
521	1000
619	1025
636	1050
537	1075

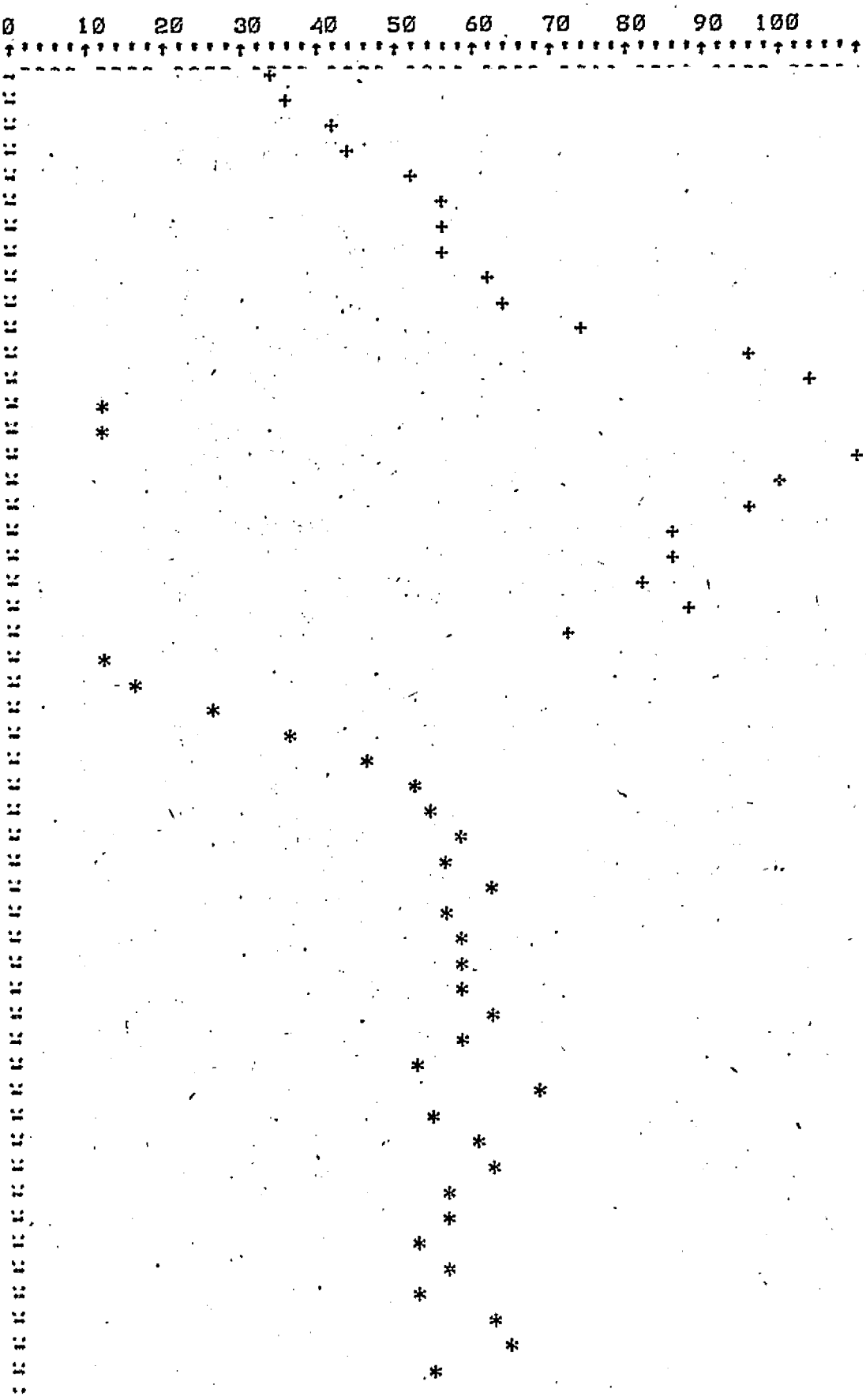

(%X10) (NM)

APPENDIX I

Copper Basin

Alligator Bark Juniper Spectra

Juniper No.	Scan No.	Cu (ppm)	Mo (ppm)	Remarks
401	1373	149	53	Somewhat questionable data.
402	1404	128	32	Somewhat questionable data.
403	1423	102	86	Cloudy conditions.
414	1426	229	65	Cloudy conditions.

††† Background Alligator Bark Juniper #401, Copper Basin - Cu 149 ppm, Mo 53 ppm

*AVERAGE OF SCANS # 1373

PERCENT DIRECTIONAL REFLECTANCE

PDR (%X10)	WVL (NM)
30	400
30	412
32	425
36	437
40	450
47	462
50	475
53	487
57	500
65	512
74	525
89	537
101	550
117	562
122	575
112	587
106	600
112	612
104	625
88	637
85	650
78	662
103	675
120	687
210	700
267	712
319	725
364	737
402	750
421	762
409	775
466	787
427	800
440	812
456	825
478	837
471	850
472	862
449	875
493	887
447	900
432	912
436	925
525	937
348	950
549	962
537	975
590	987
522	1000
416	1025
624	1050
665	1075

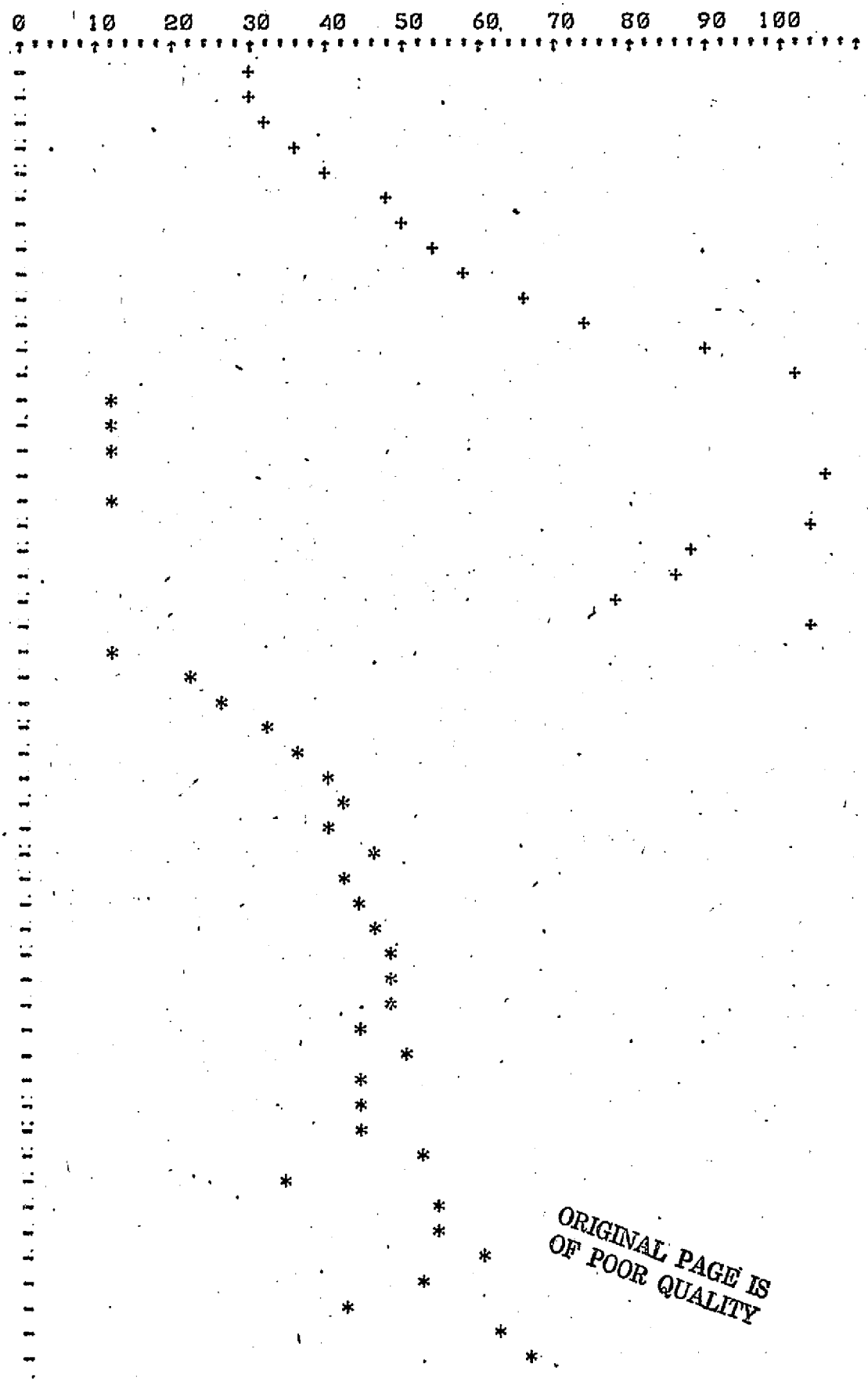

(%X10) (NM)

††† Background Alligator Bark Juniper #402, Copper Basin - Cu 128 ppm; Mo 32 ppm

†AVERAGE OF SCANS # 1404 1405 1406 1407

PERCENT DIRECTIONAL REFLECTANCE

PDR (%X10)	WVL (NM)
33	400
33	412
33	425
36	437
39	450
40	462
41	475
40	487
43	500
49	512
55	525
62	537
69	550
72	562
71	575
62	587
69	600
69	612
65	625
63	637
66	650
61	662
71	675
91	687
185	700
271	712
373	725
436	737
458	750
482	762
504	775
515	787
508	800
509	812
521	825
526	837
531	850
531	862
533	875
533	887
536	900
552	912
558	925
546	937
543	950
529	962
507	975
547	987
535	1000
556	1025
570	1050
614	1075

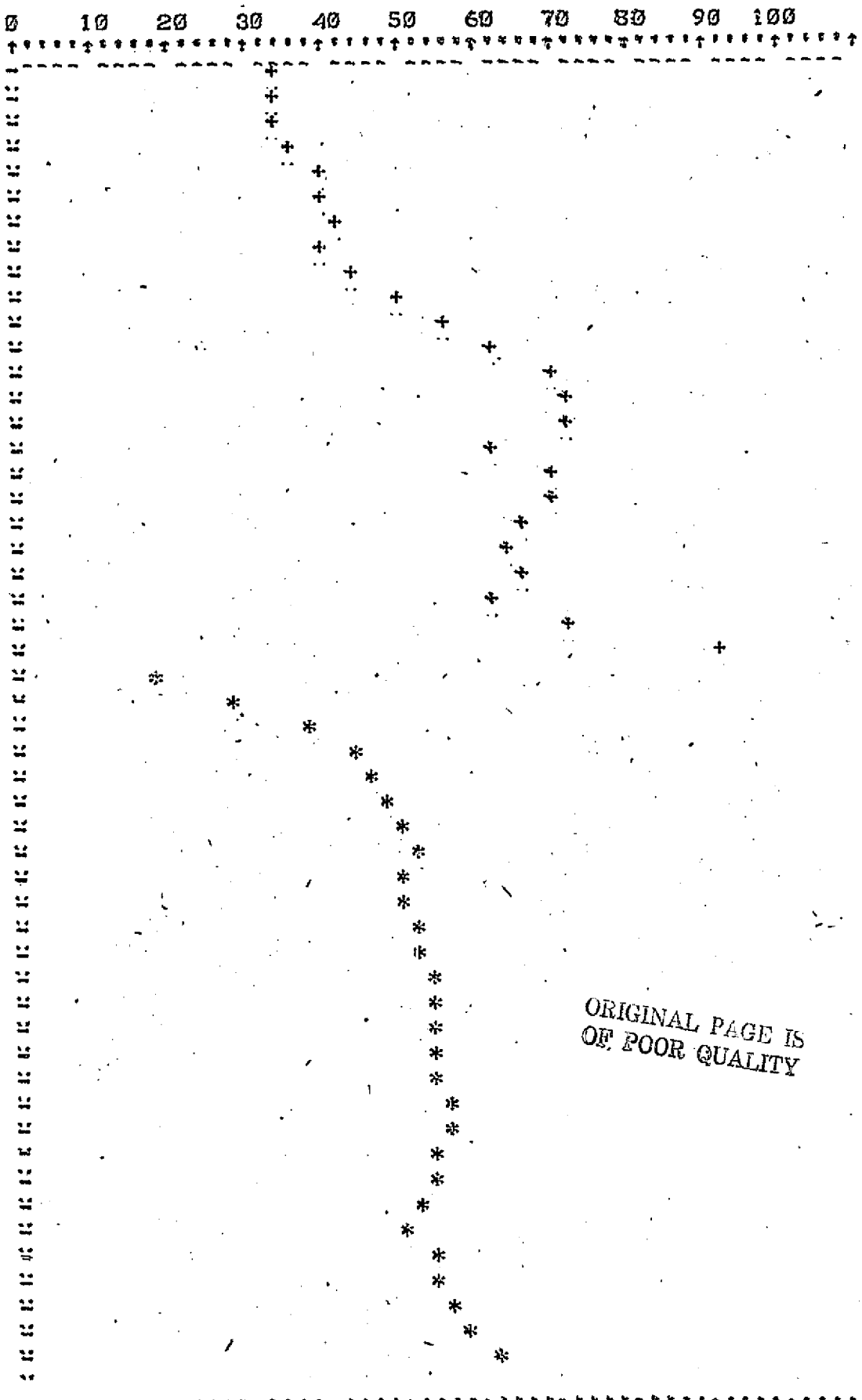

(%X10) (NM)

Backgrourd Alligator Bark Juniper #403, Cu 102 ppm, Mo 86 ppm

AVERAGE OF SCANS # 1423 1424 1425

PERCENT DIRECTIONAL REFLECTANCE

PDR (%X10)	WVL (NM)
32	400
32	412
34	425
37	437
40	450
45	462
49	475
50	487
51	500
58	512
71	525
84	537
96	550
102	562
99	575
94	587
91	600
88	612
84	625
80	637
78	650
63	662
64	675
89	687
201	700
310	712
454	725
565	737
637	750
683	762
694	775
728	787
728	800
742	812
737	825
760	837
769	850
777	862
797	875
787	887
769	900
785	912
826	925
808	937
731	950
705	962
704	975
658	987
712	1000
759	1025
846	1050
923	1075

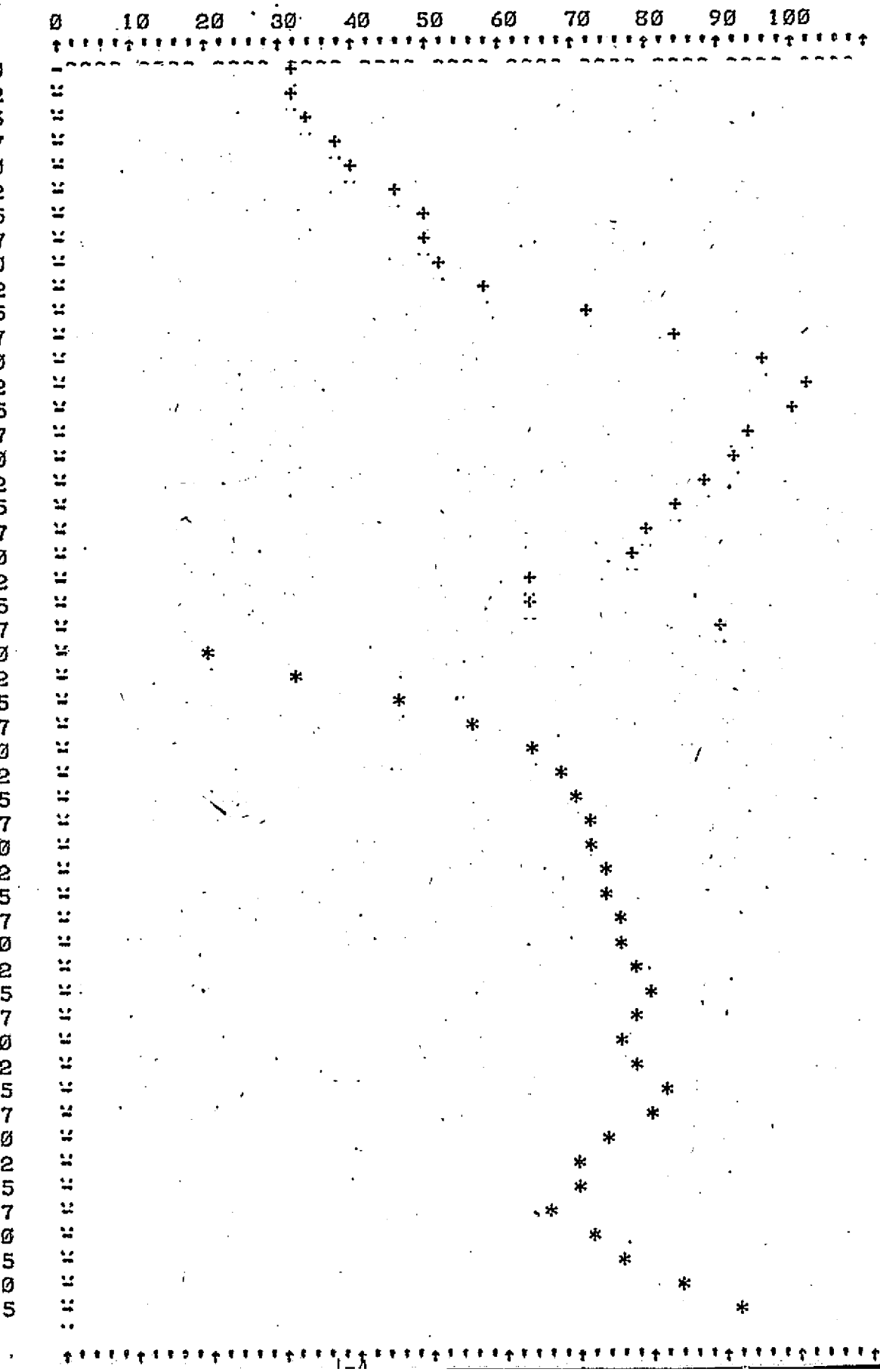

††† Background Alligator Bark Juniper #414 – Copper Basin, Cu 229 ppm Mo 6[illegible] ppm

AVERAGE OF SCANS # 1426 1427

PERCENT DIRECTIONAL REFLECTANCE

PDR (ZX10)	WVL (NM)
43	400
43	412
47	425
51	437
55	450
68	462
73	475
77	487
79	500
90	512
109	525
133	537
153	550
163	562
167	575
153	587
143	600
143	612
135	625
129	637
125	650
99	662
83	675
111	687
209	700
300	712
436	725
508	737
551	750
593	762
607	775
624	787
618	800
633	812
645	825
648	837
636	850
676	862
651	875
643	887
631	900
673	912
672	925
655	937
610	950
618	962
661	975
544	987
604	1000
626	1025
717	1050
758	1075

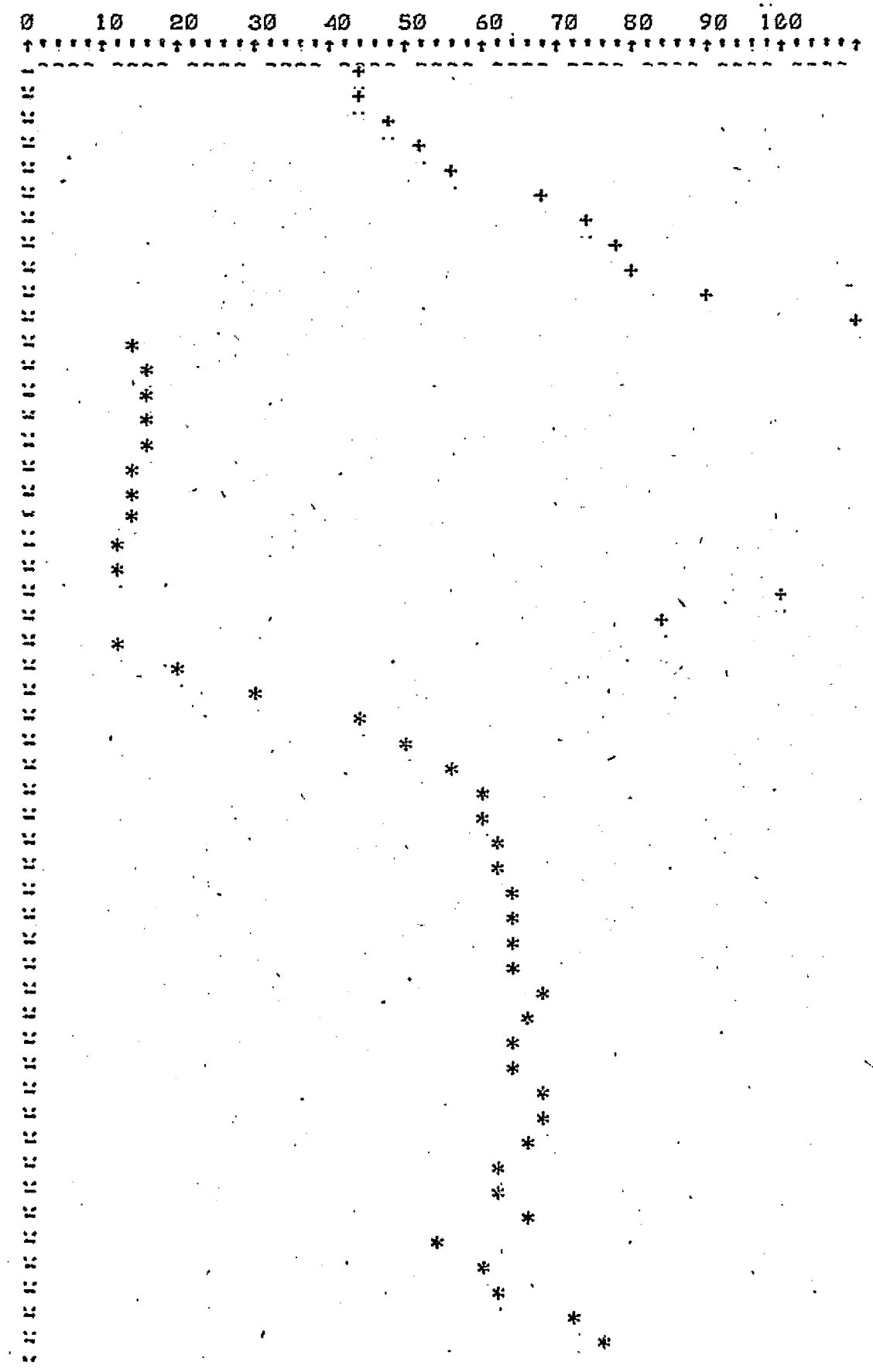

(ZX10) (NM)

APPENDIX J

Mission Logs

ROLL # ON 27 DATE 30 Oct. 72 JOB Arizona WEATHER

PHOTOGRAPHER Anderson PILOT Jim Crosson FILM 2424 MAGAZINE Rose Dark

AREA	STRIP #	STRIP DIR.	NEG. NO. FROM	NEG. NO. TO	TIME START	TIME END	SCALE	ALT.	EXPOSURE 1/25 REC.	EXPOSURE 1/25 FILTER	EXPOSURE 1/25 f	REMARKS
Copper Basin	3		1	4	1002			8.5K MSL	1 9	4400	f11	406-480 High
	2		5	8	1005				2 1	5200	f4	505-558 scattered
									3 5	6200	5.6-8	585-680 cirrus
	1		9	16	1008	cleaning	17	3.5K MT	423	8485	8	810-855
"	3		18	21	1022			"	1 9	4400	f11	406-480
	2		22	25	1025				2 5	SDC 206	4-5.6	(625) (50)
									3 11	SDC 211	f5.6	(875) (50)
	1		26	33	1030	cleaning	34		423	8485	f8	810-855
"	3		35	38	1037			"	1 9	4400	f11	406-480
	2		39	41	1040				2 5	SDC 206	4-5.6	(625) (50)
									3 11	SDC 211	f5.6	(875) (50)
	1		42	47	1044	cleaning	48		42	SDC 204	4-5.6	(525) (60)
"	3		49	51	1056			"	1 8	SDC 353	f8	(445) (40) High cirrus
	2		52 55	54 57	1102				221	SDC 218	f8	(725) (50) cleaning
									312	SDC 213	4-5.6	(683) (31)
	1		58	63	1106	cleaning	64		42	SDC 204	4-5.6	(525) (60)
"	3		65	67	1112			"	1 8	SDC 354	11-16	(450) (100)
	2		68	70	1125				2 1	SDC 203	f2.8	(575) (42)
									3 6	SDC 356	4-5.6	(825) (50)
	1		71	76	1130	cleaning	77		422	SDC 219	f8	(825) (50)
"	3		78	80	1151			"	1 9	4400	f11	406-480
	2		81	83	1154				2 12	6825	4-5.6	675-710
									3 6	SDC-356	4-5.6	(625) (50)
	1		84	89	1159	.6	90		4 19		5.6-8	710-765

ROLL # 0N27 DATE 30 Oct. 72 JOB Arizona WEATHER

PHOTOGRAPHER Anderson PILOT Jim Carson FILM 2424 MAGAZINE [illegible]

AREA	STRIP #	STRIP DIR.	NEG. NO. FROM	NEG. NO. TO	TIME START	TIME END	SCALE	ALT.	EXPOSURE REC.	EXPOSURE FILTER	EXPOSURE f	REMARKS
Bagdad			91	97	1215				1 9	4400	f11	406-480 High cirrus,
			98	103					2 1	5200	f4	505-558 broken
			104	113					3 5	6200	5.6-8	585-680
									4 23	8485	f8	810-855
									1			
									2			
									3			
									4			
									1			
									2			
									3			
									4			
									1			
									2			
									3			
									4			
									1			
									2			
									3			
									4			
									1			
									2			
									3			
									4			

J-3

ROLL # ON 28 DATE 31 Oct 72 JOB Arizona WEATHER

PHOTOGRAPHER Anderson PILOT Jim Crosson FILM 2424 MAGAZINE Rm-L & C

AREA	STRIP #	STRIP DIR.	NEG. NO. FROM	NEG. NO. TO	TIME START	TIME END	SCALE	ALT.	EXPOSURE 1/150 REC.	EXPOSURE 1/150 FILTER	EXPOSURE 1/150 f	REMARKS
Copper Barn	1		1	14	1110			9K MSL 4/R MT	1 8	SDC 353	4-5.6	(45)(40) Scattered clouds
	2		15	27	1115				2 5	SDC 206	2.8-4	(625)(50)
	3		28	40	1123				3 11	SDC 211	+4	(675)(50)
									4 22	SDC 219	+8	(825)(50)
"	4		41	53	1128			"	1			Increasing cloudiness
	5		54	67	1133				2	4		
									3			
									4			
Copper creek	6		68	82	1142			"	1			Some high scattered clouds
	7		83	91	1147				2			
	8		92	101	1152				3	4		
									4			
"	9		102	112	1156			"	1			
									2			
									3	4		
									4			
								"	1			Some snow on slope in last section of area (Barn)
									2			
									3			
									4			
									1			
									2			
									3			
									4			

ROLL # ON 29 DATE 1 Nov. 72 JOB Arizona WEATHER Clear

PHOTOGRAPHER Anderson PILOT Jim Cannon FILM 2424 MAGAZINE Non-IMC

AREA	STRIP #	STRIP DIR.	NEG. NO. FROM	NEG. NO. TO	TIME START	TIME END	SCALE	ALT.	EXPOSURE 1/150 REC.	EXPOSURE 1/150 FILTER	EXPOSURE 1/150 f	REMARKS
Copper Basin	1		1	13	1256			9K MSL	1	#400	5.6-8	406-480 B
	—	mirror shot	14						2	5200	f2.8	505-558 D
								4K INT	3	6200	4-5.6	585-650 A
	2		15	27	1303				4	8485	5.6-8	810-855 C
"	3		28	41	1307			4	1			
	4		42	54	1313				2			
	5		55	68	1319				3	"		
									4			
Copper Creek	6		69	81	1332			4	1			
	7		82	90	1337				2	"		
	8		91	99	1342				3			
									4			
	9		100	109	1346			4	1			
									2	"		
Closing shot	—		110						3			
									4			
									1			
									2			
									3			
									4			
									1			
									2			
									3			
									4			

J-5

ROLL # ON 29 DATE 1 Nov 72 JOB Cuprus WEATHER Clear

PHOTOGRAPHER Anderson PILOT Jim Carson FILM 2424 MAGAZINE

AREA	STRIP #	STRIP DIR.	NEG. NO. FROM	NEG. NO. TO	TIME START	TIME END	SCALE	ALT.	EXPOSURE REC.	EXPOSURE FILTER	EXPOSURE f	REMARKS
Copper Basin	1		111	124	1358			9K MSL	1	SOC 353	f4	(445)(440)
	2		125	137	1404				2	5200	f2.8	505-558
	3		138	151	1409				3 Not Used	SOC 210	4-5.6	(650)(1.00)
									4	8425	5.6-8	810-855
	4		152	165	1415				1			Mid-speed shutter setting
	5		166	179	1420				2			
									3			
									4			
Copper Creek	6		180	193	1428				1			
	7		194	203	1432				2			
									3			
									4			
	8		204	214	1437				1			Line # 9 will have gap in middle due to intervalometer malfunction
	9		215	224	1442				2			
									3			
									4			
Cleaning Shot			225						1			
									2			
									3			
									4			
									1			
									2			
									3			
									4			

ROLL # 0N 29 DATE 1 Nov. 72 JOB Arizona WEATHER Clear

PHOTOGRAPHER Anderson PILOT Jim Cocco FILM 2424 MAGAZINE

AREA	STRIP #	STRIP DIR.	NEG. NO. FROM	NEG. NO. TO	TIME START	TIME END	SCALE	ALT.	REC.	EXPOSURE 1/75- FILTER	EXPOSURE 1/75- f	1/150 REMARKS
Baghdad			226	234	1505			11K MSL	1	4400	5.6-8	406-480 Mid-range
									2	5200	4.2.8	505-558
			235	248	1510				3	6200	-5.6	585-680 shutter
									4	4425	5.6-8	810-855 setting
"	reshot		249	251					1			
									2			
			252	258	1516				3			
									4			
2			259	267	1523				1			
									2			
									3			
									4			
									1			
									2			
									3			
									4			
									1			
									2			
									3			
									4			
									1			
									2			
									3			
									4			